



Supporting Information

Atroposelective Access to 1,3-Oxazepine-Containing Bridged Biaryls via Carbene-Catalyzed Desymmetrization of Imines

X. Yang, L. Wei, Y. Wu, L. Zhou, X. Zhang*, Y. R. Chi**

Contents

General methods.....	S2
Reaction conditions optimization.....	S2
General procedure	S4
Synthetic application.....	S5
Determination of the rotational barriers	S7
DFT calculations	S10
Characterization data of the products	S22
^1H, ^{13}C, ^{19}F and ^{31}P NMR spectra and HPLC charts.....	S39
X-ray structure of 2k.....	S114
References.....	S114

General methods

All reactions and manipulations involving air-sensitive compounds were carried out using standard Schlenk techniques. Anhydrous toluene and THF were distilled from sodium benzophenone ketyl. Anhydrous CH_2Cl_2 and CHCl_3 were distilled from CaH_2 under an atmosphere of nitrogen. All reactions were monitored by TLC. TLC analysis was performed by illumination with a UV lamp (254 nm). All flash chromatography was packed with silica-gel as the stationary phase. ^1H NMR spectra were recorded on a Bruker (400 MHz) instrument, and chemical shifts were reported in ppm downfield from internal TMS with the solvent resonance as the internal standard (CDCl_3 , $\delta = 7.26$ ppm). ^{13}C NMR spectra were recorded on a Bruker (101 MHz) instrument, and chemical shifts were reported in ppm downfield from TMS with the solvent resonance as the internal standard (CDCl_3 , $\delta = 77$ ppm). ^{19}F NMR spectra were recorded on a Bruker (377 MHz) instrument. Optical rotations were measured on a Jasco P-1030 polarimeter. High resolution mass spectra (HRMS) (EI $^+$) were recorded on a Finnigan MAT 95 XP mass spectrometer. The amino alcohols were synthesized according to the literature procedures.^[1]

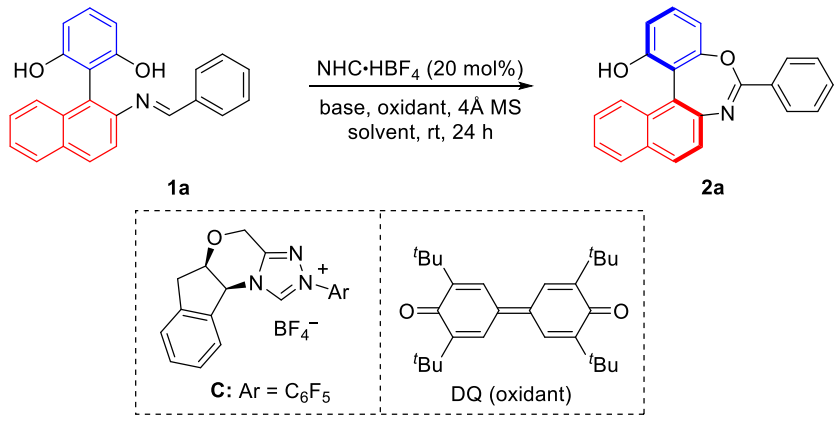
Reaction conditions optimization

Table S1. Screening of NHC catalysts.^[a]

Entry	NHC· HBF_4	Oxidant	Base	Solvent	Yield [%] ^[b]	ee [%] ^[c]
1	A	DQ	Cs_2CO_3	CH_2Cl_2	8	97
2	B	DQ	Cs_2CO_3	CH_2Cl_2	72	97
3	C	DQ	Cs_2CO_3	CH_2Cl_2	73	97
4	D	DQ	Cs_2CO_3	CH_2Cl_2	71	97
5	E	DQ	Cs_2CO_3	CH_2Cl_2	70	97
6	F	DQ	Cs_2CO_3	CH_2Cl_2	72	97

[a] Reaction conditions: **1a** (0.1 mmol), base (1.0 equiv), NHC· HBF_4 (20 mol%), 4Å MS (100 mg) and DQ (1.2 equiv) in solvent (1.0 mL) at rt. [b] Isolated yield. [c] Enantiomeric ratio of **2a** was determined via HPLC on a chiral stationary phase.

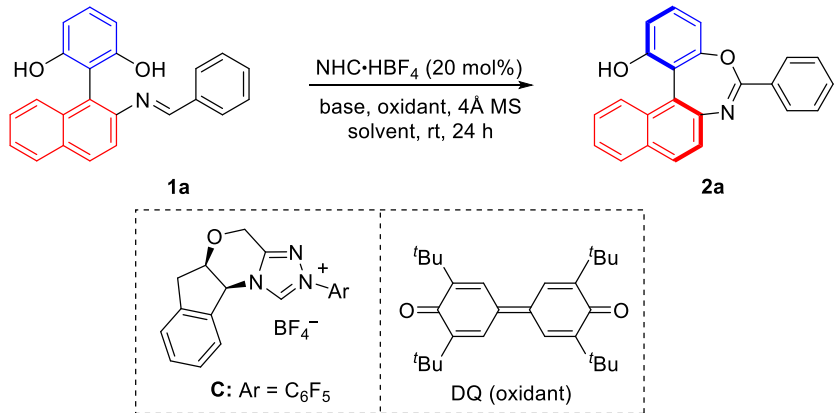
Table S2. Screening of bases.^[a]



Entry	NHC·HBF ₄	Oxidant	Base	Solvent	Yield [%] ^[b]	ee [%] ^[c]
1	C	DQ	Cs ₂ CO ₃	CH ₂ Cl ₂	73	97
2	C	DQ	K ₂ CO ₃	CH ₂ Cl ₂	72	97
3	C	DQ	DIEA	CH ₂ Cl ₂	81	97
4	C	DQ	DBU	CH ₂ Cl ₂	10	-

[a] Reaction conditions: **1a** (0.1 mmol), base (1.0 equiv), NHC·HBF₄ (20 mol%), 4 Å MS (100 mg) and DQ (1.2 equiv) in solvent (1.0 mL) at rt. [b] Isolated yield. [c] Enantiomeric ratio of **2a** was determined via HPLC on a chiral stationary phase.

Table S3. Screening of solvents.^[a]

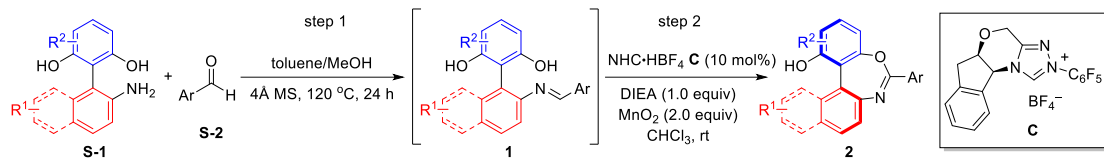


Entry	NHC·HBF ₄	Oxidant	Base	Solvent	Yield [%] ^[b]	ee [%] ^[c]
1	C	DQ	DIEA	CH ₂ Cl ₂	81	97
2	C	DQ	DIEA	toluene	trace	-
3	C	DQ	DIEA	THF	trace	-
4	C	DQ	DIEA	CHCl ₃	81	98
5	C	DQ	DIEA	DCE	78	97

[a] Reaction conditions: **1a** (0.1 mmol), base (1.0 equiv), NHC·HBF₄ (20 mol%), 4 Å MS (100 mg) and DQ (1.2 equiv) in solvent (1.0 mL) at rt. [b] Isolated yield. [c] Enantiomeric ratio of **2a** was determined via HPLC on a chiral stationary phase.

General procedure

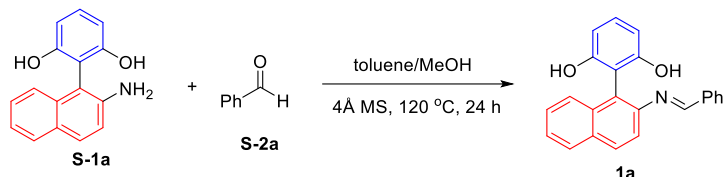
General procedure for the NHC-catalyzed desymmetrization of *in-situ* formed imines



Step 1: To a dried 4 mL tube with a stir bar was added the amino alcohol **S-1** (0.11 mmol), 4 Å MS (100 mg), anhydrous toluene (1.0 mL), anhydrous CH₃OH (50 uL) and aldehyde **S-2** (0.1 mmol) under nitrogen atmosphere. The test tube was sealed and stirred at 120 °C for 24 h. Then the reaction mixture was carefully concentrated under reduced pressure to remove the toluene and get the crude imine **1** for next step without further purification.

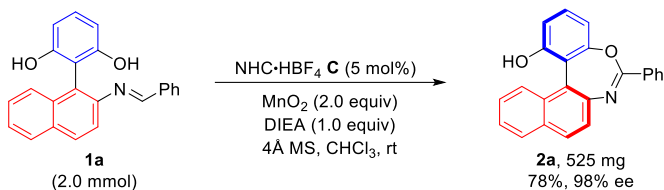
Step 2: To the above crude imine was added activated MnO₂ (2.0 equiv, 0.2 mmol, 17.4 mg), NHC precatalyst **C** (10 mol %, 4.7 mg), anhydrous CHCl₃ (1.0 mL) and DIEA (1.0 equiv, 0.1 mmol, 18 uL). After stirring at rt (20 °C) for the indicated time in the table, the reaction mixture was directly subjected to the preparative thin layer chromatography (Hexane/DCM = 1:5) to afford the desired products **2**.

General procedure for the synthesis of imine



To a dried 50 mL round bottom flask with a stir bar was added amino alcohol **S-1a** (3.0 mmol, 0.75 g), MgSO₄ (4.0 g), anhydrous toluene (20 mL), anhydrous CH₃OH (1.5 mL) and benzaldehyde **S-2a** (4.5 mmol) under nitrogen atmosphere. The round bottom flask was sealed and stirred at 120 °C for 24 h. Then the reaction mixture was cooled and filtered to remove MgSO₄. The filtrate was carefully concentrated under reduced pressure to give the crude product. After recrystallization from ethyl acetate and hexane, the imine was obtained as a yellow solid.

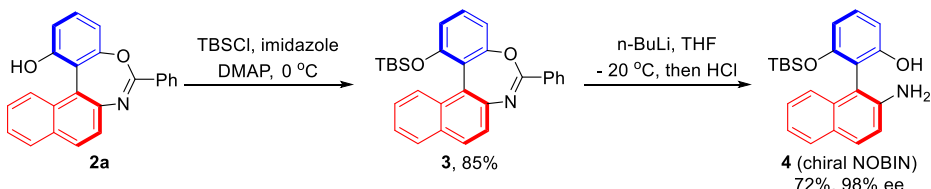
Procedure for the scale-up synthesis of **2a** with a lower catalyst loading



To a dried 50 mL round bottom flask with a stir bar was added imine (2.0 mmol, 678 mg), 4Å MS (2.0 g), activated MnO₂ (2.0 equiv, 350 mg), NHC precatalyst **C** (5 mol %, 56 mg), anhydrous CHCl₃ (10 mL) and DIEA (1.0 equiv, 0.36 mL). After stirring at rt (20 °C) for 18 h, the reaction mixture was concentrated to around 3 mL and then directly subjected to the column chromatography (Hexane/DCM = 1:3) to give the desired product **1a** (525 mg) in 78% yield and 98% ee.

Synthetic application

Synthesis of chiral NOBIN

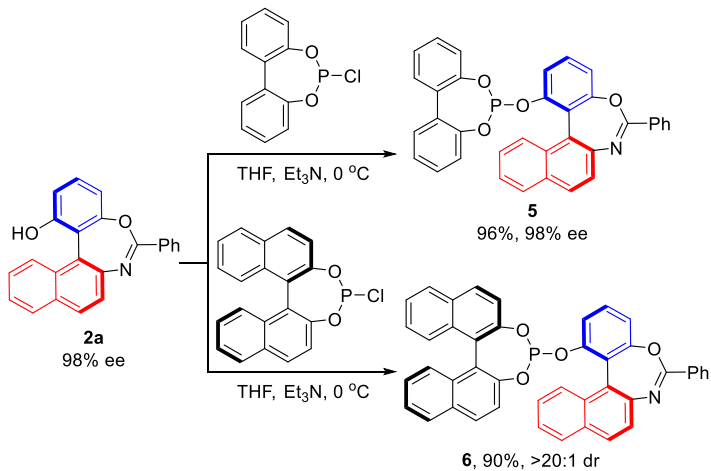


To a dried 5 mL tube with a stir bar was added compound **2a** (0.2 mmol, 67.4 mg), DMAP (0.1 equiv, 2.4 mg), imidazole (2.0 equiv, 27.2 mg) and anhydrous DCM (1.0 mL) under nitrogen atmosphere. The mixture was cooled to 0 °C and a solution of TBSCl (2.0 equiv, 60.3 mg) in DCM (1.0 mL) was slowly added. After stirring at 0 °C for 24 h until the starting material consumed, the reaction mixture was concentrate under reduced pressure and the residue was subjected to the preparative thin layer chromatography (Hexane/DCM = 5:1) to afford the desired product **3** (76.6 mg, 85% yield).

To a dried 5 mL tube with a stir bar was added compound **3** (0.1 mmol, 45.2 mg) and anhydrous THF (1.0 mL) under nitrogen atmosphere. The mixture was cooled to -20 °C and a solution of *n*-BuLi (2.0 M, 0.1 mL) was slowly added. After stirring at -20 °C for 0.5 h, saturated NH₄Cl aqueous was added to quench the reaction. To the mixture was added HCl (2.0 N) and the acidic solution was stirred for 10 min; then saturated

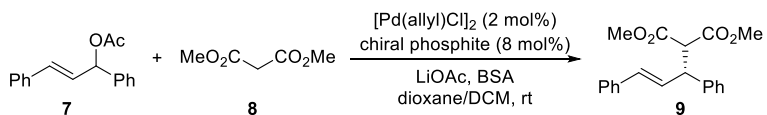
NaHCO_3 aqueous was added to neutralize the reaction mixture. Ethyl acetate was added to extract for three times. The organic phase was combined and concentrate under reduced pressure, then the residue was subjected to the preparative thin layer chromatography (Hexane/EA = 5:1) to afford the chiral NOBIN **4** (26.3 mg) in 72% yield and 98% ee.

Synthesis of chiral phosphite ligands



To a dried 4 mL test tube with a stir bar was added compound **2a** (0.2 mmol, 67.4 mg), anhydrous THF (2.0 mL) and Et_3N (0.1 mL, 4.0 equiv) under nitrogen atmosphere. The mixture was cooled to 0 °C and a solution of phosphorochloridite^[2] (2.0 equiv) in THF (1.0 mL) was slowly added. After stirring at 0 °C for 2 h until the starting material consumed, the reaction mixture was concentrate under reduced pressure and the residue was subjected to the preparative thin layer chromatography (Hexane/DCM = 2:1) to afford the desired phosphite ligands.

Application of the phosphite ligands for asymmetric alkyl allylation



To a dried 4 mL test tube with a stir bar was added $[\text{Pd}(\text{allyl})\text{Cl}]_2$ (2 mol%, 1.1 mg), chiral phosphite (8 mol%) and dioxane/DCM (1:1, 1.2 mL) under nitrogen atmosphere. The mixture was stirred at rt for 0.5 h, and then compound **7** (0.15 mmol, 37.9 mg), dimethyl malonate **8** (0.27 mmol, 35.7 mg), LiOAc (3.0 equiv, 29.7 mg) and BSA (3.0 equiv, 91.6 mg) was added. After stirring at rt for 24 h until the starting material

consumed, the reaction mixture was concentrate under reduced pressure and the residue was subjected to the preparative thin layer chromatography (Hexane/EA = 5:1) to afford the desired product **9**.

Determination of the rotational barriers

The specified 1,3-oxazepine-bridged biaryls (5 mg) was dissolved in toluene (5.0 mL) and heated at indicated temperature. Aliquots (< 0.1 mL) were diluted with *i*PrOH (0.5 mL) and directly analyzed by chiral HPLC to determine the enantiomeric ratio at the specified time. The rotational barrier (ΔG^\ddagger), rate constants for enantiomerization (k_{ent}) and racemization (k_{rac}), and half-life for racemization ($t_{1/2\text{rac}}$) were calculated based on the following equations,

$$t_{1/2\text{rac}} = \ln 2 / k_{\text{rac}}$$

$$\Delta G^\ddagger = -RT \ln(k_{\text{ent}} h / k_B T)$$

where the transmission coefficient κ is set as 1, Boltzmann constant $k_B = 1.3806503 \times 10^{-23}$ J/K, Planck constant $h = 6.62606876 \times 10^{-34}$ J s, idea gas constant $R = 8.314472$ J/(mol K).^[3]

Table S4. Change of enantiomer ratio with time for **2a** (40 °C in toluene)

t	ee (%)
0	98.818
1 h	98.248
2 h	97.806
3 h	97.206
4 h	96.278
6 h	95.224
8 h	93.922
10 h	92.496
12 h	91.414

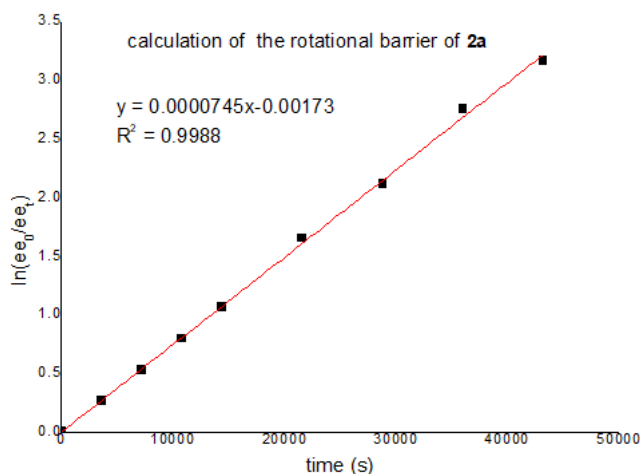
Table S5. Change of enantiomer ratio with time for **2a** (50 °C in toluene)

t	ee (%)
0	98.818
1 h	96.218
2 h	93.830
3 h	91.508

4 h	89.064
6 h	84.888
8 h	80.556
10 h	76.694
12 h	72.882

Table S6. Change of enantiomer ratio with time for **2a** (70 °C in toluene)

t/s	ee (%)	ln(ee ₀ /ee _t)
0	98.818	0
3600 (1 h)	76.098	0.26126
7200 (2 h)	58.374	0.52641
10800 (3 h)	44.648	0.79447
14400 (4 h)	34.306	1.05796
21600 (6 h)	18.992	1.64926
28800 (8 h)	11.432	2.11506
36000 (10 h)	6.32	2.74856
43200 (12h)	3.418	3.16153



$$\ln(ee_0/ee_t) = 2k_{ent}t + C$$

$$k_{ent} = 1/2 \text{ slope} = 0.0000373 \text{ s}^{-1}$$

$$k_{rac} = 2k_{ent} = 0.0000745 \text{ s}^{-1}$$

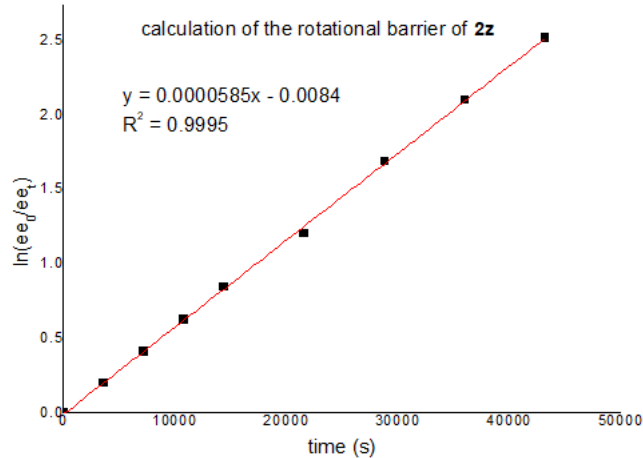
$$t_{1/2rac} = \ln 2 / k_{rac} = 9304 \text{ s} = 2.58 \text{ h}$$

$$\Delta G^\neq = -RT\ln(k_{ent}h/k_B T) = 27.1 \text{ kcal/mol}$$

Table S7. Change of enantiomer ratio with time for **2z** (70 °C in toluene)

t/s		ee (%)	ln(ee ₀ /ee _t)
0		98.904	0
3600 (1 h)		80.750	0.20279
7200 (2 h)		65.464	0.41265
10800 (3 h)		52.918	0.62541
14400 (4 h)		42.520	0.84418

21600 (6 h)		29.602	1.20631
28800 (8 h)		18.826	1.68899
36000 (10 h)		12.088	2.10194
43200 (12h)		7.818	2.52224



$$\ln(\text{ee}_0/\text{ee}_t) = 2k_{\text{ent}}t + C$$

$$k_{\text{ent}} = 1/2 \text{ slope} = 0.0000273 \text{ s}^{-1}$$

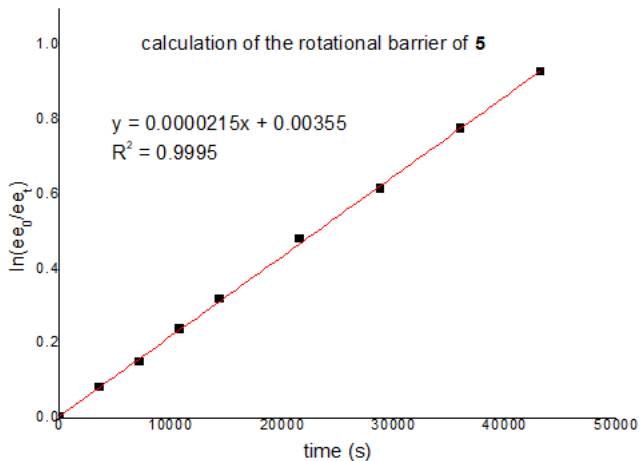
$$k_{\text{rac}} = 2k_{\text{ent}} = 0.0000585 \text{ s}^{-1}$$

$$t_{1/2\text{rac}} = \ln 2/k_{\text{rac}} = 11849 \text{ s} = 3.29 \text{ h}$$

$$\Delta G^\neq = -RT \ln(k_{\text{ent}}h/k_B T) = 27.3 \text{ kcal/mol}$$

Table S8. Change of enantiomer ratio with time for **5** (70 °C in toluene)

t/s (h)	ee (%)	$\ln(\text{ee}_0/\text{ee}_t)$
0	97.690	0
3600 (1 h)	90.072	0.08119
7200 (2 h)	83.200	0.15026
10800 (3 h)	77.026	0.23761
14400 (4 h)	71.022	0.31880
21600 (6 h)	60.488	0.47935
28800 (8 h)	52.532	0.61366
36000 (10 h)	44.988	0.7754
43200 (12h)	37.574	0.92803



$$\ln(ee_0/ee_t) = 2k_{\text{ent}}t + C$$

$$k_{\text{ent}} = 1/2 \text{ slope} = 0.0000108 \text{ s}^{-1}$$

$$k_{\text{rac}} = 2k_{\text{ent}} = 0.0000215 \text{ s}^{-1}$$

$$t_{1/2\text{rac}} = \ln 2 / k_{\text{rac}} = 32239 \text{ s} = 8.96 \text{ h}$$

$$\Delta G^\ddagger = -RT \ln(k_{\text{ent}}h/k_B T) = 28.1 \text{ kcal/mol}$$

DFT calculations

Computational Methods

Conformational sampling

Conformational samplings were carried out at GFN2-xTB^{4–6} level of theory using the CREST (Conformer-Rotamer Ensemble Sampling Tool) program version 2.12 by Grimme and co-workers.^{7,8} The conformers and rotamers ensemble was generated using the iterative metadynamics based on genetic z-matrix crossing (iMTD-GC). Conformers were further optimized at GFN2-xTB level with very tight (*-opt vtight*) optimization in the presence of ALPB implicit solvation model for chloroform (solvent used in the experimental reactions) and for toluene (solvent used in the rotational barriers measurement). The 10 lowest energy conformers were further optimized at density functional theory (DFT) level and the lowest DFT energy conformer is used for further analysis/usage.

Density functional theory (DFT) calculations

DFT calculations were carried out using the *Gaussian 16* rev. B.01 program.⁹ The global hybrid functional M06-2X¹⁰ with Karlsruhe-family basis set of double- ζ valence def2-SVP^{11,12} for all atoms were employed for all gas-phase optimizations. Single point

(SP) corrections were performed using M06-2X functional and def2-TZVP¹¹ basis set for all atoms. The implicit SMD continuum solvation model¹³ was used to account for the solvent effect of chloroform (solvent used in the experimental reactions) and of toluene (solvent used in the rotational barriers measurement). Gibbs energies were evaluated at the room temperature (for reaction) and at 70°C (for rotational barriers measurements), using the entropic quasi-harmonic treatment scheme of Grimme¹⁴ and the enthalpy quasi-harmonic treatment of Head-Gordon,¹⁴ at a cut off frequency of 100 cm⁻¹. The free energies were further corrected using standard concentration of 1 mol/L, which was used in solvation calculations. Data analysis was carried out using the GoodVibes code version 3.1.1.¹⁵ Gibbs energies evaluated at SMD(chloroform/toluene)-M06-2X/def2-TZVP//M06-2X/def2-SVP level of theory are given in kcal/mol. Non-covalent interactions (NCIs) were analyzed using NCIPLLOT¹⁶ calculations. The *wfn* files for NCIPLLOT were generated at M06-2X/def2-SVP level of theory. NCI indices calculated with NCIPLLOT were visualized at a gradient isosurface value of $s = 0.5$ au. These are colored according to the sign of the second eigenvalue (λ_2) of the Laplacian of the density ($\nabla^2\rho$) over the range of -0.1 (blue = attractive) to +0.1 (red = repulsive). Molecular orbitals are visualized using an isosurface value of 0.05 au throughout. All molecular structures and molecular orbitals were visualized using PyMOL software.¹⁷

Computational rotational barriers studies

The rotational barriers for the enantiomerization of the structures **2a**, **2z**, **2ab** and **5** (Scheme S1) are studied computationally. For structure **5** which has many degrees of freedom, thorough conformational sampling was carried out using the CREST program^{7,8} at GFN2-xTB⁴⁻⁶ level in the presence of ALPB implicit toluene. A relaxed PES scan of the dihedral angle along the C–C axial axis is performed, in accordance to the protocol outlined in reference.¹² The highest energy structure is then used as the guess structure to locate the actual rotational transition structure. The TSs for the enantiomerization via rotation for each of these structures were then successfully located and verified by intrinsic reaction coordinate (IRC)^{18,19} analyses (see attached IRC movies, on DOI: [10.5281/zenodo.6789750](https://doi.org/10.5281/zenodo.6789750), for details).

steric clashes preventing ease of enantiomerization			freely rotatable bond without steric hinderance
2a expt: $\Delta G^\ddagger = 27.1 \text{ kcal mol}^{-1}$ calc: $\Delta G^\ddagger = 27.9 \text{ kcal mol}^{-1}$	2z expt: $\Delta G^\ddagger = 27.3 \text{ kcal mol}^{-1}$ calc: $\Delta G^\ddagger = 28.0 \text{ kcal mol}^{-1}$	5 expt: $\Delta G^\ddagger = 28.1 \text{ kcal mol}^{-1}$ calc: $\Delta G^\ddagger = 28.9 \text{ kcal mol}^{-1}$	2ab cannot be determined $\Delta G^\ddagger = 13.9 \text{ kcal mol}^{-1}$

Scheme S1. Structures for which the transition states for their enantiomerization are studied. The experimentally determined rotational barriers are shown.

Figure S1 shows the DFT optimized structures of the transition states of the enantiomerization of these structures. We can see that the DFT-computed rotational barriers are in very good agreement with the experimentally obtained barriers; the computed barriers for structures **2a**, **2z**, and **5** are $27.9 \text{ kcal mol}^{-1}$, $28.0 \text{ kcal mol}^{-1}$ and $28.9 \text{ kcal mol}^{-1}$, respectively, which are within 1 kcal mol^{-1} of the experimentally determined barriers (Scheme S1).

Structure	Reactant	TS for enantiomerization
2a	$\Delta G^\ddagger = 0.0 \text{ kcal mol}^{-1}$	$\Delta G^\ddagger = 27.9 \text{ kcal mol}^{-1}$
2z	$\Delta G^\ddagger = 0.0 \text{ kcal mol}^{-1}$	$\Delta G^\ddagger = 28.0 \text{ kcal mol}^{-1}$

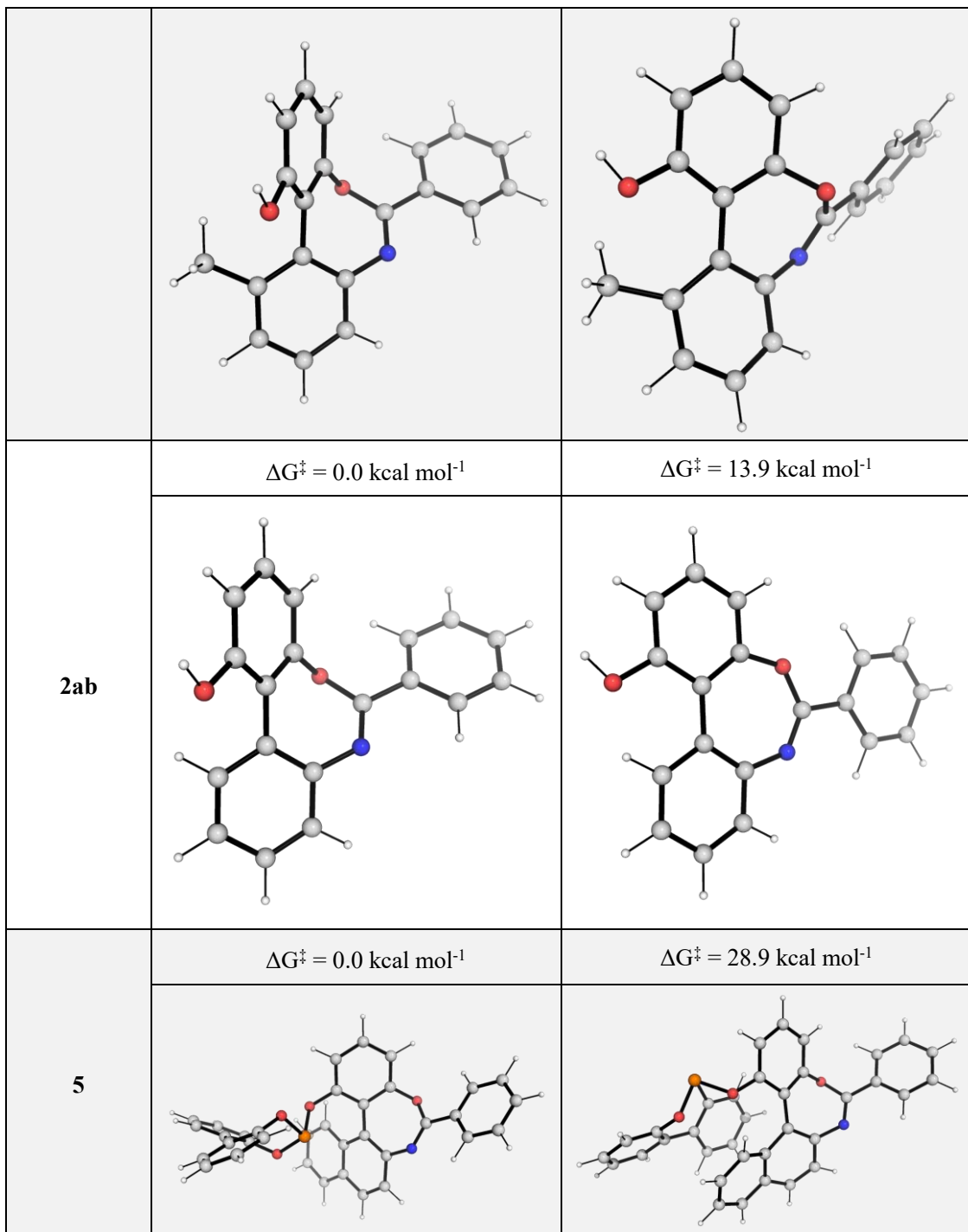


Figure S1. DFT-optimized transition state structures for the enantiomerization of various structures.

Computed rotational barriers are taken relative to each structure as the “reactant”. Rotational barriers are calculated at SMD(toluen)-M06-2X/def2-TZVP//M06-2X/def2-SVP level of theory at 70°C and are given in kcal mol^{-1} .

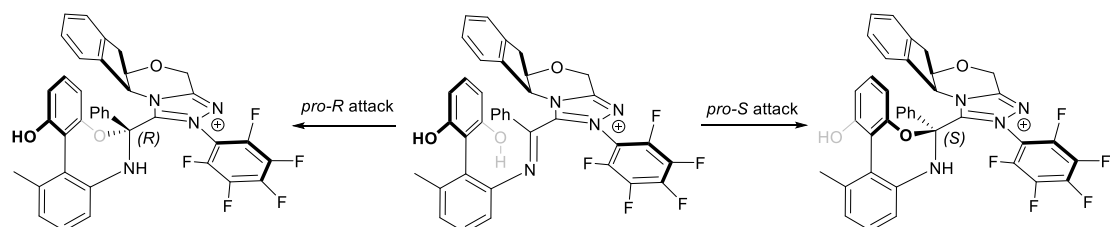
Structure **2ab** is computed to have a rotational barrier of $13.9 \text{ kcal mol}^{-1}$. This translates to a half-life of 1.8 millisecond (*ms*) at room temperature, and for example, 28.5s at -60°C and 15 minutes at -80 °C using simple transition state theory for estimation. Thus,

structure **2ab** is expected to enantiomerize rapidly and no enantiomeric excess (ee) can be observed at the reaction condition.

From these studies, we see that the *ortho*-substituent on the phenyl ring is essential in preventing easy enantiomerization by offering steric hinderance to rotation along the axis such that distinct enantiomers can exist at the reaction conditions/temperature (structures **2a**, **2z** and **5** in Scheme S1), whereas the lack of the substituent at this position (structure **2ab**) allows for free rotation along the axial axis, making the enantiomerization easy to occur and the product non-resolvable (Scheme S1).

Enantioselectivity determining transition state

To study the origin of the experimentally observed enantioselectivity, we focused on the enantio-determining step, which is the attack of the imine carbon atom in the azolium intermediate by the two different hydroxyl groups (Scheme S2).



Scheme S2. Schematic representations of the enantio-determining step arising from the attack of the imine carbon by different hydroxyl ($-\text{OH}$) groups.

The lowest energy conformer for the azolium intermediate was found via GFN2-xTB CREST conformational sampling followed by DFT optimization of the 10 lowest energy conformers and taking the lowest energy structure on the DFT potential energy surface (PES). We tried to locate the TSs for these C–O bond formation event, however, to no success. The relaxed PES scan along the bond forming C–O distance suggest that there may not be any TSs for the C–O bond formation for this azolium intermediate, as the PES scan plots in Figure S2 shows that the C–O covalently bonded structures formed via this intermediate would be very thermodynamically uphill ($\sim 60\text{--}80$ kcal mol $^{-1}$).

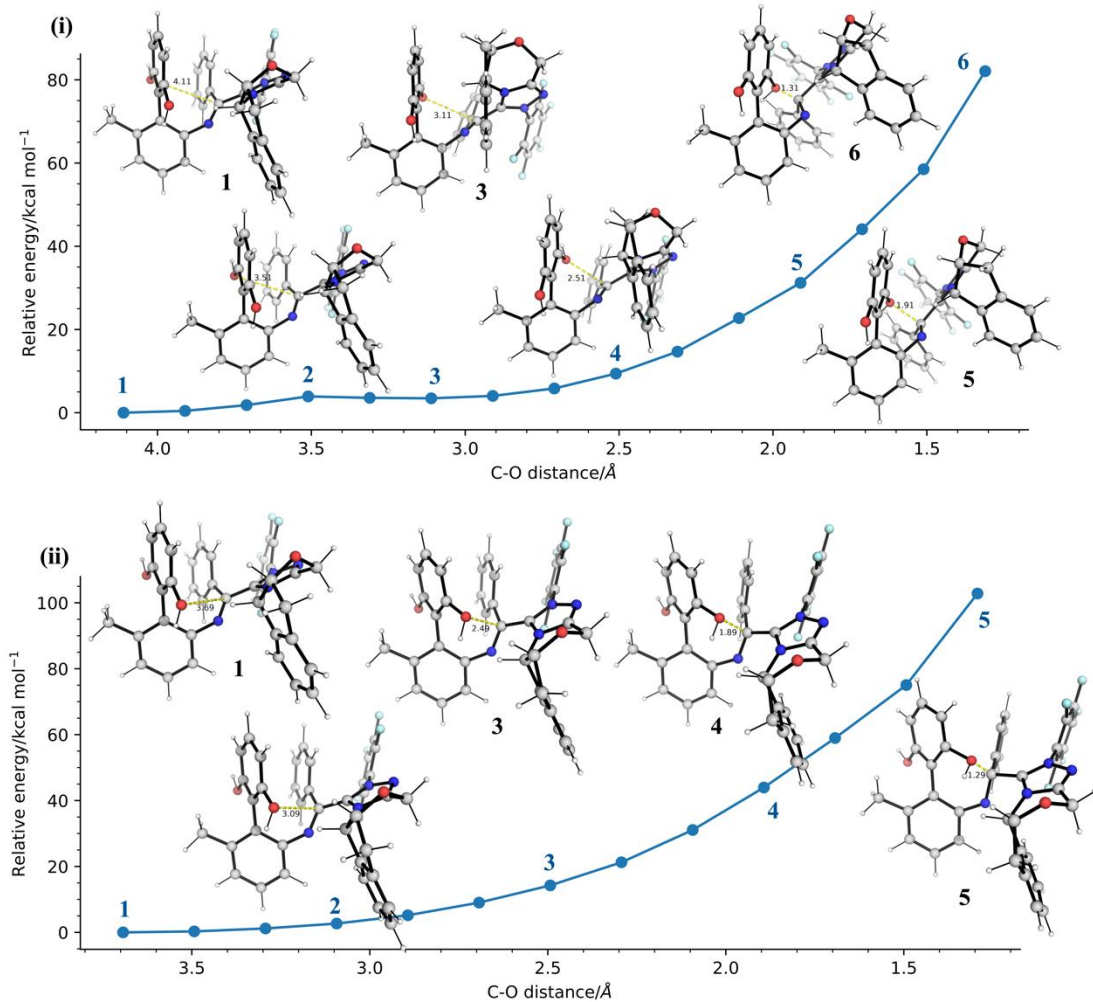
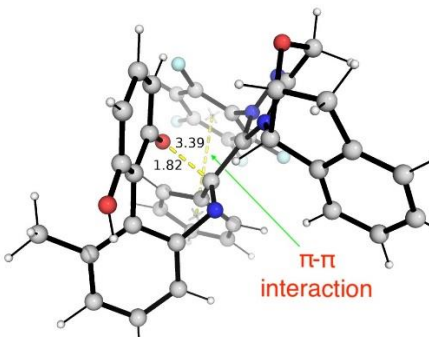
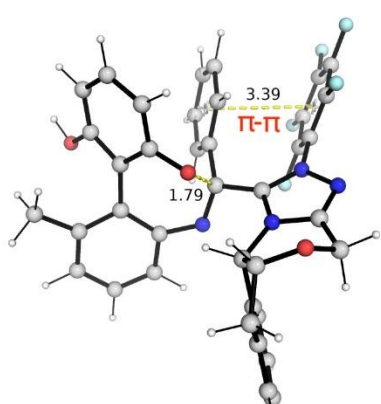
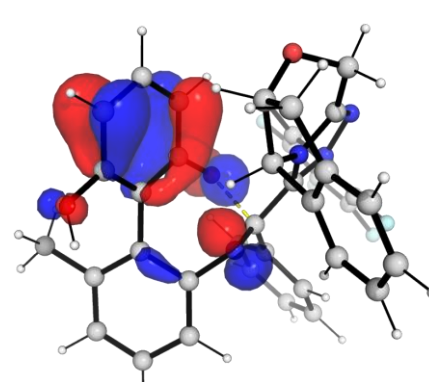
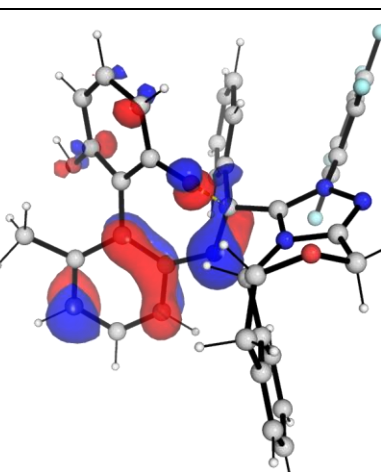


Figure S2. Relaxed potential energy surface (PES) scan for the C–O bond formation for (i) *pro-R* attack and (ii) *pro-S* attack computed at M06-2X/def2-SVP level of theory. Energies are taken relative to the lowest energy conformer from CREST+DFT optimization (structures at point **1**) and their units are given in kcal mol⁻¹. Note that both attacks result from the attack of the (*Si*)-face of the imine.

We hypothesized that the phenol OH groups may be *reversibly* deprotonated by the base present in the reaction and since we are interested in the *relative* barrier difference between the two enantiogenic reaction pathways, we considered instead the TSs for which the deprotonated phenoxide attacks the imine C=N carbon. The TSs for these two pathways leading to different enantiomeric outcomes are shown in Figure S3.

From the frontier molecular orbitals (FMOs) analysis (HOMOs and LUMOs) in Figure S3, we can see that there is productive overlap between the HOMO and the LUMO in **TS-major**, as we can see that in this TS structure, as the C–O σ bond is formed, the

HOMO shows $\sigma_{\text{C}-\text{O}}$ orbital and the LUMO shows $\sigma^*_{\text{C}-\text{O}}$ orbital. On the other hand, there is no such productive orbital overlap in **TS-minor**; in fact, the HOMO shows $\sigma^*_{\text{C}-\text{O}}$ anti-bonding characteristics not favorable for C–O σ bond formation. The non-covalent interaction (NCI) plots show that both TS structures benefit from $\pi-\pi$ interactions between the aryl rings, although it is hard to quantify numerically which is more favorable from the NCI plots alone.

	TS-major	TS-minor
$\Delta\Delta G^\ddagger$	0.0 kcal mol ⁻¹	8.3 kcal mol ⁻¹
DFT structure	 <p>3.39 1.82 $\pi-\pi$ interaction</p>	 <p>3.39 1.79 $\pi-\pi$</p>
HOMO		

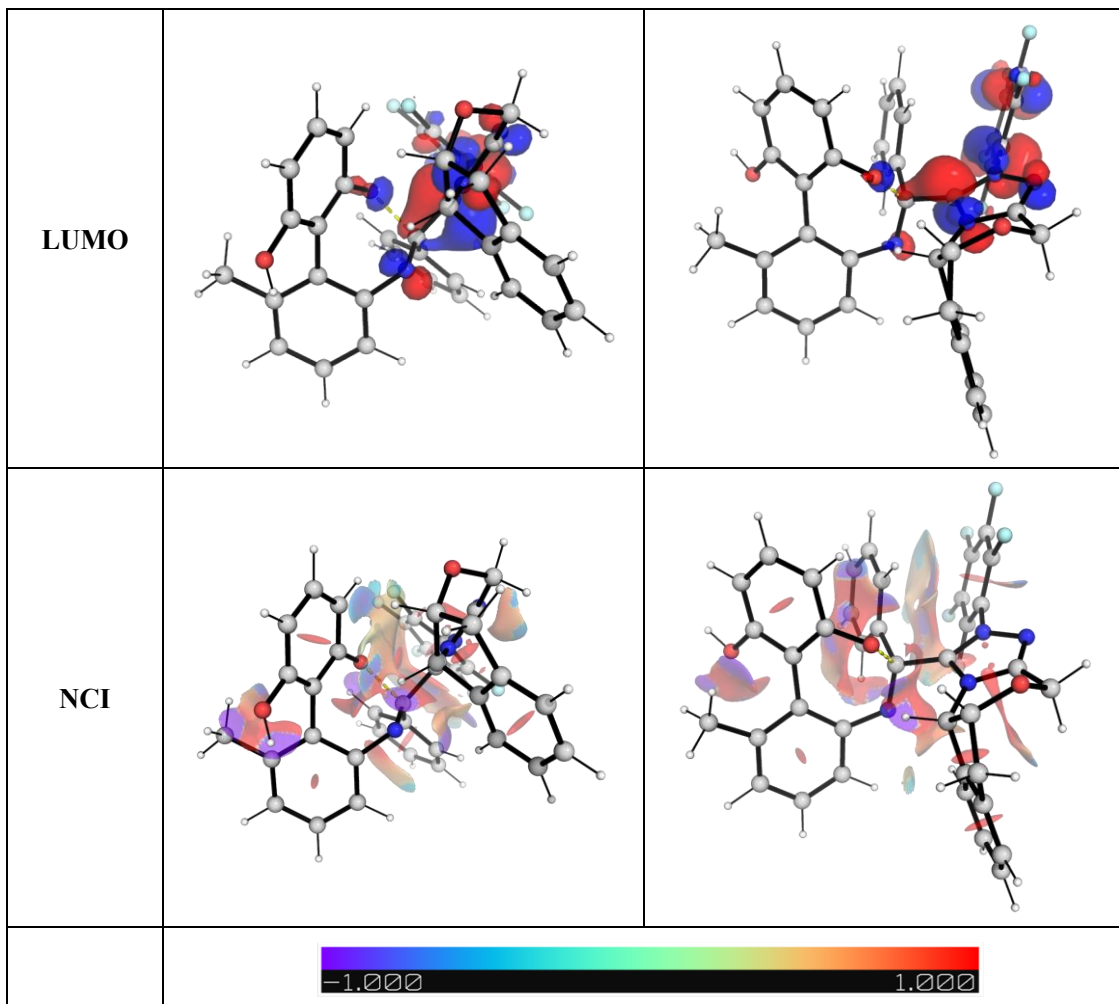


Figure S3. DFT-optimized TS structures, their HOMOs and LUMOs (isosurface value = 0.05 au) and non-covalent interaction (NCI) plots. Key bond distances are given in Å. Relative activation barriers ($\Delta\Delta G^\ddagger$) are given in kcal mol⁻¹.

To gain further insights into the origins for the enantioselectivity, we performed a distortion-interaction^{20,21}/activation strain (DI-AS) model²¹⁻²⁵ analysis. The DI-AS model is applied to these key TSs. Geometries are taken from along the IRC reaction coordinate at every 3 points interval and single point gas-phase calculations were performed at M06-2x/def2-TZVP level of theory to obtain DI-AS profiles shown in Figure S4. From the plot, we can see that the distortions are similar and indeed the interactions, e.g., arising from productive orbital overlaps, are more favorable in **TS-major**, in agreement with the qualitative FMO analysis outlined above.

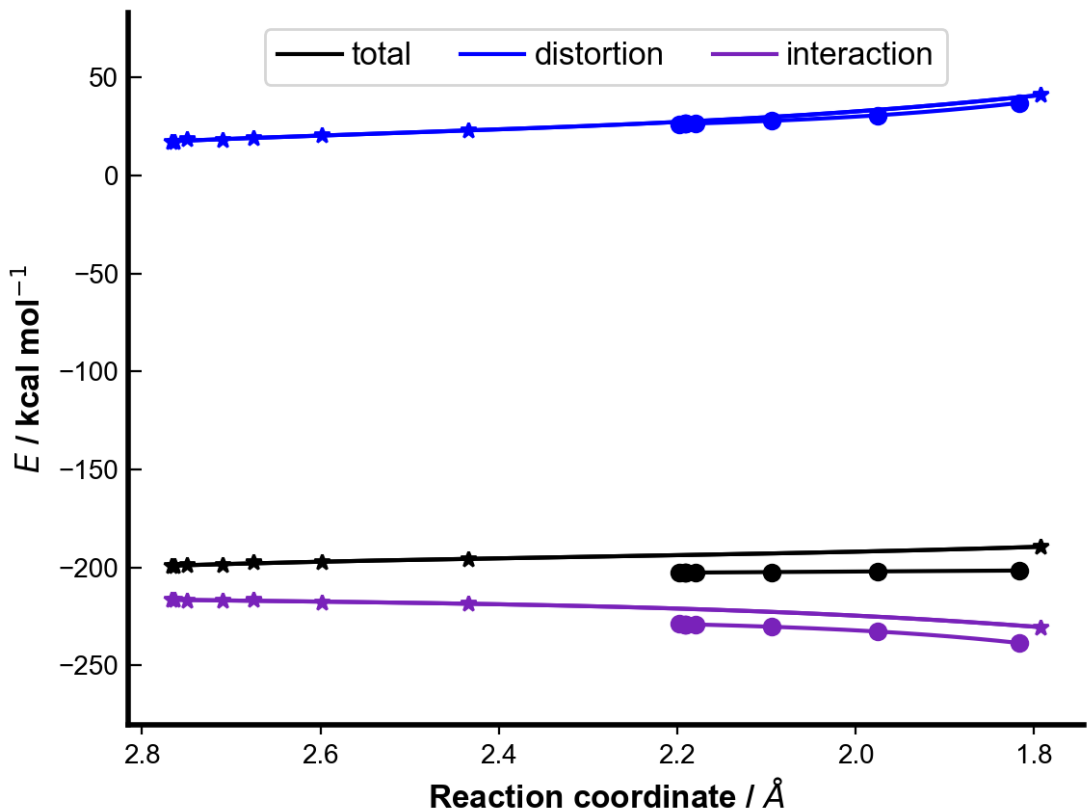


Figure S4. The activation strain or distortion-interaction analyses applied to the IRC paths along the enantio-determining transition states for the major product formation, **TS_major** (in full circle markers) and for the minor product formation, **TS_minor** (in star markers). All energies are calculated at M06-2X/def2TZVPP in gas-phase and used without any further corrections.

Optimized structures and absolute energies, zero-point energies

Geometries of **all optimized structures** (in .xyz format with their associated energy in Hartrees) and **movies of relevant IRC analyses** are included in a separate folder named *DFT_xyz_structures* with an associated readme.txt file. All these data have been uploaded to zenodo.org (DOI: [10.5281/zenodo.6789750](https://doi.org/10.5281/zenodo.6789750)).

Absolute values (in Hartrees) for SCF energy, zero-point vibrational energy (ZPE), enthalpy and quasi-harmonic Gibbs free energy for M06-2X/def2-SVP optimized conformers and single point corrections in SMD(chloroform) and SMD(toluene) using M06-2X/def2-TZVP functional are also included.

Reaction in chloroform at room temperature

SP

SMD(chlorof

Structures	E/au	ZPE/au	H/au	T.S/au	qh-G/au	orm) M06-	2X/def2TZV
------------	------	--------	------	--------	---------	-----------	------------

P

azolium_interm

ediate	-2404.632404	0.576779	-2404.0145	0.112084	-2404.124898	-2407.410891
--------	--------------	----------	------------	----------	--------------	--------------

azolium_interm

ediate_c2	-2404.632404	0.576779	-2404.0145	0.112073	-2404.124893	-2407.410895
-----------	--------------	----------	------------	----------	--------------	--------------

azolium_interm

ediate_c3	-2404.631826	0.576909	-2404.0139	0.110037	-2404.123171	-2407.41172
-----------	--------------	----------	------------	----------	--------------	-------------

azolium_interm

ediate_c4	-2404.627097	0.576836	-2404.0091	0.111341	-2404.119286	-2407.40892
-----------	--------------	----------	------------	----------	--------------	-------------

azolium_interm

ediate_c5	-2404.627097	0.576839	-2404.0091	0.111334	-2404.119279	-2407.408921
-----------	--------------	----------	------------	----------	--------------	--------------

azolium_interm

ediate_c6	-2404.627097	0.576839	-2404.0091	0.111334	-2404.119279	-2407.40892
-----------	--------------	----------	------------	----------	--------------	-------------

azolium_interm

ediate_c7	-2404.627097	0.576839	-2404.0091	0.111334	-2404.119279	-2407.40892
-----------	--------------	----------	------------	----------	--------------	-------------

azolium_interm

ediate_c8	-2404.628587	0.576936	-2404.0105	0.111493	-2404.120662	-2407.407794
-----------	--------------	----------	------------	----------	--------------	--------------

	-2404.626571	0.576685	-2404.0088	0.110973	-2404.118611	-2407.407717
--	--------------	----------	------------	----------	--------------	--------------

azolium_interm

ediate_c9**azolium_interm**

ediate_c10	-2404.630864	0.577324	-2404.0126	0.11033	-2404.121951	-2407.408342
-------------------	--------------	----------	------------	---------	--------------	--------------

TS_major	-2404.190044	0.564275	-2403.5864	0.106169	-2403.692056	-2406.923720
-----------------	--------------	----------	------------	----------	--------------	--------------

TS_minor	-2404.168133	0.563523	-2403.5652	0.106584	-2403.670891	-2406.909806
-----------------	--------------	----------	------------	----------	--------------	--------------

Rotational barriers in toluene at 70°C temperature**SP****SMD(toluen)**

Structures	E/au	ZPE/au	H/au	T.S/au	qh-G/au) M06-
-------------------	-------------	---------------	-------------	---------------	----------------	---------------

2X/def2TZV**P**

structure_2z_c1	-975.257279	0.303297	-974.93005	0.075448	-975.00527	-976.351019
------------------------	-------------	----------	------------	----------	------------	-------------

structure_2z_c2	-975.252813	0.302787	-974.92591	0.075746	-975.001403	-976.348351
------------------------	-------------	----------	------------	----------	-------------	-------------

TS_2z	-975.209407	0.302432	-974.88387	0.073406	-974.956819	-976.304921
--------------	-------------	----------	------------	----------	-------------	-------------

structure_2ab_c

1	-935.992428	0.275517	-935.69495	0.071469	-935.766135	-937.043127
----------	-------------	----------	------------	----------	-------------	-------------

structure_2ab_c

2	-935.988846	0.275186	-935.69156	0.071782	-935.763047	-937.040873
----------	-------------	----------	------------	----------	-------------	-------------

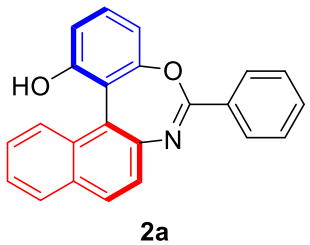
TS_2ab	-935.967993	0.27453	-935.67174	0.072578	-935.743107	-937.01781
---------------	-------------	---------	------------	----------	-------------	------------

structure_2a_c1	-1089.462521	0.322975	-1089.1141	0.078707	-1089.192478	-1090.679728
------------------------	--------------	----------	------------	----------	--------------	--------------

structure_2a_c2	-1089.456658	0.322525	-1089.1085	0.079073	-1089.187254	-1090.675833
------------------------	--------------	----------	------------	----------	--------------	--------------

TS_2a	-1089.414947	0.322051	-1089.0681	0.077147	-1089.144865	-1090.632020
structure_5	-2042.009443	0.485312	-2041.4835	0.115706	-2041.596027	-2044.043655
structure_5_c2	-2042.009443	0.485311	-2041.4835	0.115704	-2041.596027	-2044.043655
structure_5_c3	-2042.009443	0.485312	-2041.4835	0.115699	-2041.596024	-2044.043656
structure_5_c4	-2042.011153	0.485274	-2041.4853	0.114743	-2041.597321	-2044.044057
structure_5_c5	-2042.011153	0.485274	-2041.4853	0.114743	-2041.597321	-2044.044057
structure_5_c6	-2042.011397	0.485264	-2041.4856	0.11382	-2041.5971	-2044.043975
structure_5_c7	-2042.01202	0.485083	-2041.4863	0.115084	-2041.598361	-2044.042934
structure_5_c8	-2042.012341	0.485234	-2041.4866	0.112541	-2041.597339	-2044.041603
structure_5_c9	-2042.012341	0.485233	-2041.4866	0.11254	-2041.597338	-2044.041602
structure_5_c10	-2042.012341	0.485233	-2041.4866	0.112538	-2041.597339	-2044.041600
TS_5	-2041.972592	0.484544	-2041.4485	0.109402	-2041.556388	-2044.000321

Characterization data of the products



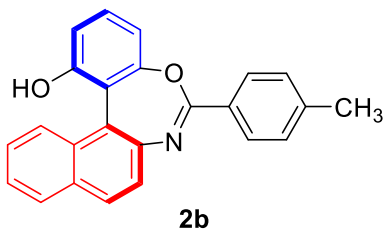
(S)-6-phenylbenzo[f]naphtho[2,1-d][1,3]oxazepin-1-ol (2a): yellow solid, 26.9 mg, 80% yield

¹H NMR (400 MHz, CDCl₃) δ 8.43 – 8.27 (m, 2H), 7.93 (d, *J* = 8.4 Hz, 2H), 7.81 (d, *J* = 8.4 Hz, 1H), 7.66 – 7.41 (m, 6H), 7.33 (t, *J* = 8.2 Hz, 1H), 7.03 – 6.84 (m, 2H), 5.03 (s, 1H);

¹³C NMR (101 MHz, CDCl₃) δ 159.6, 158.6, 154.1, 144.1, 132.0, 131.9, 131.7, 130.4, 129.4, 129.3, 129.2, 128.9, 128.6, 127.4, 126.2, 125.9, 125.8, 122.7, 116.1, 113.7, 113.1; **IR v_{max}** (film, cm⁻¹): 1608.6, 1504.5, 1269.2, 1170.8, 1004.9, 779.2; **[α]_D²⁵** = +98.0 (c = 1.0, CHCl₃);

HRMS (ESI, m/z): calcd. for [M+H]⁺: 338.1181, found: 338.1187;

HPLC analysis: 98% ee, (CHIRALCEL IA column, *n*-hexane/*i*-PrOH = 90/10, flow rate = 1.0 mL/min, λ = 254 nm, t_{major} = 11.3 min, t_{minor} = 18.0 min).



(S)-6-(*p*-tolyl)benzo[f]naphtho[2,1-d][1,3]oxazepin-1-ol (2b): yellow solid, 28.4 mg, 81% yield

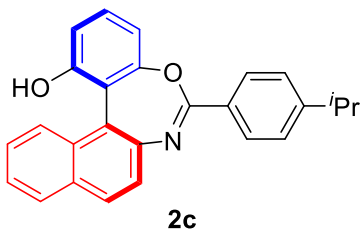
¹H NMR (400 MHz, CDCl₃) δ 8.23 (d, *J* = 8.2 Hz, 2H), 7.91 (d, *J* = 8.6 Hz, 2H), 7.79 (d, *J* = 8.3 Hz, 1H), 7.66 – 7.41 (m, 3H), 7.34 – 7.28 (m, 3H), 6.94 – 6.89 (m, 2H), 5.05 (s, 1H), 2.43 (s, 3H);

¹³C NMR (101 MHz, CDCl₃) δ 159.6, 158.8, 154.1, 144.2, 142.6, 131.6, 130.2, 129.4, 129.3, 129.2 (2C), 129.1, 128.8, 127.3, 126.2, 125.8, 125.7, 122.5, 116.1, 113.6, 113.1, 21.6;

IR v_{max} (film, cm⁻¹): 1607.3, 1478.5, 1264.5, 1173.8, 1103.2, 765.4; **[α]_D²⁵** = +51.9 (c = 1.0, CHCl₃);

HRMS (ESI, m/z): calcd. for [M+Na]⁺: 374.1157, found: 374.1158;

HPLC analysis: 98% ee, (CHIRALCEL IA column, *n*-hexane/*i*-PrOH = 90/10, flow rate = 1.0 mL/min, λ = 254 nm, t_{major} = 15.6 min, t_{minor} = 23.0 min).



(S)-6-(4-isopropylphenyl)benzo[f]naphtho[2,1-d][1,3]oxazepin-1-ol (2c): yellow oil, 31.0 mg, 82% yield

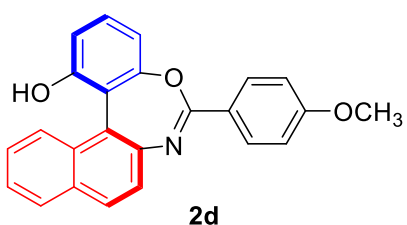
¹H NMR (400 MHz, CDCl₃) δ 8.27 (d, *J* = 8.3 Hz, 2H), 7.92 (d, *J* = 8.5 Hz, 2H), 7.80 (d, *J* = 8.4 Hz, 1H), 7.64 – 7.43 (m, 3H), 7.41 – 7.26 (m, 3H), 7.06 – 6.77 (m, 2H), 5.05 (s, 1H), 3.06 – 2.88 (m, 1H), 1.29 (d, *J* = 6.9 Hz, 6H);

¹³C NMR (101 MHz, CDCl₃) δ 159.6, 158.7, 154.0, 153.4, 144.2, 131.6, 130.2, 129.4 (2C), 129.3, 129.2, 128.8, 127.3, 126.7, 126.2, 125.8, 125.7, 122.5, 116.1, 113.6, 113.1, 34.2, 23.8, 23.7;

IR v_{max} (film, cm⁻¹): 1598.3, 1532.6, 1218.2, 1143.6, 1024.3, 768.2; [α]_D²⁵ = +47.6 (c = 1.0, CHCl₃);

HRMS (ESI, m/z): calcd. for [M+Na]⁺: 402.1470, found: 402.1475;

HPLC analysis: 99% ee, (CHIRALCEL IA column, *n*-hexane/*i*-PrOH = 80/20, flow rate = 0.6 mL/min, λ = 254 nm, t_{major} = 13.8 min, t_{minor} = 16.4 min).



(S)-6-(4-methoxyphenyl)benzo[f]naphtho[2,1-d][1,3]oxazepin-1-ol (2d): yellow oil, 22.0 mg, 60% yield

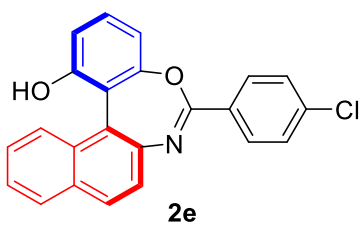
¹H NMR (400 MHz, CDCl₃) δ 8.29 (d, *J* = 9.0 Hz, 2H), 7.92 (d, *J* = 8.4 Hz, 2H), 7.79 (d, *J* = 8.4 Hz, 1H), 7.62 – 7.47 (m, 3H), 7.33 (t, *J* = 8.2 Hz, 1H), 6.99 (d, *J* = 9.0 Hz, 2H), 6.94 – 6.90 (m, 2H), 5.03 (s, 1H), 3.88 (s, 3H);

¹³C NMR (101 MHz, CDCl₃) δ 162.8, 159.6, 158.6, 154.1, 144.4, 131.5, 131.2 (2C), 130.2, 129.2, 128.8, 127.3, 126.2, 125.7, 125.6, 124.3, 122.3, 116.1, 113.9, 113.6, 113.0, 55.4;

IR v_{max} (film, cm⁻¹): 1636.3, 1508.6, 1245.3, 1150.2, 1076.8, 765.2; [α]_D²⁵ = +35.8 (c = 1.0, CHCl₃);

HRMS (ESI, m/z): calcd. for [M+Na]⁺: 390.1106, found: 390.1101;

HPLC analysis: 98% ee, (CHIRALCEL IA column, *n*-hexane/*i*-PrOH = 90/10, flow rate = 1.0 mL/min, λ = 254 nm, t_{minor} = 24.4 min, t_{major} = 27.8 min).



(S)-6-(4-chlorophenyl)benzo[f]naphtho[2,1-d][1,3]oxazepin-1-ol (2e): yellow solid, 26.7 mg, 72% yield

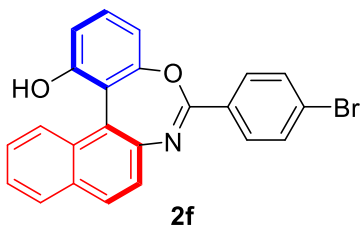
¹H NMR (400 MHz, CDCl₃) δ 8.26 (d, *J* = 8.7 Hz, 2H), 7.92 (d, *J* = 8.6 Hz, 2H), 7.79 (d, *J* = 8.3 Hz, 1H), 7.64 – 7.49 (m, 3H), 7.46 (d, *J* = 8.7 Hz, 2H), 7.34 (t, *J* = 8.2 Hz, 1H), 6.98 – 6.83 (m, 2H), 5.04 (s, 1H);

¹³C NMR (101 MHz, CDCl₃) δ 159.4, 157.5, 154.1, 143.8, 138.3, 131.7, 130.5, 130.4 (2C), 129.4, 129.2, 128.9, 128.8, 127.4, 126.1, 126.0, 125.7, 122.7, 115.9, 113.8, 112.9;

IR v_{max} (film, cm⁻¹): 1634.3, 1527.5, 1245.2, 1156.3, 1023.6, 736.8; [α]_D²⁵ = +77.4 (c = 1.0, CHCl₃);

HRMS (ESI, m/z): calcd. for [M+Na]⁺: 394.0611, found: 394.0610;

HPLC analysis: 97% ee, (CHIRALCEL IA column, *n*-hexane/*i*-PrOH = 90/10, flow rate = 1.0 mL/min, λ = 254 nm, t_{major} = 13.8 min, t_{minor} = 15.3 min).



(S)-6-(4-bromophenyl)benzo[f]naphtho[2,1-d][1,3]oxazepin-1-ol (2f): yellow solid, 24.9 mg, 60% yield

¹H NMR (400 MHz, CDCl₃) δ 8.19 (d, *J* = 8.6 Hz, 2H), 7.93 (d, *J* = 8.6 Hz, 2H), 7.79 (d, *J* = 8.3 Hz, 1H), 7.70 – 7.47 (m, 5H), 7.34 (t, *J* = 8.2 Hz, 1H), 7.00 – 6.82 (m, 2H), 5.04 (s, 1H);

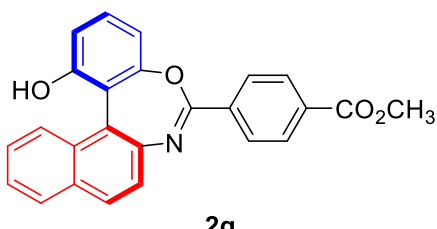
¹³C NMR (101 MHz, CDCl₃) δ 159.4, 157.7, 154.1, 143.7, 131.9, 131.7, 130.9, 130.7,

130.4 (2C), 129.4, 129.2, 128.8, 127.4, 126.9, 126.0, 125.8, 122.7, 115.9, 113.8, 112.9;

IR v_{max} (film, cm⁻¹): 1633.2, 1524.5, 1267.3, 1156.8, 1032.8, 765.2; [α]_D²⁵ = +72.9 (c = 1.0, CHCl₃);

HRMS (ESI, m/z): calcd. for [M+Na]⁺: 438.0106, found: 438.0094;

HPLC analysis: 97% ee, (CHIRALCEL AD-H column, *n*-hexane/*i*-PrOH = 90/10, flow rate = 1.0 mL/min, λ = 254 nm, t_{major} = 18.3 min, t_{minor} = 20.7 min).



methyl (S)-4-(1-hydroxybenzo[f]naphtho[2,1-d][1,3]oxazepin-6-yl)benzoate (2g): yellow solid, 30.8 mg, 78% yield

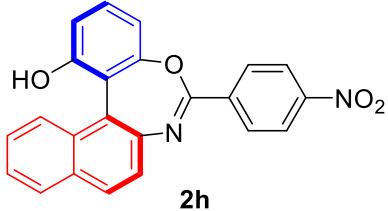
¹H NMR (400 MHz, CDCl₃) δ 8.39 (d, *J* = 8.6 Hz, 2H), 8.14 (d, *J* = 8.6 Hz, 2H), 7.93 (d, *J* = 9.0 Hz, 2H), 7.81 (d, *J* = 8.3 Hz, 1H), 7.63 – 7.46 (m, 3H), 7.35 (t, *J* = 8.2 Hz, 1H), 6.93 (d, *J* = 8.2 Hz, 2H), 5.12 (s, 1H), 3.94 (s, 3H);

¹³C NMR (101 MHz, CDCl₃) δ 166.4, 159.4, 157.5, 154.2, 143.6, 135.9, 132.8, 131.8, 130.4, 129.7, 129.4, 129.2, 129.1, 128.8, 127.4, 126.1, 126.0, 125.9, 122.9, 115.9, 113.9, 112.9, 52.3;

IR ν_{max} (film, cm^{-1}): 1683.6, 1589.6, 1267.3, 1168.9, 1023.8, 768.8; $[\alpha]_D^{25} = +74.9$ ($c = 1.0, \text{CHCl}_3$);

HRMS (ESI, m/z): calcd. for $[\text{M}+\text{Na}]^+$: 418.1055, found: 418.1049;

HPLC analysis: 98% ee, (CHIRALCEL AD-H column, *n*-hexane/*i*-PrOH = 90/10, flow rate = 1.0 mL/min, $\lambda = 254$ nm, $t_{\text{major}} = 20.3$ min, $t_{\text{minor}} = 28.1$ min).



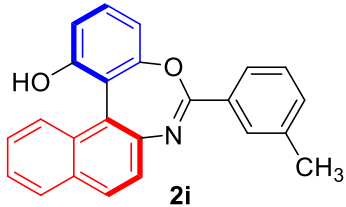
(S)-6-(4-nitrophenyl)benzo[f]naphtho[2,1-d][1,3]oxazepin-1-ol (2h): yellow solid, 28.6 mg, 75% yield

$^1\text{H NMR}$ (400 MHz, CDCl_3) δ 8.47 (d, $J = 9.0$ Hz, 2H), 8.31 (d, $J = 9.0$ Hz, 2H), 7.96 – 7.93 (m, 2H), 7.81 (d, $J = 8.3$ Hz, 1H), 7.65 – 7.48 (m, 3H), 7.37 (t, $J = 8.2$ Hz, 1H), 6.96 – 6.90 (m, 2H), 5.06 (s, 1H);

$^{13}\text{C NMR}$ (101 MHz, CDCl_3) δ 159.3, 156.2, 154.3, 149.7, 143.3, 137.6, 131.9, 130.6 (2C), 130.0, 129.5, 129.1, 128.8, 127.6, 126.4, 125.9, 123.7, 123.1, 115.7, 114.2, 112.7; **IR ν_{max}** (film, cm^{-1}): 1654.3, 1526.7, 1239.4, 1158.8, 1003.8, 778.6; $[\alpha]_D^{25} = +61.2$ ($c = 1.0, \text{CHCl}_3$);

HRMS (ESI, m/z): calcd. for $[\text{M}+\text{Na}]^+$: 405.0851, found: 405.0862;

HPLC analysis: 96% ee, (CHIRALCEL IA column, *n*-hexane/*i*-PrOH = 90/10, flow rate = 1.0 mL/min, $\lambda = 254$ nm, $t_{\text{minor}} = 22.2$ min, $t_{\text{major}} = 27.5$ min).



(S)-6-(*m*-tolyl)benzo[f]naphtho[2,1-d][1,3]oxazepin-1-ol (2i): yellow oil, 25.3 mg, 72% yield

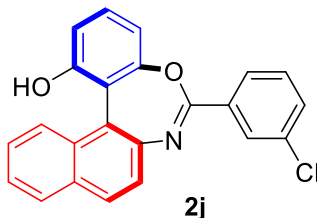
$^1\text{H NMR}$ (400 MHz, CDCl_3) δ 8.14 (d, $J = 6.7$ Hz, 2H), 7.93 (d, $J = 8.5$ Hz, 2H), 7.80 (d, $J = 8.4$ Hz, 1H), 7.65 – 7.46 (m, 3H), 7.41 – 7.31 (m, 3H), 7.00 – 6.85 (m, 2H), 5.04 (s, 1H), 2.45 (s, 3H);

$^{13}\text{C NMR}$ (101 MHz, CDCl_3) δ 159.5, 158.7, 154.1, 144.1, 138.3, 132.8, 131.7, 131.6, 130.3, 129.8, 129.3, 129.2, 128.8, 128.4, 127.4, 126.4, 126.1, 125.9, 125.8, 122.6, 116.0, 113.6, 113.1, 21.4;

IR ν_{max} (film, cm^{-1}): 1607.8, 1506.7, 1270.8, 1169.3, 1016.7, 768.3; $[\alpha]_D^{25} = +41.4$ ($c = 1.0, \text{CHCl}_3$);

HRMS (ESI, m/z): calcd. for $[\text{M}+\text{Na}]^+$: 374.1157, found: 374.1154;

HPLC analysis: 98% ee, (CHIRALCEL IA column, *n*-hexane/*i*-PrOH = 90/10, flow rate = 1.0 mL/min, $\lambda = 254$ nm, $t_{\text{major}} = 8.9$ min, $t_{\text{minor}} = 16.2$ min).



(S)-6-(3-chlorophenyl)benzo[f]naphtho[2,1-d][1,3]oxazepin-1-ol (2j): yellow oil, 23.7 mg, 64% yield

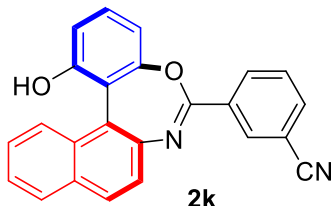
¹H NMR (400 MHz, CDCl₃) δ 8.31 (s, 1H), 8.21 (d, *J* = 7.8 Hz, 1H), 7.94 (d, *J* = 8.5 Hz, 2H), 7.80 (d, *J* = 8.3 Hz, 1H), 7.65 – 7.47 (m, 4H), 7.43 (t, *J* = 7.9 Hz, 1H), 7.35 (t, *J* = 8.2 Hz, 1H), 6.93 (dd, *J* = 8.1 Hz, 1.3 Hz, 2H), 5.02 (s, 1H);

¹³C NMR (101 MHz, CDCl₃) δ 159.4, 157.1, 154.1, 143.7, 134.7, 133.7, 131.9, 131.8, 130.4, 129.8, 129.4, 129.2, 129.1, 128.8, 127.5, 127.2, 126.1, 126.0, 125.8, 122.8, 115.8, 113.9, 112.9;

IR v_{max} (film, cm⁻¹): 1654.6, 1523.6, 1258.3, 1169.7, 1023.5, 732.6; [α]_D²⁵ = +55.6 (c = 1.0, CHCl₃);

HRMS (ESI, m/z): calcd. for [M+Na]⁺: 394.0611, found: 394.0615;

HPLC analysis: 98% ee, (CHIRALCEL IA column, *n*-hexane/*i*-PrOH = 90/10, flow rate = 1.0 mL/min, λ = 254 nm, t_{major} = 8.6 min, t_{minor} = 18.3 min).



(S)-3-(1-hydroxybenzo[f]naphtho[2,1-d][1,3]oxazepin-6-yl)benzonitrile (2k): yellow solid, 27.0 mg, 75% yield

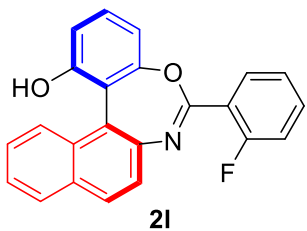
¹H NMR (400 MHz, ⁶d-acetone) δ 8.85 (br, 1H), 8.71 (s, 1H), 8.68 (d, *J* = 8.0 Hz, 1H), 8.07 – 7.92 (m, 3H), 7.89 – 7.87 (m, 1H), 7.80 (t, *J* = 7.8 Hz, 1H), 7.56 – 7.49 (m, 3H), 7.40 (t, *J* = 8.2 Hz, 1H), 7.13 (dd, *J* = 8.1 Hz, 0.8 Hz, 1H), 7.00 (dd, *J* = 8.2 Hz, 0.8 Hz, 1H);

¹³C NMR (101 MHz, ⁶d-acetone) δ 161.1, 157.2, 156.8, 143.3, 136.0, 134.1, 134.0, 133.1, 132.6, 131.9, 131.3, 131.0, 129.7, 128.9, 128.8, 126.7, 126.4, 126.3, 125.6, 118.7, 117.0, 114.7, 112.8;

IR v_{max} (film, cm⁻¹): 1632.7, 1523.6, 1254.3, 1168.5, 1026.7, 736.5; [α]_D²⁵ = +56.7 (c = 0.2, CHCl₃);

HRMS (ESI, m/z): calcd. for [M+Na]⁺: 385.0953, found: 385.0956;

HPLC analysis: 98% ee, (CHIRALCEL IA column, *n*-hexane/*i*-PrOH = 80/20, flow rate = 0.6 mL/min, λ = 254 nm, t_{major} = 14.5 min, t_{minor} = 23.0 min).



(S)-6-(2-fluorophenyl)benzo[f]naphtho[2,1-d][1,3]oxazepin-1-ol (2l): yellow oil, 18.7 mg, 53% yield

¹H NMR (400 MHz, CDCl₃) δ 8.22 (td, *J* = 7.8 Hz, 1.7 Hz, 1H), 7.94 (d, *J* = 8.5 Hz, 2H), 7.81 (d, *J* = 8.3 Hz, 1H), 7.68 – 7.45 (m, 4H), 7.34 (t, *J* = 8.2 Hz, 1H), 7.29 – 7.14 (m, 2H), 6.95 – 6.90 (m, 2H), 5.00 (s, 1H);

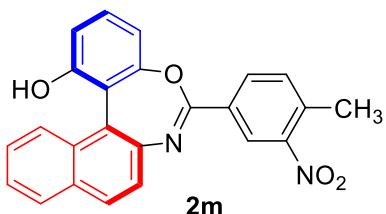
¹³C NMR (101 MHz, CDCl₃) δ 161.8 (d, *J* = 260.5 Hz), 159.8, 155.6 (d, *J* = 6.3 Hz), 154.0, 143.8, 133.3 (d, *J* = 8.9 Hz), 132.1, 131.8, 130.3, 129.3, 129.1, 128.8, 127.4, 126.1 (d, *J* = 10.3 Hz), 125.8, 124.0 (d, *J* = 3.9 Hz), 122.7, 120.4 (d, *J* = 8.6 Hz), 117.3, 117.1, 115.9, 113.9, 113.2 (d, *J* = 1.8 Hz);

¹⁹F NMR (377 MHz, CDCl₃) δ -107.6 (s, 1F);

IR v_{max} (film, cm⁻¹): 1653.8, 1524.6, 1238.4, 1168.7, 1054.3, 739.6; [α]_D²⁵ = -70.9 (c = 1.0, CHCl₃);

HRMS (ESI, m/z): calcd. for [M+Na]⁺: 378.0906, found: 378.0910;

HPLC analysis: 97% ee, (CHIRALCEL IA column, *n*-hexane/*i*-PrOH = 90/10, flow rate = 1.0 mL/min, λ = 254 nm, t_{major} = 10.3 min, t_{minor} = 19.7 min).



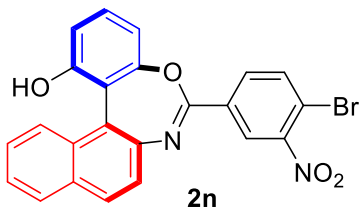
(S)-6-(4-methyl-3-nitrophenyl)benzo[f]naphtho[2,1-d][1,3]oxazepin-1-ol (2m): yellow solid, 28.5 mg, 72% yield

¹H NMR (400 MHz, CDCl₃) δ 8.89 (d, *J* = 1.6 Hz, 1H), 8.41 (dd, *J* = 8.0 Hz, 1.7 Hz, 1H), 7.93 (d, *J* = 8.4 Hz, 2H), 7.80 (d, *J* = 8.3 Hz, 1H), 7.63 – 7.50 (m, 3H), 7.45 (d, *J* = 8.1 Hz, 1H), 7.37 (t, *J* = 8.2 Hz, 1H), 7.03 – 6.82 (m, 2H), 5.05 (s, 1H), 2.67 (s, 3H); **¹³C NMR** (101 MHz, CDCl₃) δ 159.3, 156.1, 154.2, 149.4, 143.4, 137.1, 133.1, 132.9, 131.8, 131.4, 130.5, 129.5, 129.1, 128.8, 127.5, 126.2, 125.9, 125.8, 125.2, 122.9, 115.7, 114.0, 112.8, 20.5;

IR v_{max} (film, cm⁻¹): 1645.3, 1523.7, 1256.2, 1160.9, 1043.8, 756.2; [α]_D²⁵ = +96.2 (c = 1.0, CHCl₃);

HRMS (ESI, m/z): calcd. for [M+Na]⁺: 419.1008, found: 419.1005;

HPLC analysis: 98% ee, (CHIRALCEL IA column, *n*-hexane/*i*-PrOH = 80/20, flow rate = 0.6 mL/min, λ = 254 nm, t_{major} = 15.3 min, t_{minor} = 24.8 min).



(S)-6-(4-bromo-3-nitrophenyl)benzo[f]naphtho[2,1-d][1,3]oxazepin-1-ol (2n): yellow solid, 29.0 mg, 63% yield

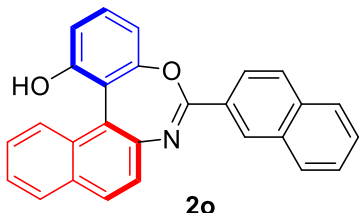
¹H NMR (400 MHz, CDCl₃) δ 8.75 (d, *J* = 2.0 Hz, 1H), 8.34 (dd, *J* = 8.4 Hz, 2.1 Hz, 1H), 7.96 (d, *J* = 8.7 Hz, 2H), 7.86 (d, *J* = 8.4 Hz, 1H), 7.80 (d, *J* = 8.2 Hz, 1H), 7.65 – 7.50 (m, 3H), 7.38 (t, *J* = 8.2 Hz, 1H), 6.96 (dd, *J* = 8.2 Hz, 0.9 Hz, 1H), 6.89 (dd, *J* = 8.1 Hz, 0.9 Hz, 1H), 5.03 (s, 1H);

¹³C NMR (101 MHz, CDCl₃) δ 159.1, 155.2, 154.3, 150.1, 143.1, 135.4, 132.9, 132.8, 131.9, 130.7, 129.6, 129.1, 128.9, 127.7, 126.4, 125.9, 125.8 (2C), 123.0, 118.0, 115.6, 114.3, 112.7;

IR v_{max} (film, cm⁻¹): 1658.7, 1543.6, 1238.7, 1159.6, 1054.3, 719.8; [α]_D²⁵ = +71.3 (c = 1.0, CHCl₃);

HRMS (ESI, m/z): calcd. for [M+Na]⁺: 482.9956, found: 482.9962;

HPLC analysis: 97% ee, (CHIRALCEL IA column, *n*-hexane/*i*-PrOH = 90/10, flow rate = 1.0 mL/min, λ = 254 nm, t_{major} = 28.1 min, t_{minor} = 32.4 min).



(S)-6-(naphthalen-2-yl)benzo[f]naphtho[2,1-d][1,3]oxazepin-1-ol (2o): yellow solid, 24.0 mg, 63% yield

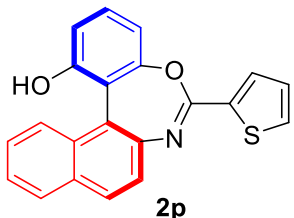
¹H NMR (400 MHz, CDCl₃) δ 8.87 (s, 1H), 8.38 (dd, *J* = 8.7 Hz, 1.7 Hz, 1H), 8.07 – 8.01 (m, 1H), 7.98 – 7.79 (m, 5H), 7.68 – 7.48 (m, 5H), 7.34 (t, *J* = 8.2 Hz, 1H), 7.03 (dd, *J* = 8.1 Hz, 0.9 Hz, 1H), 6.92 (dd, *J* = 8.2, 0.9 Hz, 1H), 5.03 (s, 1H);

¹³C NMR (101 MHz, CDCl₃) δ 159.5, 158.6, 154.1, 144.1, 135.1, 132.8, 131.7, 130.3, 130.0, 129.4, 129.3 (2C), 129.2, 128.8, 128.4, 128.0, 127.8, 127.4, 126.6, 126.2, 12.0, 125.8, 125.6, 122.6, 116.1, 113.7, 113.1;

IR v_{max} (film, cm⁻¹): 1645.8, 1523.7, 1219.4, 1158.9, 1032.7, 765.4; [α]_D²⁵ = +55.5 (c = 1.0, CHCl₃);

HRMS (ESI, m/z): calcd. for [M+Na]⁺: 410.1157, found: 410.1152;

HPLC analysis: 98% ee, (CHIRALCEL AD-H column, *n*-hexane/*i*-PrOH = 90/10, flow rate = 1.0 mL/min, λ = 254 nm, t_{major} = 19.3 min, t_{minor} = 26.6 min).



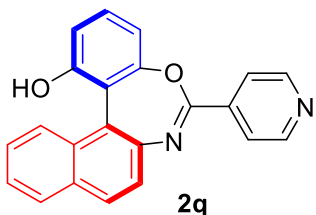
(S)-6-(thiophen-2-yl)benzo[f]naphtho[2,1-d][1,3]oxazepin-1-ol (2p): yellow oil, 18.4 mg, 54% yield

¹H NMR (400 MHz, CDCl₃) δ 8.01 – 7.88 (m, 3H), 7.79 (d, *J* = 8.3 Hz, 1H), 7.64 – 7.47 (m, 4H), 7.37 (t, *J* = 8.2 Hz, 1H), 7.15 (dd, *J* = 4.9 Hz, 3.8 Hz, 1H), 6.95 (t, *J* = 7.2 Hz, 2H), 5.01 (s, 1H);

¹³C NMR (101 MHz, CDCl₃) δ 159.5, 154.6, 154.1, 143.8, 136.8, 131.9, 131.8, 131.7, 130.4, 129.4, 129.3, 128.8, 128.0, 127.4, 126.1, 125.9, 125.7, 122.5, 115.8, 113.9, 113.0; **IR v_{max}** (film, cm⁻¹): 1638.6, 1524.5, 1276.2, 1145.8, 1094.7, 739.2; **[α]_D²⁵** = +98.8 (*c* = 1.0, CHCl₃);

HRMS (ESI, m/z): calcd. for [M+Na]⁺: 366.0565, found: 366.0569;

HPLC analysis: 98% ee, (CHIRALCEL IA column, *n*-hexane/*i*-PrOH = 90/10, flow rate = 1.0 mL/min, λ = 254 nm, t_{major} = 14.1 min, t_{minor} = 21.9 min).



(S)-6-(pyridin-4-yl)benzo[f]naphtho[2,1-d][1,3]oxazepin-1-ol (2q): yellow oil, 28.7 mg, 85% yield

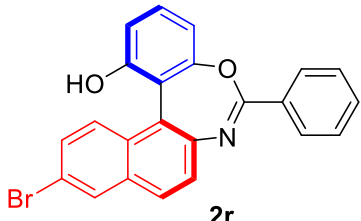
¹H NMR (400 MHz, CDCl₃) δ 8.61 (d, *J* = 6.0 Hz, 2H), 8.10 (d, *J* = 6.1 Hz, 2H), 7.90 – 7.85 (m, 3H), 7.63 – 7.46 (m, 3H), 7.35 (t, *J* = 8.2 Hz, 1H), 6.95 (d, *J* = 8.1 Hz, 1H), 6.89 (d, *J* = 8.1 Hz, 1H), 6.60 (br, 1H);

¹³C NMR (101 MHz, CDCl₃) δ 159.5, 156.2, 154.9, 149.9, 143.0, 139.6, 131.9, 130.4, 129.5, 129.4, 128.6, 127.2, 126.4, 126.2, 125.6, 123.9, 122.5, 115.9, 114.3, 112.5;

IR v_{max} (film, cm⁻¹): 1628.7, 1532.6, 1278.2, 1140.8, 1047.8, 739.5; **[α]_D²⁵** = +96.7 (*c* = 1.0, CHCl₃);

HRMS (ESI, m/z): calcd. for [M+Na]⁺: 361.0953, found: 361.0951;

HPLC analysis: 98% ee, (CHIRALCEL IC column, *n*-hexane/*i*-PrOH = 90/10, flow rate = 1.0 mL/min, λ = 254 nm, t_{minor} = 14.2 min, t_{major} = 16.7 min).



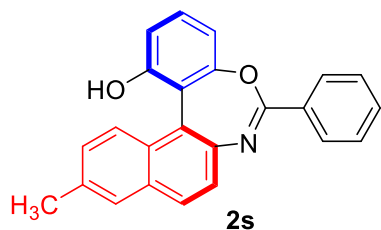
(S)-11-bromo-6-phenylbenzo[f]naphtho[2,1-d][1,3]oxazepin-1-ol (2r): yellow solid, 29.9 mg, 72% yield

¹H NMR (400 MHz, CDCl₃) δ 8.38 – 8.24 (m, 2H), 8.06 (d, *J* = 1.9 Hz, 1H), 7.81 (d, *J* = 8.7 Hz, 1H), 7.66 (d, *J* = 9.1 Hz, 1H), 7.61 – 7.46 (m, 5H), 7.33 (t, *J* = 8.2 Hz, 1H), 6.95 – 6.88 (m, 2H), 5.06 (s, 1H);

¹³C NMR (101 MHz, CDCl₃) δ 159.6, 158.8, 154.0, 144.2, 132.7, 132.1, 131.6, 130.6, 130.5, 130.3, 129.2, 128.6, 128.2, 128.1, 128.0, 127.2, 123.1, 119.9, 115.7, 113.8, 113.2; **IR v_{max}** (film, cm⁻¹): 1627.6, 1543.8, 1219.7, 1132.5, 1022.6, 745.9; [α]_D²⁵ = +52.4 (c = 0.2, CHCl₃);

HRMS (ESI, m/z): calcd. for [M+Na]⁺: 438.0106, found: 438.0117;

HPLC analysis: 98% ee, (CHIRALCEL IA column, *n*-hexane/*i*-PrOH = 90/10, flow rate = 0.5 mL/min, λ = 254 nm, t_{major} = 24.9 min, t_{minor} = 49.3 min).



(S)-11-methyl-6-phenylbenzo[f]naphtho[2,1-d][1,3]oxazepin-1-ol (2s): yellow oil, 28.1 mg, 80% yield

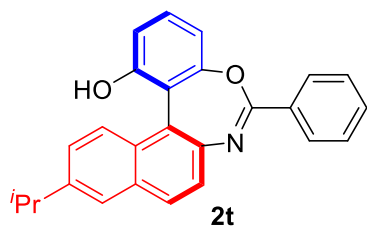
¹H NMR (400 MHz, CDCl₃) δ 8.39 – 8.25 (m, 2H), 7.82 (d, *J* = 8.7 Hz, 1H), 7.69 (d, *J* = 8.5 Hz, 2H), 7.60 – 7.43 (m, 4H), 7.39 (dd, *J* = 8.9 Hz, 1.5 Hz, 1H), 7.31 (t, *J* = 8.2 Hz, 1H), 6.94 – 6.88 (m, 2H), 5.09 (s, 1H), 2.52 (s, 3H);

¹³C NMR (101 MHz, CDCl₃) δ 159.4, 158.2, 154.1, 143.2, 135.7, 131.9, 131.8, 130.2,

129.5, 129.2, 128.7, 128.5, 127.9, 127.3, 126.1, 125.6, 122.5, 116.1, 113.6, 113.0, 21.4; **IR v_{max}** (film, cm⁻¹): 1635.7, 1523.4, 1259.3, 1145.2, 1053.1, 719.2; [α]_D²⁵ = +79.5 (c = 1.0, CHCl₃);

HRMS (ESI, m/z): calcd. for [M+Na]⁺: 374.1157, found: 374.1154;

HPLC analysis: 99% ee, (CHIRALCEL IA column, *n*-hexane/*i*-PrOH = 90/10, flow rate = 0.5 mL/min, λ = 254 nm, t_{major} = 24.3 min, t_{minor} = 49.0 min).



(S)-11-isopropyl-6-phenylbenzo[f]naphtho[2,1-d][1,3]oxazepin-1-ol (2t): yellow oil, 28.3 mg, 75% yield

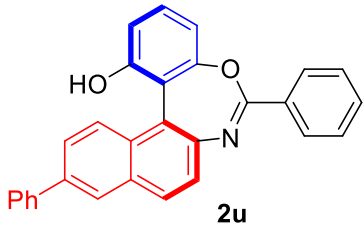
¹H NMR (400 MHz, CDCl₃) δ 8.40 – 8.27 (m, 2H), 7.88 (d, *J* = 8.6 Hz, 1H), 7.78 – 7.70 (m, 2H), 7.60 – 7.43 (m, 5H), 7.32 (t, *J* = 8.2 Hz, 1H), 6.94 – 6.89 (m, 2H), 5.07 (s, 1H), 3.17 – 3.01 (m, 1H), 1.36 (d, *J* = 1.8 Hz, 3H), 1.34 (d, *J* = 1.8 Hz, 3H);

¹³C NMR (101 MHz, CDCl₃) δ 159.4, 158.2, 154.1, 146.5, 143.3, 132.2, 131.9, 131.8, 130.2, 129.2, 129.0, 128.5, 127.7, 127.3, 126.1, 125.7, 125.2, 122.4, 116.1, 113.6, 113.0, 33.97, 23.9, 23.8;

IR v_{max} (film, cm⁻¹): 1635.6, 1523.5, 1226.2, 1135.1, 1023.5, 732.4; [α]_D²⁵ = +103.7 (c = 1.0, CHCl₃);

HRMS (ESI, m/z): calcd. for [M+Na]⁺: 402.1470, found: 402.1480;

HPLC analysis: 99% ee, (CHIRALCEL IA column, *n*-hexane/*i*-PrOH = 90/10, flow rate = 1.0 mL/min, λ = 254 nm, $t_{\text{major}} = 10.0$ min, $t_{\text{minor}} = 18.9$ min).



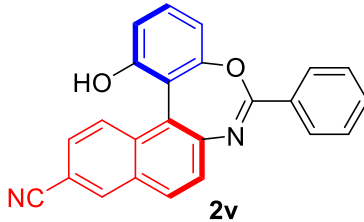
(S)-6,11-diphenylbenzo[f]naphtho[2,1-d][1,3]oxazepin-1-ol (2u): yellow solid, 26.3 mg, 64% yield

¹H NMR (400 MHz, CDCl₃) δ 8.40 – 8.27 (m, 2H), 8.13 (d, J = 1.5 Hz, 1H), 7.99 (d, J = 8.7 Hz, 1H), 7.89 – 7.82 (m, 2H), 7.78 – 7.69 (m, 2H), 7.62 (d, J = 8.7 Hz, 1H), 7.58 – 7.43 (m, 5H), 7.41 – 7.33 (m, 2H), 6.95 (td, J = 8.3 Hz, 0.9 Hz, 2H), 5.08 (s, 1H); **¹³C NMR** (101 MHz, CDCl₃) δ 159.5, 158.5, 154.1, 144.0, 140.4, 138.5, 132.0, 131.9, 131.8, 130.4, 129.5, 129.2, 128.9, 128.6, 128.4, 127.6, 127.3, 126.9, 126.6, 126.5, 126.4, 122.6, 116.0, 113.7, 113.1;

IR v_{max} (film, cm⁻¹): 1635.6, 1518.5, 1232.2, 1119.8, 1025.9, 736.2; $[\alpha]_D^{25} = +83.1$ ($c = 1.0$, CHCl₃);

HRMS (ESI, m/z): calcd. for [M+Na]⁺: 436.1313, found: 436.1319;

HPLC analysis: 99% ee, (CHIRALCEL IA column, *n*-hexane/*i*-PrOH = 90/10, flow rate = 0.5 mL/min, λ = 254 nm, $t_{\text{major}} = 31.5$ min, $t_{\text{minor}} = 71.0$ min).



(S)-1-hydroxy-6-phenylbenzo[f]naphtho[2,1-d][1,3]oxazepine-11-carbonitrile (2v): yellow solid, 19.5 mg, 54% yield

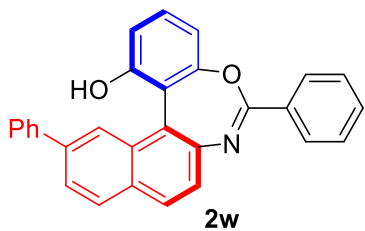
¹H NMR (400 MHz, ⁶d-acetone) δ 9.16 (s, 1H), 8.50 (d, J = 1.4 Hz, 1H), 8.46 – 8.36 (m, 2H), 8.14 (d, J = 8.7 Hz, 1H), 8.02 (d, J = 8.8 Hz, 1H), 7.79 – 7.51 (m, 5H), 7.43 (t, J = 8.2 Hz, 1H), 7.09 (d, J = 7.8 Hz, 1H), 7.02 (d, J = 8.2 Hz, 1H);

¹³C NMR (101 MHz, ⁶d-acetone) δ 160.3, 158.9, 156.0, 145.5, 133.9, 132.7, 132.4, 131.5, 130.8, 130.4, 129.6, 129.3, 129.1, 128.8, 126.8, 126.0, 125.6, 118.9, 115.6, 113.7, 112.2, 108.4;

IR v_{max} (film, cm⁻¹): 1658.6, 1574.6, 1276.2, 1123.5, 1038.2, 736.2; $[\alpha]_D^{25} = +56.7$ ($c = 0.1$, CHCl₃);

HRMS (ESI, m/z): calcd. for [M+Na]⁺: 385.0953, found: 385.0956;

HPLC analysis: 94% ee, (CHIRALCEL IA column, *n*-hexane/*i*-PrOH = 90/10, flow rate = 1.0 mL/min, λ = 254 nm, $t_{\text{major}} = 14.9$ min, $t_{\text{minor}} = 34.4$ min).



(S)-6,12-diphenylbenzo[f]naphtho[2,1-d][1,3]oxazepin-1-ol (2w): yellow solid, 33.0 mg, 80% yield

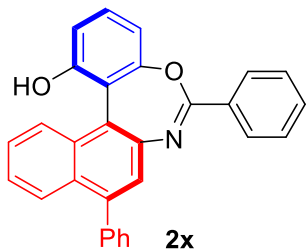
¹H NMR (400 MHz, CDCl₃) δ 8.35 – 8.33 (m, 2H), 7.98 – 7.91 (m, 3H), 7.75 (dd, *J* = 8.4 Hz, 1.7 Hz, 1H), 7.70 – 7.62 (m, 2H), 7.61 – 7.39 (m, 6H), 7.36 – 7.30 (m, 2H), 6.95 (d, *J* = 8.2 Hz, 2H); 5.16 (s, 1H);

¹³C NMR (101 MHz, CDCl₃) δ 159.5, 158.6, 154.2, 144.4, 140.9, 140.1, 131.9, 131.8, 130.7, 130.4, 129.5, 129.3, 129.2, 129.0, 128.9, 128.5, 127.5 (2C), 126.1, 125.6, 123.9, 122.9, 116.0, 113.8, 113.1;

IR v_{max} (film, cm⁻¹): 1635.7, 1556.2, 1236.1, 1128.9, 1032.4, 736.2; [α]_D²⁵ = +120.6 (c = 1.0, CHCl₃);

HRMS (ESI, m/z): calcd. for [M+Na]⁺: 436.1313, found: 436.1317;

HPLC analysis: 98% ee, (CHIRALCEL IA column, *n*-hexane/*i*-PrOH = 90/10, flow rate = 1.0 mL/min, λ = 254 nm, t_{major} = 16.9 min, t_{minor} = 45.6 min).



(S)-6,9-diphenylbenzo[f]naphtho[2,1-d][1,3]oxazepin-1-ol (2x): yellow oil, 31.0 mg, 75% yield

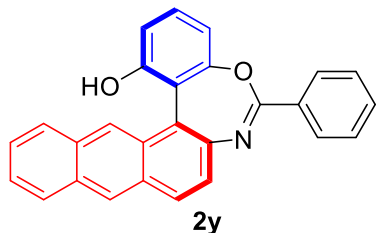
¹H NMR (400 MHz, CDCl₃) δ 8.39 – 8.28 (m, 2H), 7.99 (d, *J* = 8.4 Hz, 1H), 7.87 (d, *J* = 8.4 Hz, 1H), 7.62 – 7.41 (m, 11H), 7.34 (t, *J* = 8.2 Hz, 1H), 6.98 – 6.92 (m, 2H), 5.11 (s, 1H);

¹³C NMR (101 MHz, CDCl₃) δ 159.4, 158.7, 154.1, 143.4, 141.5, 139.7, 131.9, 131.8, 130.3, 130.1, 130.0, 129.7, 129.2, 128.5, 128.3, 127.6, 127.3, 127.1, 127.0, 126.1, 126.0, 122.1, 116.1, 113.7, 113.1;

IR v_{max} (film, cm⁻¹): 1628.6, 1514.5, 1239.1, 1130.1, 1024.6, 729.2; [α]_D²⁵ = +113.4 (c = 1.0, CHCl₃);

HRMS (ESI, m/z): calcd. for [M+Na]⁺: 436.1313, found: 436.1317;

HPLC analysis: 97% ee, (CHIRALCEL IB column, *n*-hexane/*i*-PrOH = 90/10, flow rate = 1.0 mL/min, λ = 254 nm, t_{minor} = 7.5 min, t_{major} = 9.5 min).



(S)-6,9-diphenylbenzo[f]naphtho[2,1-d][1,3]oxazepin-1-ol (2y): yellow oil, 27.8 mg, 72% yield

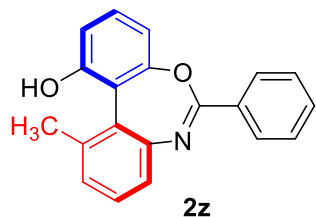
¹H NMR (400 MHz, CDCl₃) δ 8.49 (s, 1H), 8.37 – 8.34 (m, 3H), 8.11 – 7.89 (m, 3H), 7.62 – 7.43 (m, 6H), 7.39 (t, *J* = 8.2 Hz, 1H), 6.98 (d, *J* = 8.2 Hz, 2H), 5.12 (s, 1H);

¹³C NMR (101 MHz, CDCl₃) δ 159.2, 158.4, 154.2, 143.8, 132.4, 132.0, 131.8, 131.4, 130.4, 129.9, 129.7, 129.3, 128.6, 128.5, 127.8, 127.4, 127.2, 126.3, 126.1, 126.0, 124.5, 122.0, 116.2, 113.9, 113.2;

IR v_{max} (film, cm⁻¹): 1628.7, 1514.2, 1346.1, 1180.2, 1014.7, 729.2; [α]_D²⁵ = +84.2 (c = 1.0, CHCl₃);

HRMS (ESI, m/z): calcd. for [M+Na]⁺: 410.1157, found: 410.1154;

HPLC analysis: 97% ee, (CHIRALCEL IA column, *n*-hexane/*i*-PrOH = 90/10, flow rate = 1.0 mL/min, λ = 254 nm, t_{major} = 17.1 min, t_{minor} = 37.3 min).



(S)-11-methyl-6-phenyldibenzo[d,f][1,3]oxazepin-1-ol (2z): yellow oil, 21.0 mg, 70% yield

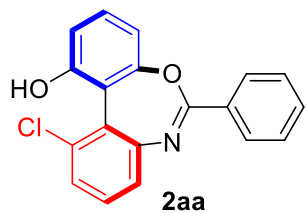
¹H NMR (400 MHz, CDCl₃) δ 8.33 – 8.23 (m, 2H), 7.53 – 7.42 (m, 3H), 7.33 (t, *J* = 7.7 Hz, 1H), 7.29 – 7.13 (m, 3H), 6.86 (dd, *J* = 8.1 Hz, 0.9 Hz, 1H), 6.79 (dd, *J* = 8.2 Hz, 0.9 Hz, 1H), 5.33 (s, 1H), 2.39 (s, 3H);

¹³C NMR (101 MHz, CDCl₃) δ 159.7, 158.1, 154.1, 145.6, 136.8, 132.0, 131.7, 129.7, 129.0, 128.5, 128.4, 127.9, 126.6, 124.2, 117.1, 113.1, 112.6, 20.3;

IR v_{max} (film, cm⁻¹): 1628.7, 1524.5, 1279.1, 1160.5, 1024.5, 729.5; [α]_D²⁵ = +54.6 (c = 1.0, CHCl₃);

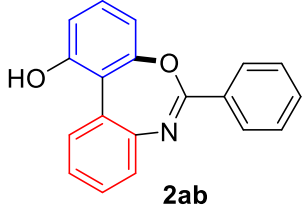
HRMS (ESI, m/z): calcd. for [M+Na]⁺: 324.1000, found: 324.0993;

HPLC analysis: 99% ee, (CHIRALCEL IA column, *n*-hexane/*i*-PrOH = 90/10, flow rate = 1.0 mL/min, λ = 254 nm, t_{major} = 9.8 min, t_{minor} = 13.4 min).

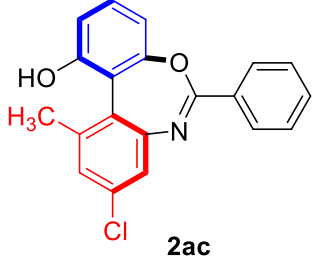


(R)-11-chloro-6-phenyldibenzo[d,f][1,3]oxazepin-1-ol (2aa): yellow oil, 21.2 mg, 66% yield

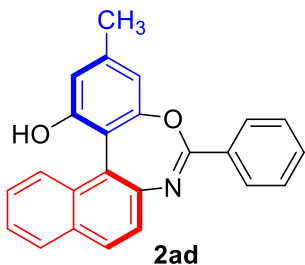
¹H NMR (400 MHz, CDCl₃) δ 8.28 – 8.26 (m, 2H), 7.55 – 7.51 (m, 1H), 7.51 – 7.44 (m, 2H), 7.40 – 7.31 (m, 3H), 7.27 – 7.23 (m, 1H), 6.97 – 6.73 (m, 2H), 5.35 (br, 1H);
¹³C NMR (101 MHz, CDCl₃) δ 159.7, 159.3, 154.4, 146.9, 132.3, 132.1, 131.5, 130.5, 129.2, 129.1, 128.5, 127.0, 126.7, 125.2, 115.8, 114.1, 112.8;
IR v_{max} (film, cm⁻¹): 1625.2, 1514.2, 1259.3, 1156.2, 1024.6, 739.8; [α]_D²⁵ = +48.6 (c = 0.2, CHCl₃);
HRMS (ESI, m/z): calcd. for [M+Na]⁺: 344.0454, found: 344.0456;
HPLC analysis: 99% ee, (CHIRALCEL IA column, *n*-hexane/*i*-PrOH = 90/10, flow rate = 1.0 mL/min, λ = 254 nm, t_{major} = 11.5 min, t_{minor} = 17.9 min).



6-phenyldibenzo[d,f][1,3]oxazepin-1-ol (2ab): yellow oil, 22.9 mg, 80% yield, 0% ee
¹H NMR (400 MHz, CDCl₃) δ 8.34 – 8.21 (m, 2H), 7.81 (dd, *J* = 7.8 Hz, 1.2 Hz, 1H), 7.57 – 7.32 (m, 5H), 7.27 – 7.17 (m, 2H), 6.87 – 6.83 (m, 2H), 6.00 (br, 1H);
¹³C NMR (101 MHz, CDCl₃) δ 158.8, 157.7, 153.9, 144.8, 131.9, 131.8, 129.6, 129.1, 128.7, 128.5, 128.4, 127.6, 127.5, 125.3, 118.2, 113.9, 113.1;
IR v_{max} (film, cm⁻¹): 1628.2, 1514.7, 1249.1, 1135.6, 1024.8, 736.2;
HRMS (ESI, m/z): calcd. for [M+Na]⁺: 310.0844, found: 310.0850.



(S)-9-chloro-11-methyl-6-phenyldibenzo[d,f][1,3]oxazepin-1-ol (2ac): yellow oil, 24.1 mg, 72% yield
¹H NMR (400 MHz, CDCl₃) δ 8.33 – 8.19 (m, 2H), 7.57 – 7.41 (m, 3H), 7.28 – 7.16 (m, 3H), 6.86 (dd, *J* = 8.1 Hz, 0.8 Hz, 1H), 6.77 (dd, *J* = 8.2 Hz, 0.8 Hz, 1H), 5.26 (s, 1H), 2.37 (s, 3H);
¹³C NMR (101 MHz, CDCl₃) δ 159.5, 158.9, 154.0, 146.6, 138.7, 133.7, 132.0, 131.6, 130.0, 129.1, 128.5, 127.5, 125.4, 123.9, 116.5, 113.3, 112.8, 20.3;
IR v_{max} (film, cm⁻¹): 1609.4, 1568.9, 1223.2, 1150.8, 1032.7, 743.2; [α]_D²⁵ = +37.6 (c = 1.0, CHCl₃);
HRMS (ESI, m/z): calcd. for [M+Na]⁺: 358.0611, found: 358.0616;
HPLC analysis: 99% ee, (CHIRALCEL IA column, *n*-hexane/*i*-PrOH = 90/10, flow rate = 1.0 mL/min, λ = 254 nm, t_{minor} = 9.8 min, t_{major} = 12.7 min).



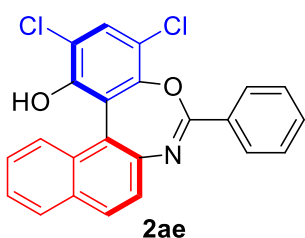
(S)-3-methyl-6-phenylbenzo[f]naphtho[2,1-d][1,3]oxazepin-1-ol (2ad): yellow solid, 21.0 mg, 60% yield

¹H NMR (400 MHz, CDCl₃) δ 8.36 – 8.33 (m, 2H), 7.93 – 7.90 (m, 2H), 7.81 (d, *J* = 8.4 Hz, 1H), 7.64 – 7.44 (m, 6H), 6.76 (d, *J* = 4.9 Hz, 2H), 4.94 (s, 1H), 2.36 (s, 3H); **¹³C NMR** (101 MHz, CDCl₃) δ 159.4, 158.4, 153.6, 143.9, 141.1, 132.0, 131.8, 131.7, 129.3, 129.2, 129.0, 128.8, 128.5, 127.3, 126.2, 125.8 (2C), 122.8, 114.3, 113.8, 113.1, 21.2;

IR v_{max} (film, cm⁻¹): 1628.7, 1514.3, 1246.2, 1148.8, 1032.5, 732.1; [α]_D²⁵ = +125.5 (c = 1.0, CHCl₃);

HRMS (ESI, m/z): calcd. for [M+Na]⁺: 374.1157, found: 374.1160;

HPLC analysis: 98% ee, (CHIRALCEL IA column, *n*-hexane/*i*-PrOH = 90/10, flow rate = 1.0 mL/min, λ = 254 nm, t_{major} = 19.7 min, t_{minor} = 24.0 min).



(S)-2,4-dichloro-6-phenylbenzo[f]naphtho[2,1-d][1,3]oxazepin-1-ol (2ae): yellow solid, 32.5 mg, 80% yield

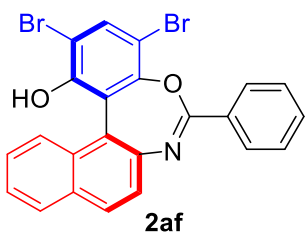
¹H NMR (400 MHz, CDCl₃) δ 8.49 – 8.37 (m, 2H), 7.98 – 7.85 (m, 2H), 7.63 – 7.61 (m, 1H), 7.57 – 7.40 (m, 7H), 5.65 (s, 1H);

¹³C NMR (101 MHz, CDCl₃) δ 158.7, 154.4, 148.1, 143.5, 132.0, 131.8, 131.6, 130.1, 129.9, 129.8, 129.3, 128.5, 128.1, 126.8, 126.1, 125.8, 125.5, 122.2, 118.7, 117.8, 117.6;

IR v_{max} (film, cm⁻¹): 1623.2, 1523.6, 1217.2, 1179.8, 1040.9, 756.2; [α]_D²⁵ = +45.2 (c = 1.0, CHCl₃);

HRMS (ESI, m/z): calcd. for [M+H]⁺: 406.0402, found: 406.0403;

HPLC analysis: 92% ee, (CHIRALCEL IA column, *n*-hexane/*i*-PrOH = 90/10, flow rate = 0.5 mL/min, λ = 254 nm, t_{major} = 21.1 min, t_{minor} = 33.7 min).



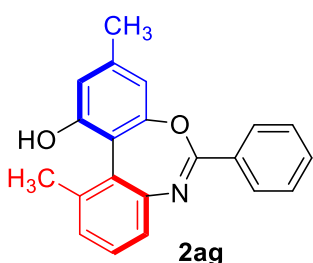
(S)-2,4-dibromo-6-phenylbenzo[f]naphtho[2,1-d][1,3]oxazepin-1-ol (2af): yellow solid, 35.6 mg, 72% yield

¹H NMR (400 MHz, CDCl₃) δ 8.49 – 8.36 (m, 2H), 7.95 – 7.86 (m, 2H), 7.78 (s, 1H), 7.64 – 7.57 (m, 1H), 7.56 – 7.40 (m, 6H), 5.66 (s, 1H);

¹³C NMR (101 MHz, CDCl₃) δ 158.9, 156.3, 149.8, 143.5, 134.8, 132.0, 131.9, 131.6, 130.1 (2C), 129.7, 128.5, 128.0, 126.9, 126.0, 125.9, 125.5, 122.3, 118.4, 107.4, 105.7; **IR v_{max}** (film, cm⁻¹): 1616.5, 1526.5, 1239.2, 1168.8, 1024.9, 731.2; [α]_D²⁵ = +88.3 (c = 1.0, CHCl₃);

HRMS (ESI, m/z): calcd. for [M+Na]⁺: 515.9211, found: 515.9198;

HPLC analysis: 92% ee, (CHIRALCEL IA column, *n*-hexane/*i*-PrOH = 90/10, flow rate = 0.5 mL/min, λ = 254 nm, t_{major} = 20.7 min, t_{minor} = 40.4 min).



(S)-3,11-dimethyl-6-phenyldibenzo[d,f][1,3]oxazepin-1-ol (2ag): yellow oil, 23.0 mg, 73% yield

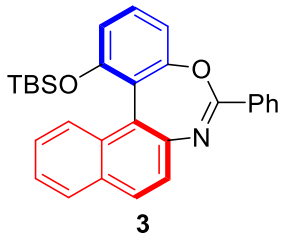
¹H NMR (400 MHz, CDCl₃) δ 8.32 – 8.23 (m, 2H), 7.56 – 7.41 (m, 3H), 7.35 – 7.22 (m, 2H), 7.17 (d, *J* = 7.4 Hz, 1H), 6.65 (d, *J* = 19.8 Hz, 2H), 2.39 (s, 3H), 2.29 (s, 3H);

¹³C NMR (101 MHz, CDCl₃) δ 159.5, 158.0, 153.6, 145.5, 140.5, 136.7, 132.2, 131.6, 129.0, 128.4, 128.1, 128.0, 126.8, 124.2, 114.1, 113.7, 113.4, 21.2, 20.3;

IR v_{max} (film, cm⁻¹): 1653.4, 1524.5, 1267.2, 1150.2, 1078.9, 739.2; [α]_D²⁵ = +27.9 (c = 1.0, CHCl₃);

HRMS (ESI, m/z): calcd. for [M+Na]⁺: 338.1157, found: 338.1152;

HPLC analysis: 99% ee, (CHIRALCEL IA column, *n*-hexane/*i*-PrOH = 90/10, flow rate = 1.0 mL/min, λ = 254 nm, t_{minor} = 17.1 min, t_{major} = 18.4 min).



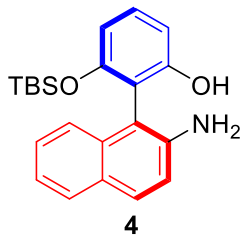
(R)-1-((tert-butyldimethylsilyl)oxy)-6-phenylbenzo[f]naphtho[2,1-d][1,3]oxazepine (3):

¹H NMR (400 MHz, CDCl₃) δ 8.41 – 8.31 (m, 2H), 7.92 – 7.76 (m, 3H), 7.58 – 7.38 (m, 6H), 7.31 (t, *J* = 8.2 Hz, 1H), 7.02 (dd, *J* = 8.2 Hz, 1.0 Hz, 1H), 6.84 (dd, *J* = 8.1 Hz, 1.0 Hz, 1H), 0.41 (s, 9H), -0.14 (s, 3H), -0.65 (s, 3H);

¹³C NMR (101 MHz, CDCl₃) δ 160.2, 158.2, 154.4, 143.0, 132.3, 131.7, 131.4, 131.3, 129.3, 129.2, 128.6, 128.5 (2C), 127.5, 125.7, 125.6, 125.2, 125.0, 121.5, 118.1, 114.1, 24.9, 17.5, 1.0, -4.7;

IR v_{max} (film, cm⁻¹): 1650.6, 1537.5, 1217.2, 1156.8, 1023.9, 776.2; [α]_D²⁵ = +77.4 (c = 1.0, CHCl₃);

HRMS (ESI, m/z): calcd. for [M+H]⁺: 452.2046, found: 452.2051.



(R)-2-(2-aminonaphthalen-1-yl)-3-((tert-butyldimethylsilyl)oxy)phenol (4):

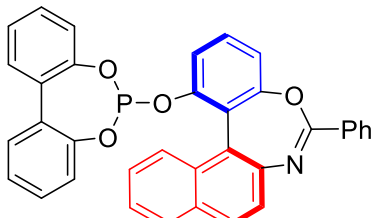
¹H NMR (400 MHz, CDCl₃) δ 7.75 (d, *J* = 8.4 Hz, 2H), 7.39 – 7.19 (m, 4H), 7.06 (d, *J* = 8.7 Hz, 1H), 6.79 (d, *J* = 8.2 Hz, 1H), 6.62 (d, *J* = 8.1 Hz, 1H), 0.48 (s, 9H), 0.02 (s, 3H), -0.15 (s, 3H);

¹³C NMR (101 MHz, CDCl₃) δ 155.1, 154.6, 143.3, 133.8, 130.0, 129.7, 128.2, 127.9, 126.7, 123.9, 122.4, 118.0, 114.0, 111.7, 108.7, 108.6, 24.9, 17.4, -4.5, -4.8;

IR v_{max} (film, cm⁻¹): 1623.6, 1590.5, 1265.2, 1130.8, 1067.9, 745.2; [α]_D²⁵ = -18.4 (c = 1.0, CHCl₃);

HRMS (ESI, m/z): calcd. for [M+H]⁺: 366.1889, found: 366.1905;

HPLC analysis: 98% ee, (CHIRALCEL AD-H column, *n*-hexane/*i*-PrOH = 95/5, flow rate = 1.0 mL/min, λ = 254 nm, t_{minor} = 9.7 min, t_{major} = 11.6 min).



5

(R)-1-(dibenzo[d,f][1,3,2]dioxaphosphhepin-6-yloxy)-6-phenylbenzo[f]naphtho[2,1-d][1,3]oxazepine (5):

¹H NMR (400 MHz, CDCl₃) δ 8.36 (dd, *J* = 8.1 Hz, 1.5 Hz, 2H), 7.96 – 7.89 (m, 2H), 7.77 (d, *J* = 8.4 Hz, 1H), 7.62 – 7.34 (m, 7H), 7.32 – 7.25 (m, 2H), 7.24 – 7.04 (m, 6H), 6.68 – 6.66 (m, 1H), 6.33 – 6.31 (m, 1H);

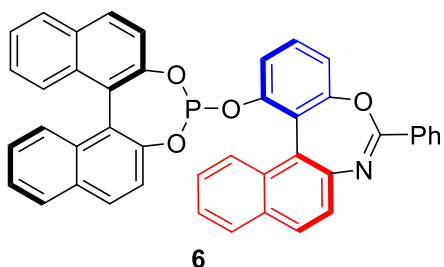
¹³C NMR (101 MHz, CDCl₃) δ 159.9, 157.8, 150.3 (d, *J* = 6.9 Hz), 148.8, 148.7, 148.6, 143.3, 131.8, 131.4, 131.0, 130.8 (d, *J* = 3.2 Hz), 130.6 (d, *J* = 3.2 Hz), 129.7, 129.6, 129.5, 129.3, 129.2, 129.0, 128.9, 128.5, 127.9, 127.7, 126.3, 125.4, 125.2, 125.1, 125.0, 124.2, 121.8, 121.7, 118.2, 118.1, 117.1;

³¹P NMR (162 MHz, CDCl₃) δ 142.1 (s);

IR v_{max} (film, cm⁻¹): 1642.2, 1523.6, 1206.2, 1145.8, 1023.7, 679.3; [α]_D²⁵ = +98.8 (c = 1.0, CHCl₃);

HRMS (ESI, m/z): calcd. for [M+H]⁺: 552.1365, found: 552.1354;

HPLC analysis: 98% ee, (CHIRALCEL IA column, *n*-hexane/*i*-PrOH = 90/10, flow rate = 0.5 mL/min, λ = 254 nm, t_{minor} = 13.6 min, t_{major} = 27.5 min).



(13c*R*)-1-(((11b*R*)-dinaphtho[2,1-d:1',2'-f][1,3,2]dioxaphosphhepin-4-yl)oxy)-6-phenylbenzo[f]naphtho[2,1-d][1,3]oxazepine (6):

¹H NMR (400 MHz, CDCl₃) δ 8.43 – 8.27 (m, 2H), 8.03 – 7.68 (m, 6H), 7.64 – 7.02 (m, 17H), 6.40 (d, *J* = 8.8 Hz, 1H);

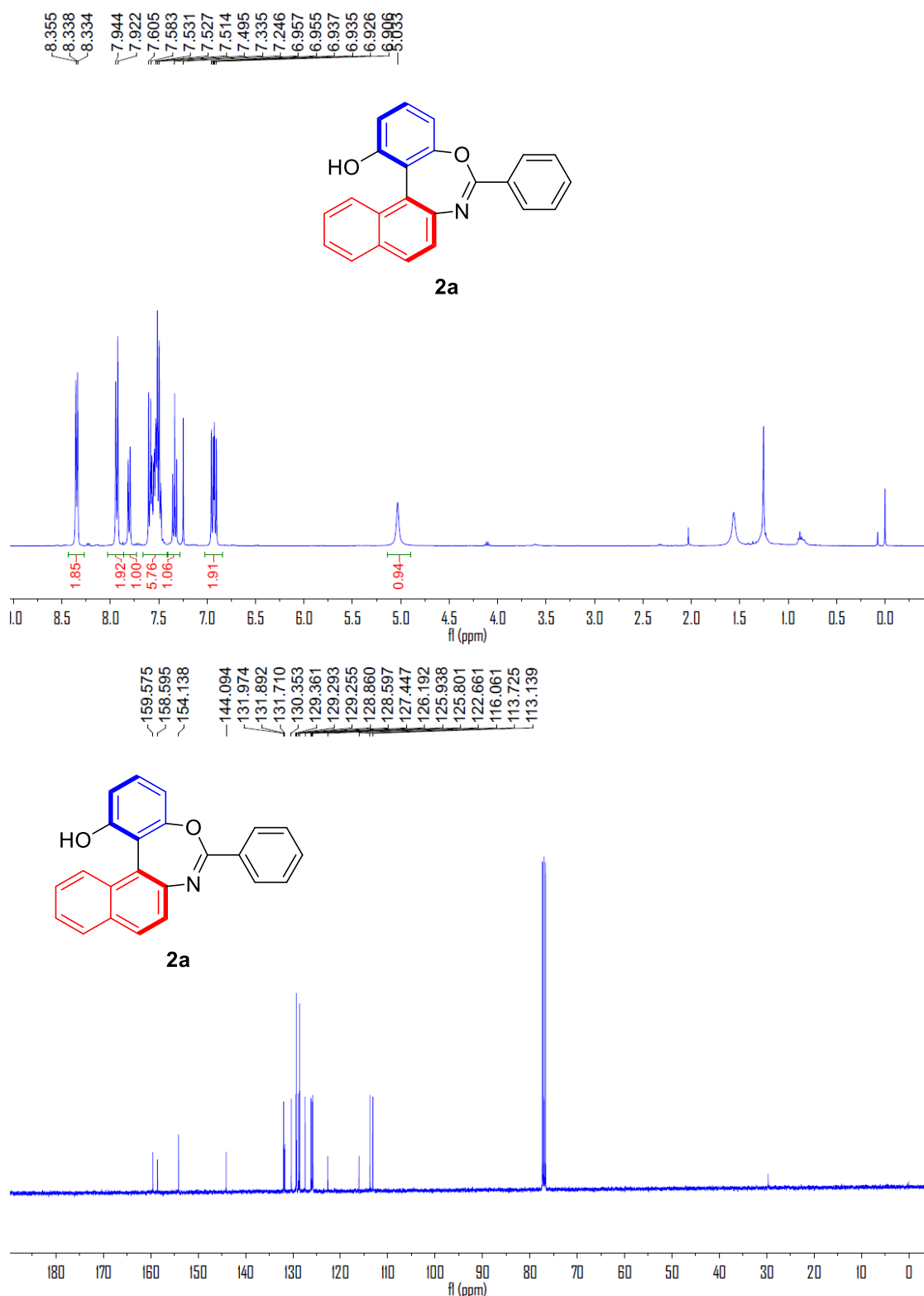
¹³C NMR (101 MHz, CDCl₃) δ 159.7, 157.7, 150.3 (d, *J* = 4.9 Hz), 147.4 (d, *J* = 4.6 Hz), 146.6 (d, *J* = 2.6 Hz), 143.2, 132.6, 132.2, 131.9, 131.8, 131.5, 131.4, 131.0, 130.9, 130.8, 130.2, 129.7, 129.5, 129.2, 129.1, 128.6, 128.3, 128.1, 127.8, 127.7, 126.9, 126.8, 126.4, 126.1, 125.9, 125.6, 125.4, 125.0, 124.8, 124.2, 123.9 (d, *J* = 5.2 Hz), 122.3 (d, *J* = 2.4 Hz), 121.5, 121.3, 117.8, 117.7 (d, *J* = 9.3 Hz), 116.8;

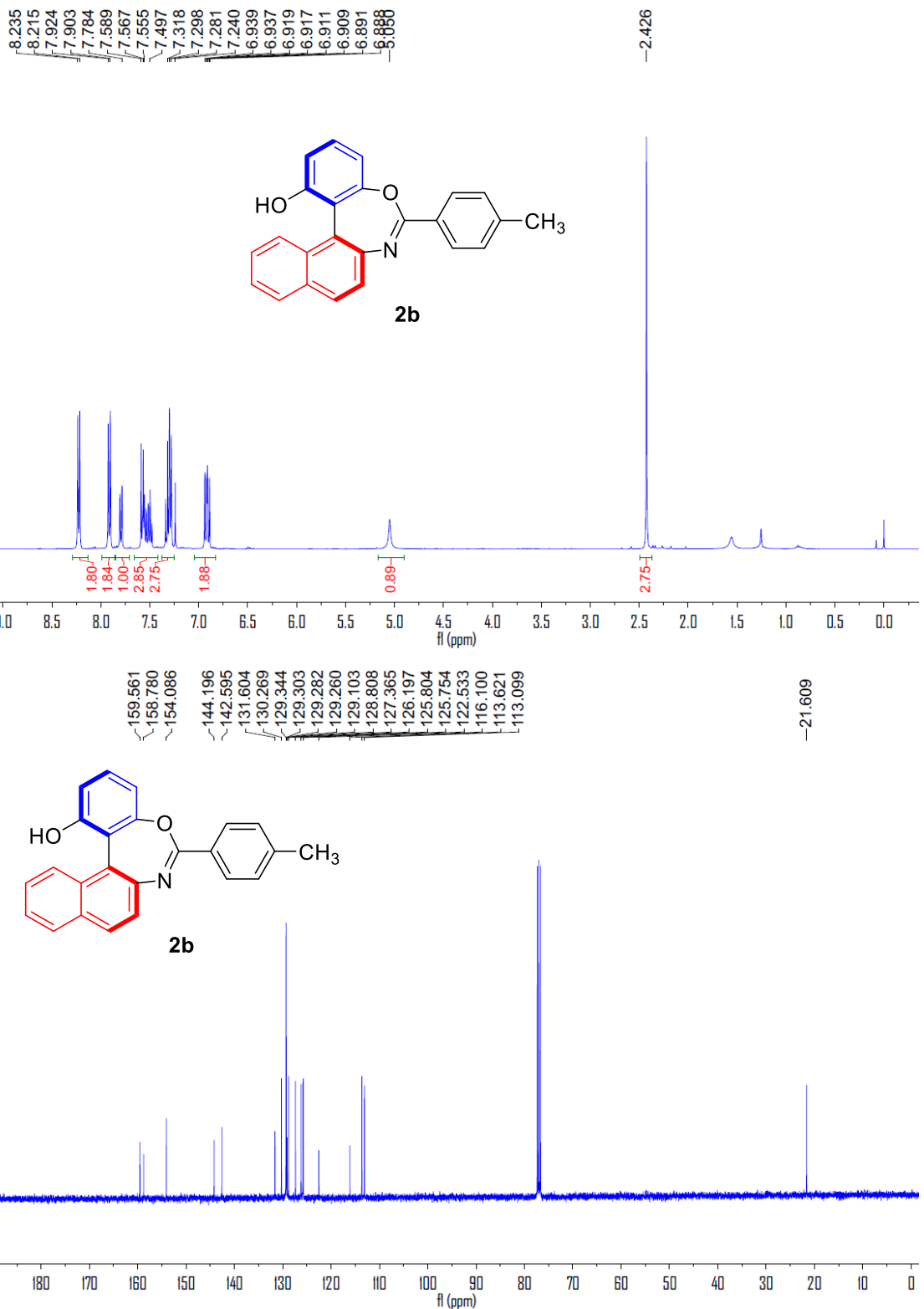
³¹P NMR (162 MHz, CDCl₃) δ 142.2 (s);

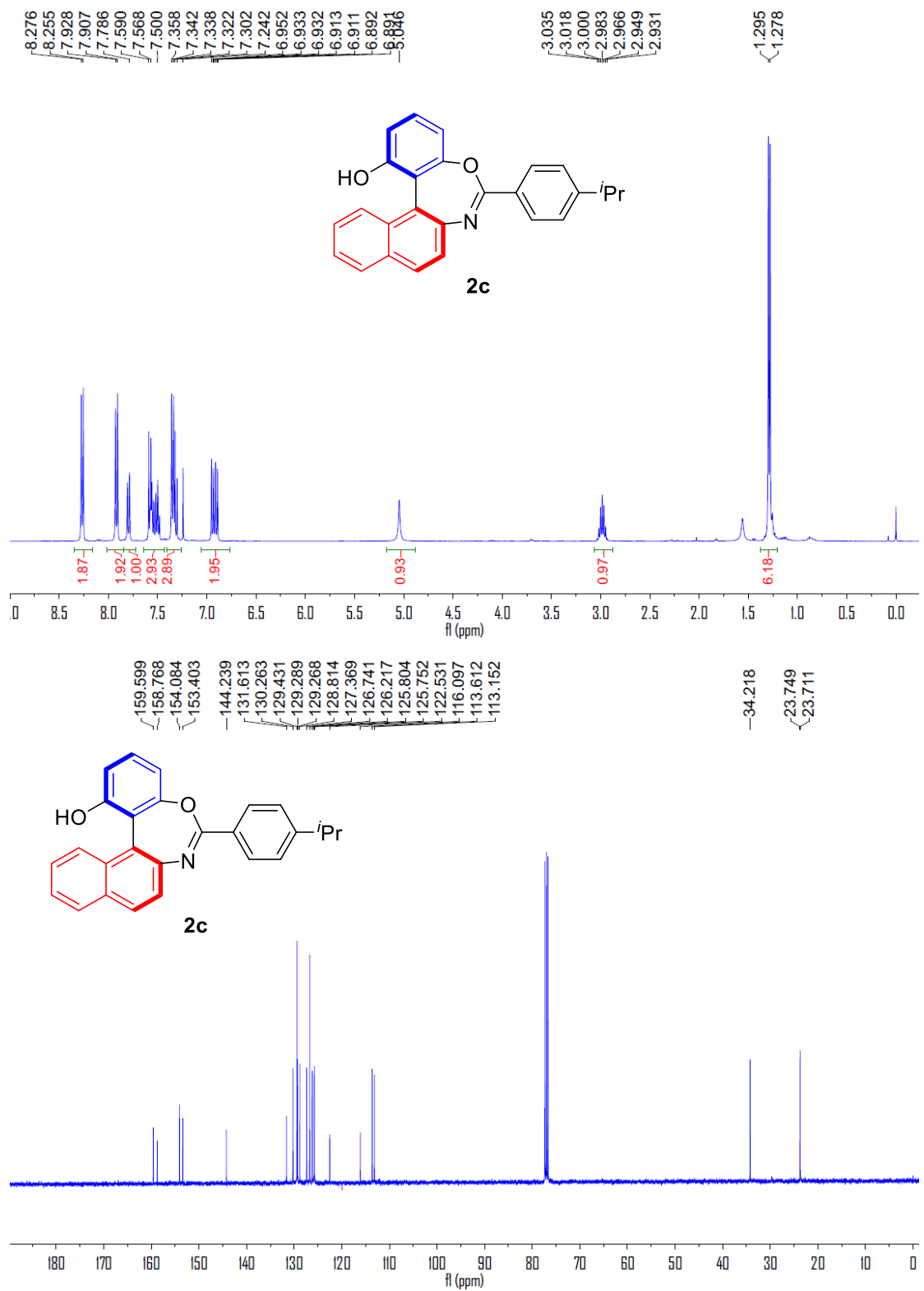
IR v_{max} (film, cm⁻¹): 1623.6, 1536.5, 1223.4, 1130.8, 1014.9, 689.1; [α]_D²⁵ = +47.4 (c = 1.0, CHCl₃);

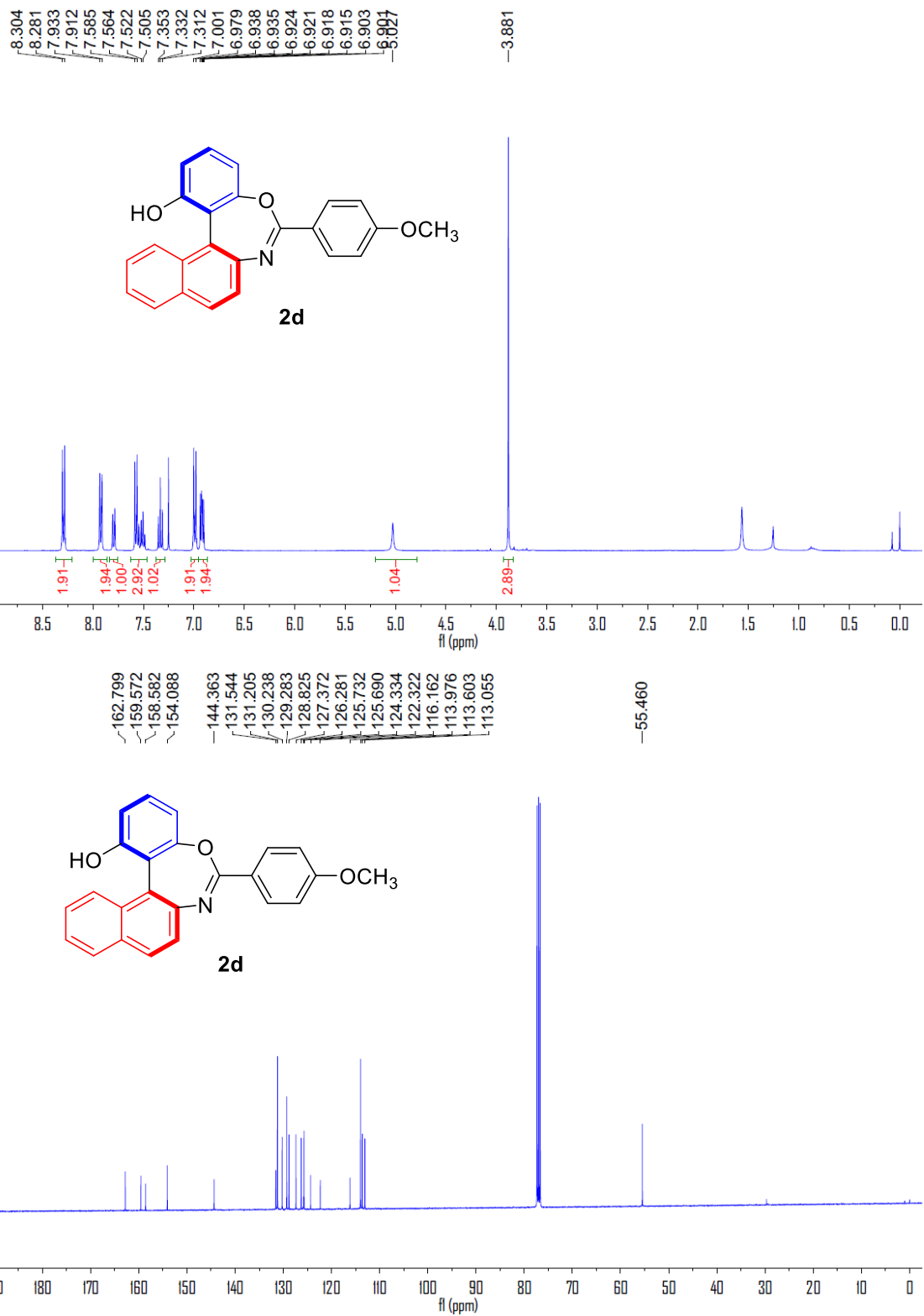
HRMS (ESI, m/z): calcd. for [M+H]⁺: 652.1678, found: 652.1681.

^1H , ^{13}C , ^{19}F and ^{31}P spectra and HPLC charts

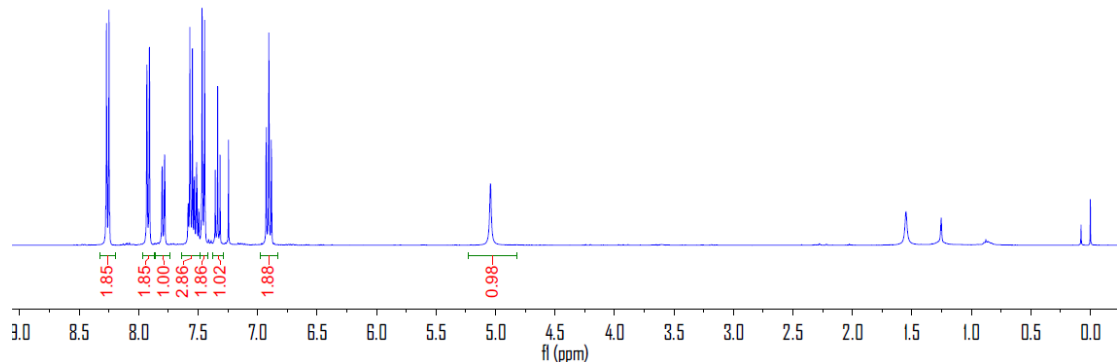
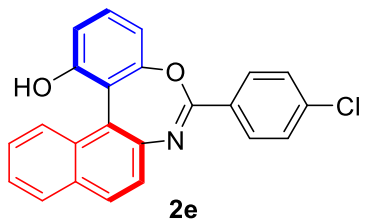




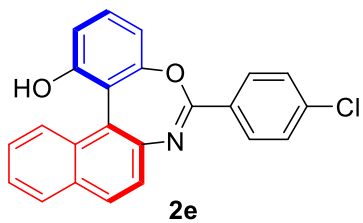




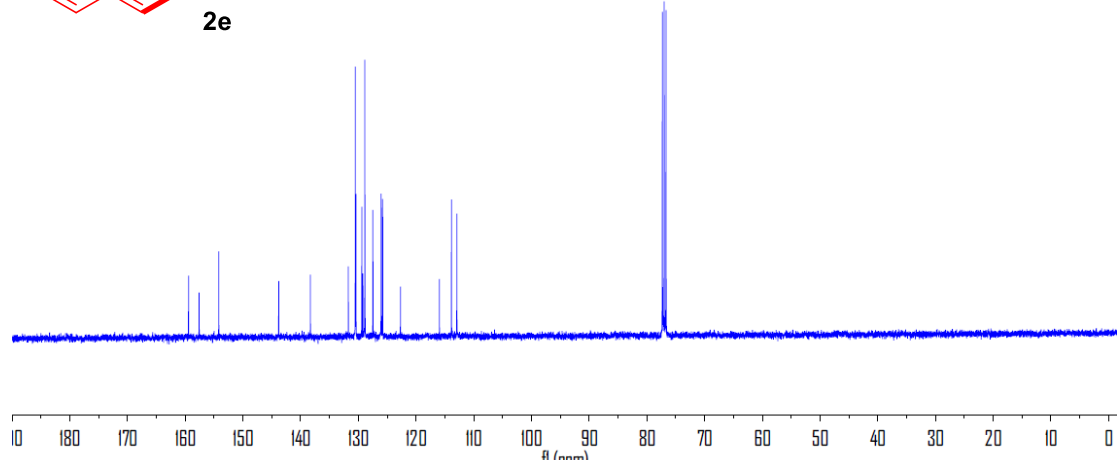
8.271
8.249
7.931
7.910
7.802
7.782
7.570
7.548
7.530
7.513
7.467
7.445
7.356
7.336
7.316
7.245
6.929
6.927
6.906
6.885
6.883



~159.420
~157.592
143.797
138.398
131.734
130.529
130.404
129.401
129.202
128.879
128.844
127.481
126.048
126.023
125.791
122.700
115.951
113.888
112.928

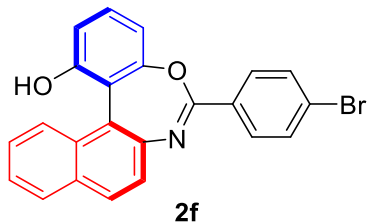


2e

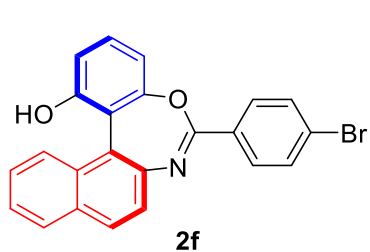
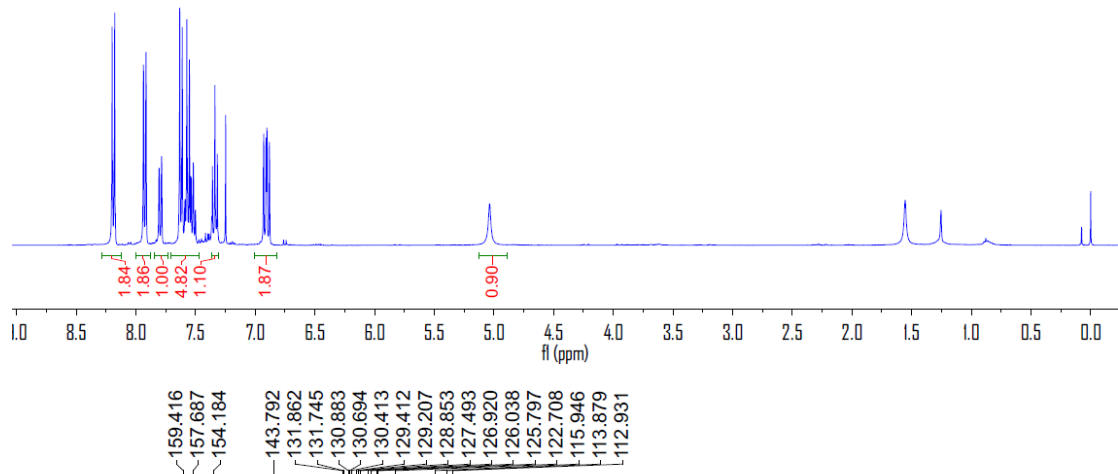


8.198
8.177
7.936
7.915
7.632
7.611
7.573
7.551
7.337
7.317
6.928
6.910
6.908
6.902
6.881
6.879

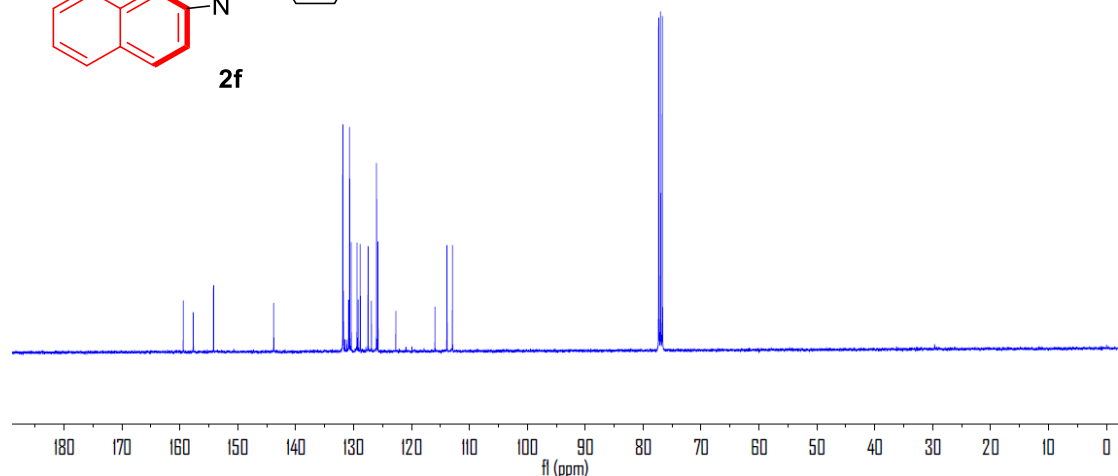
-5.036

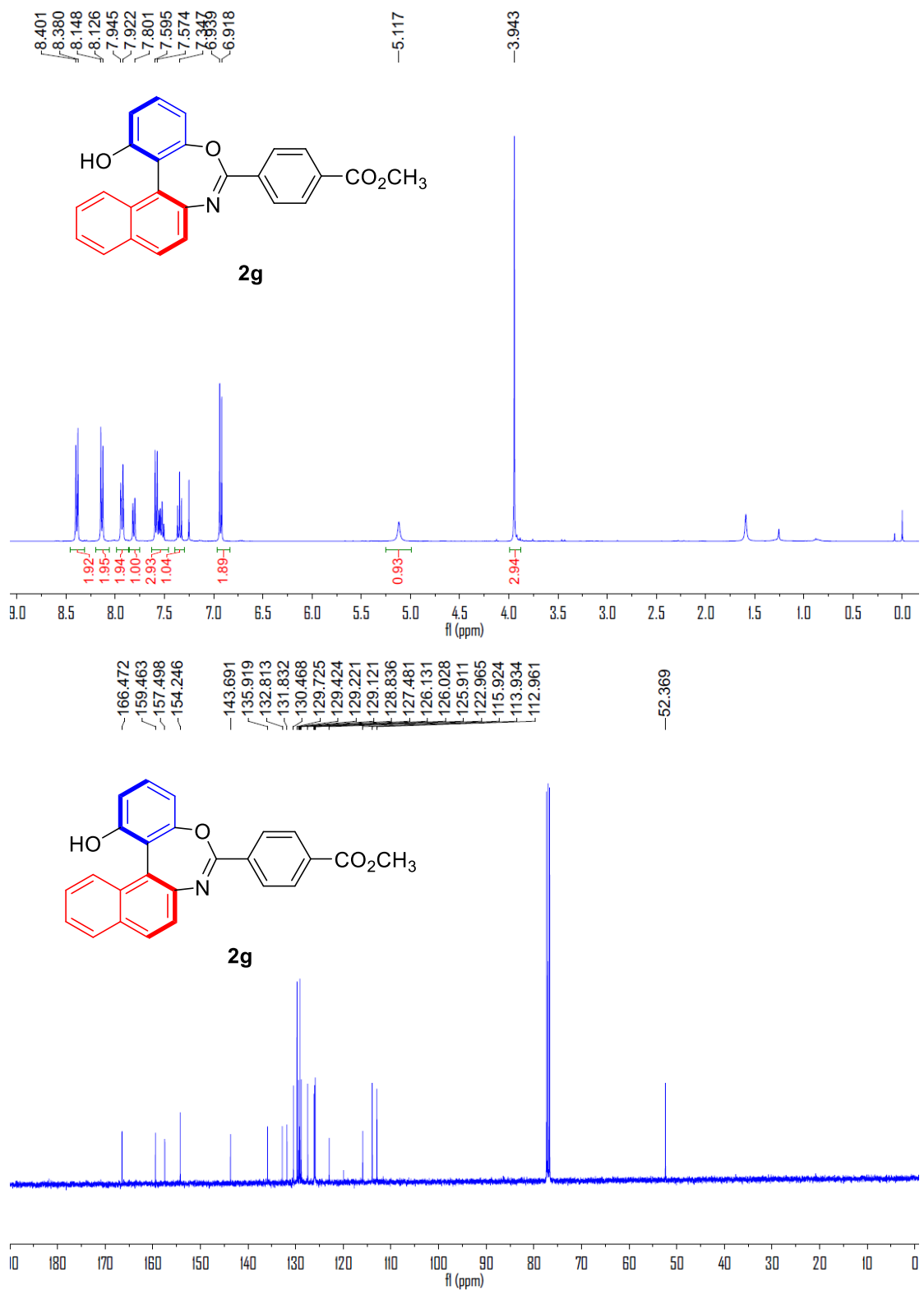


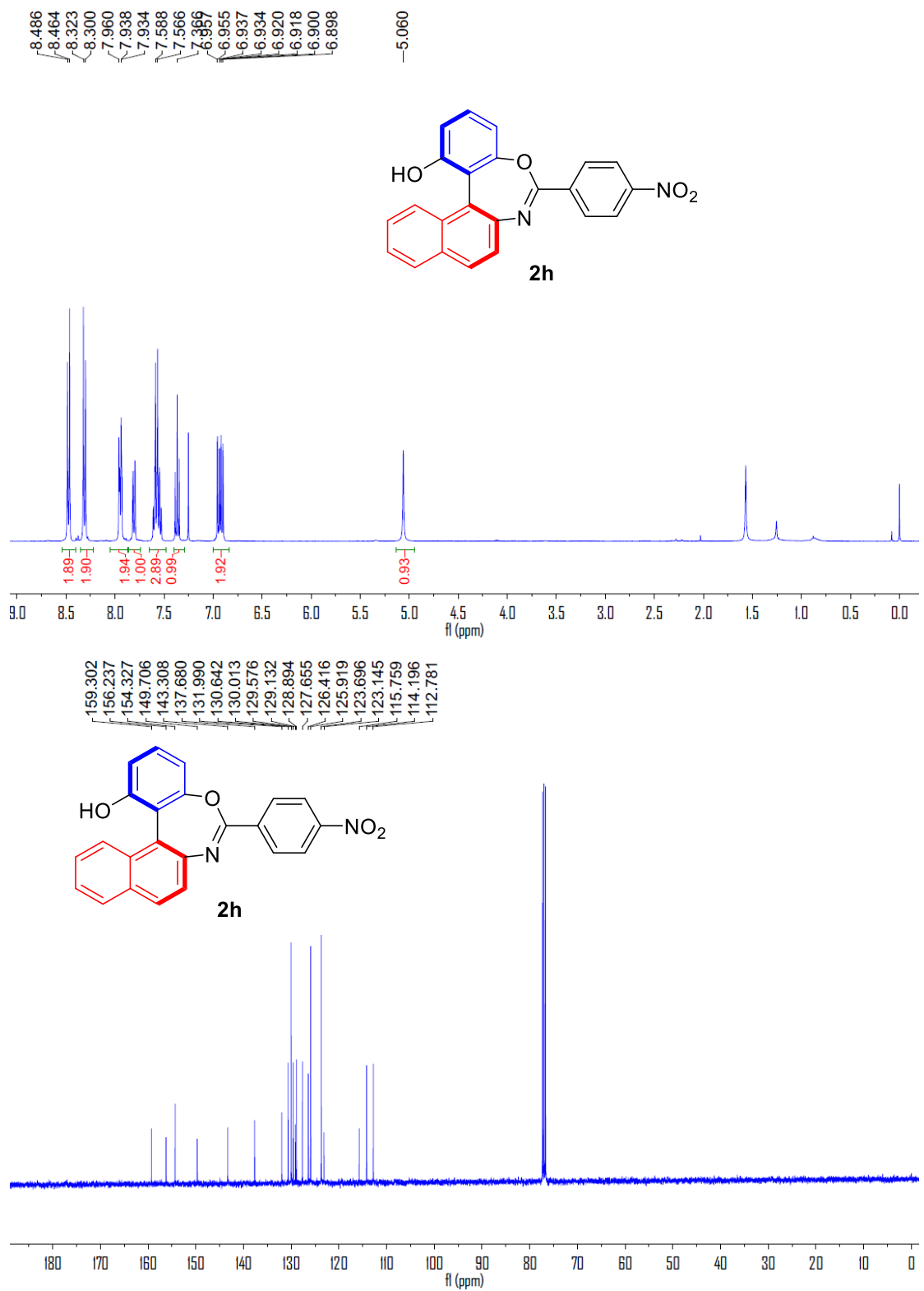
2f

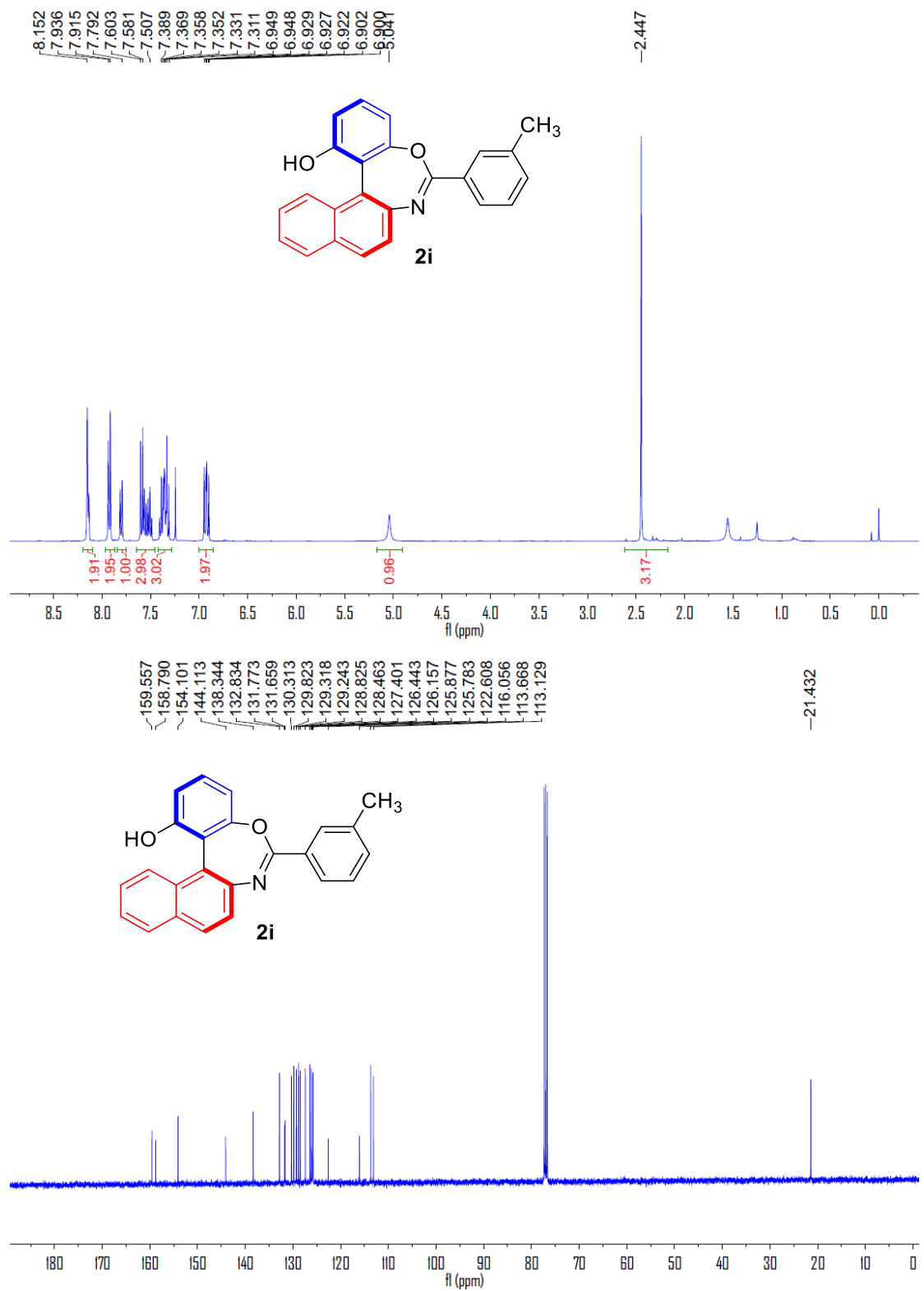


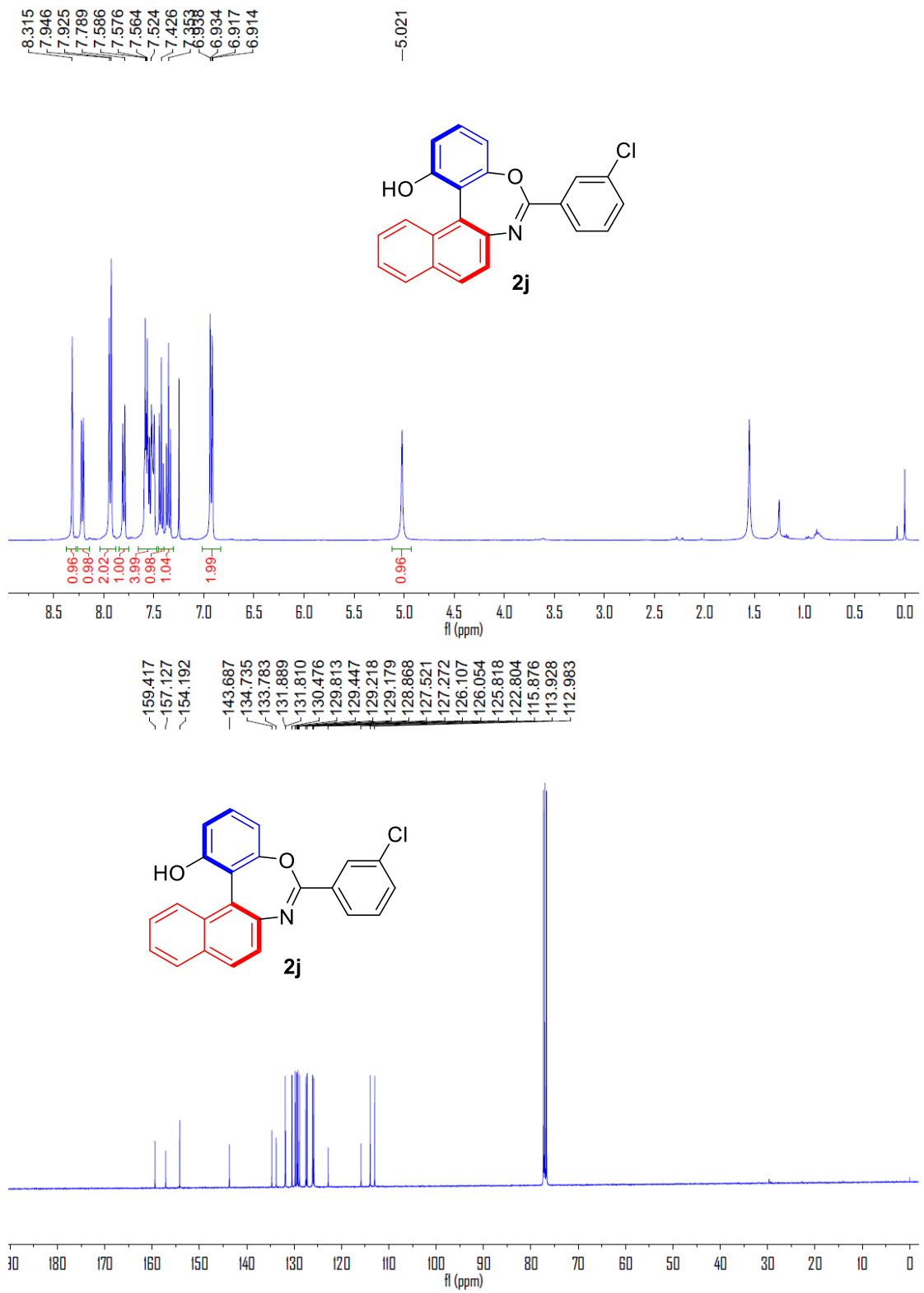
2f

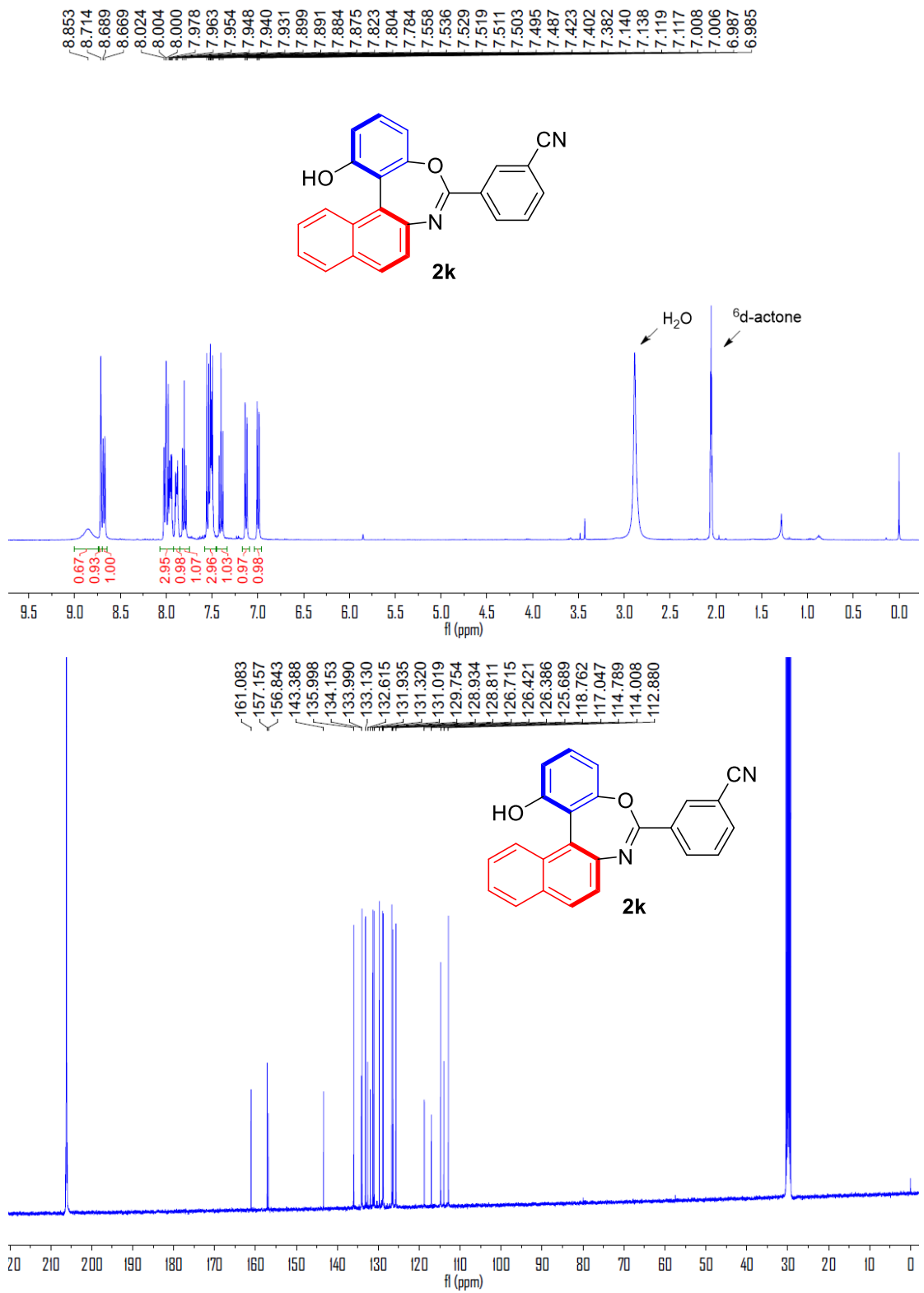


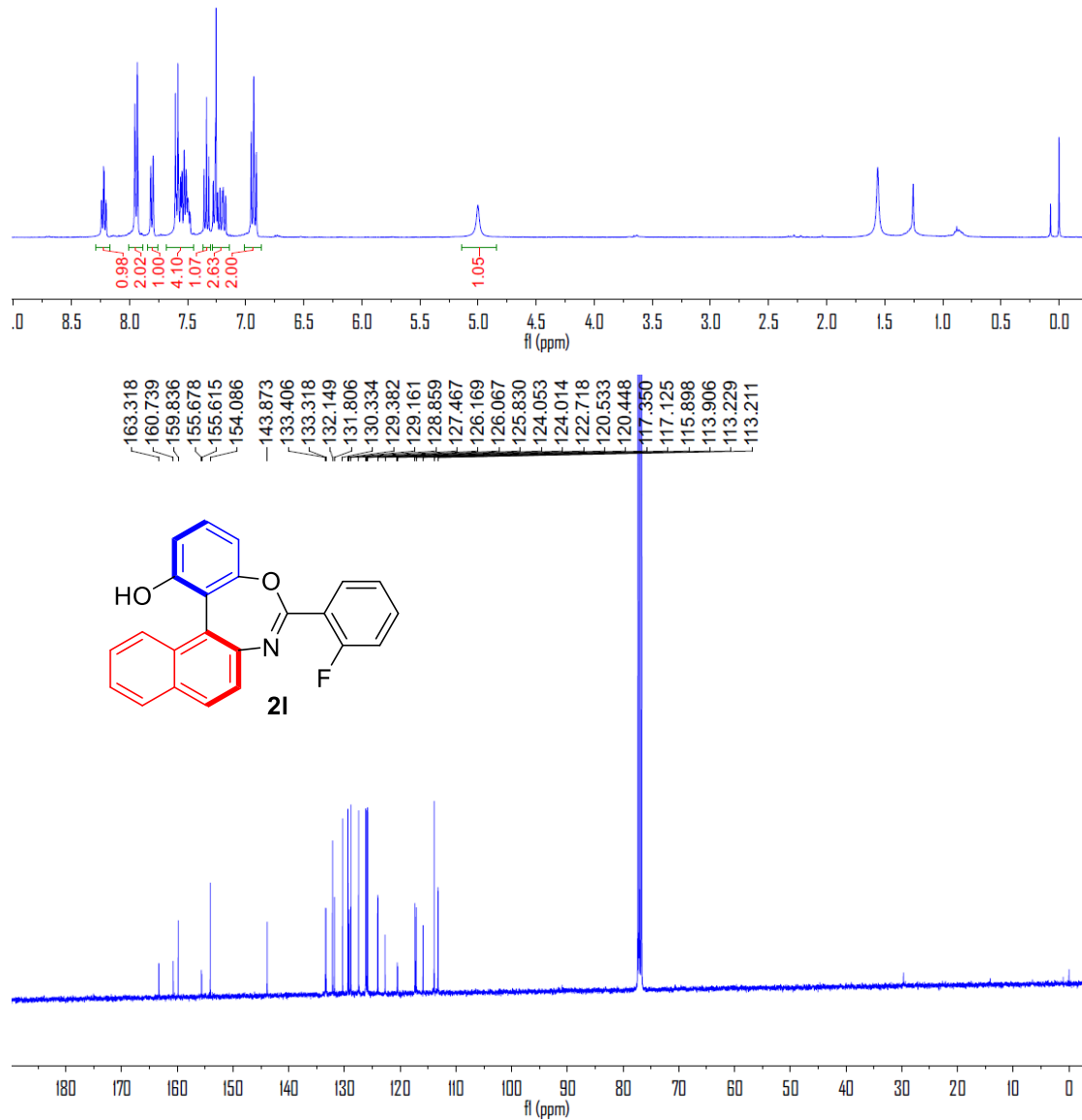
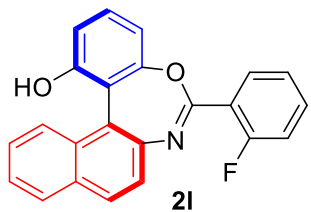
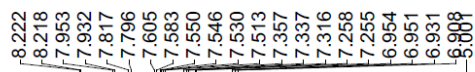


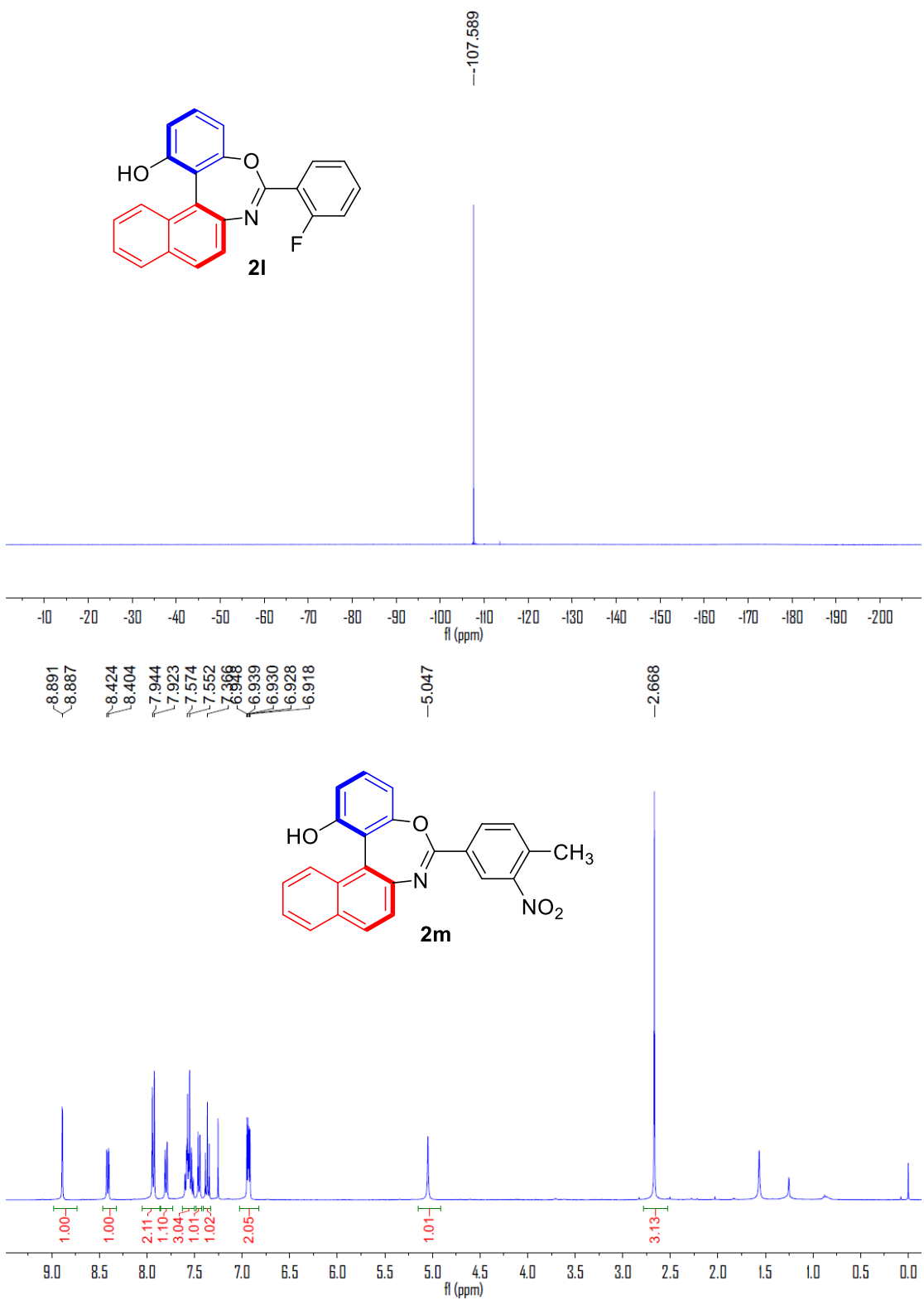


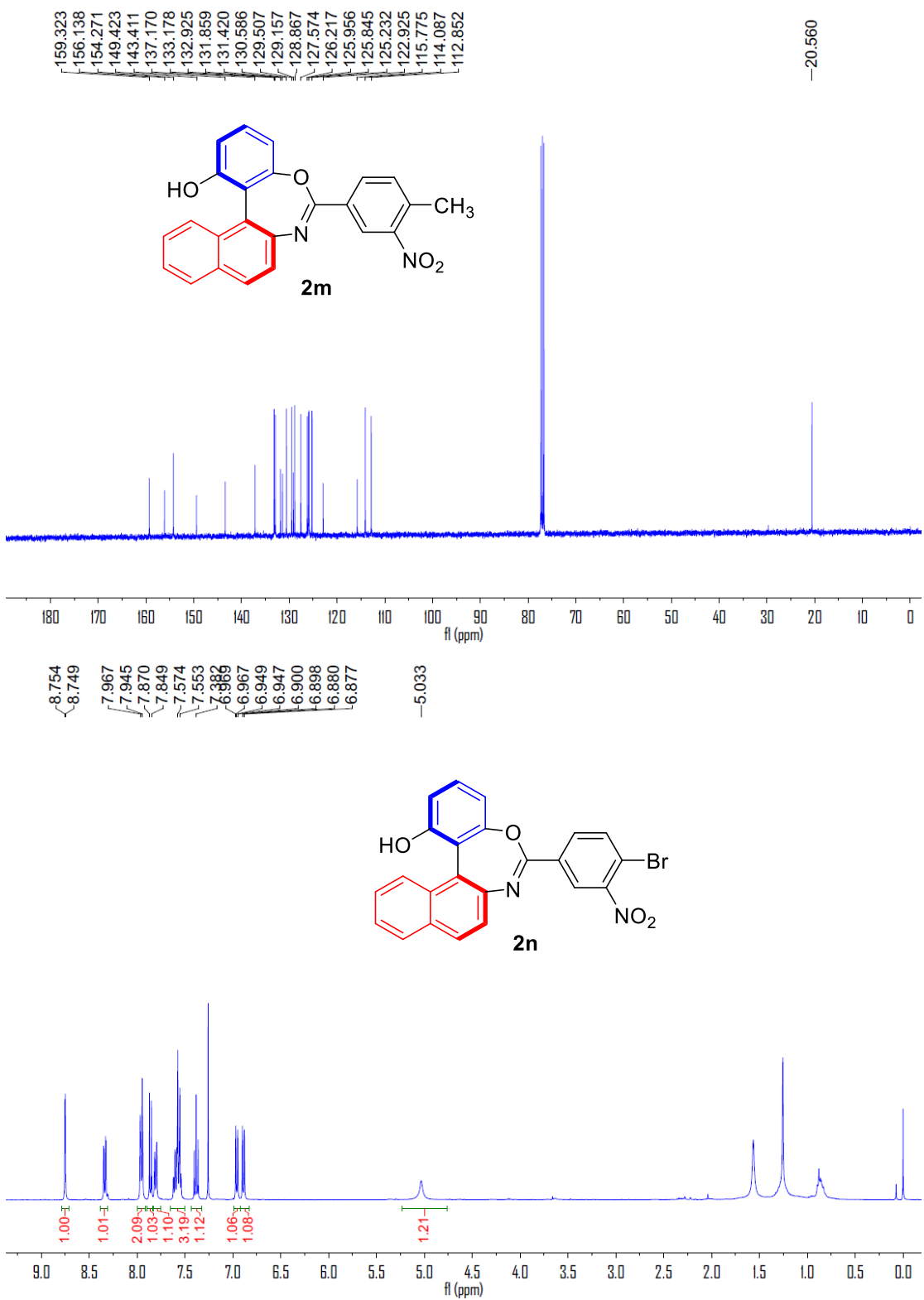


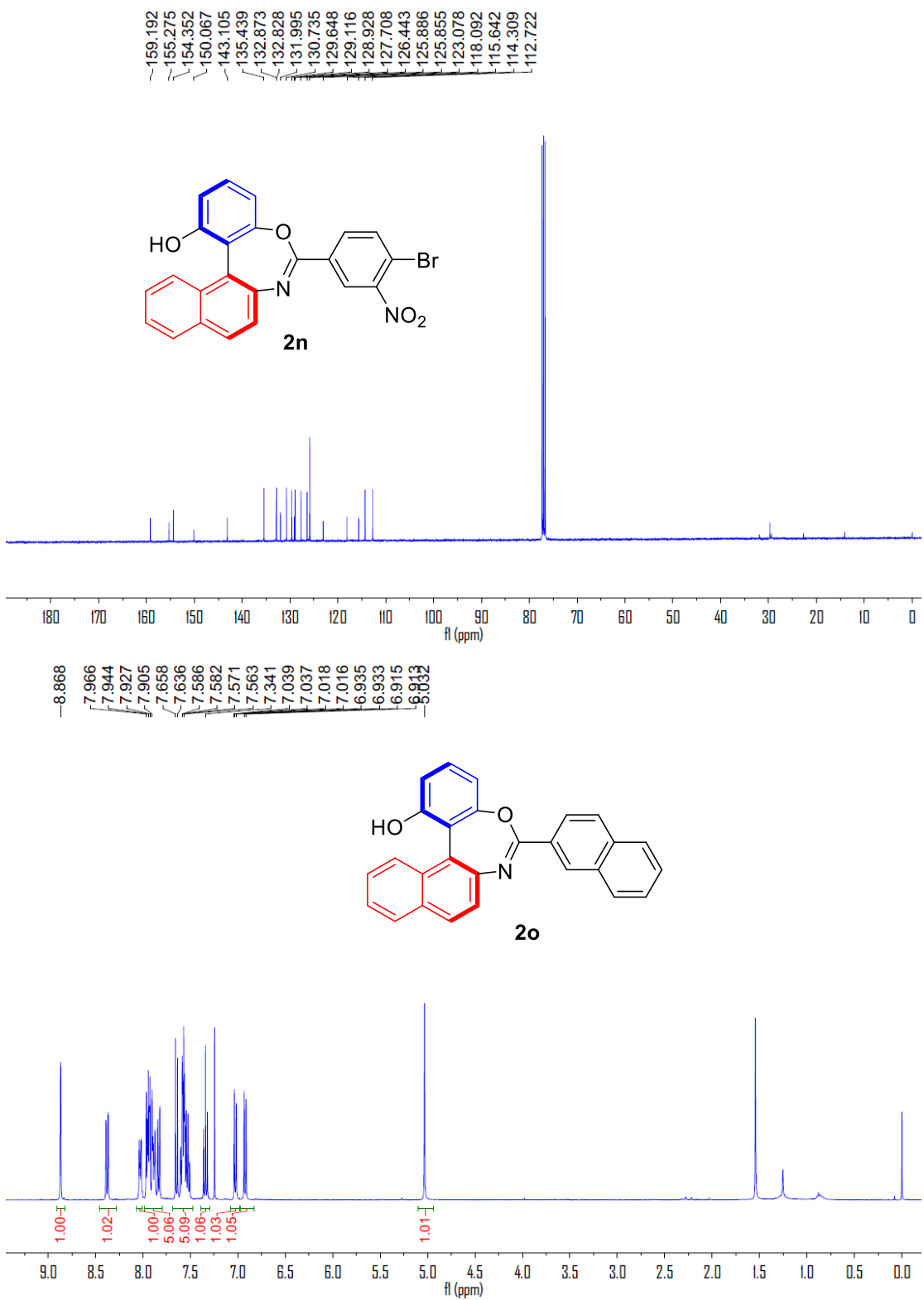


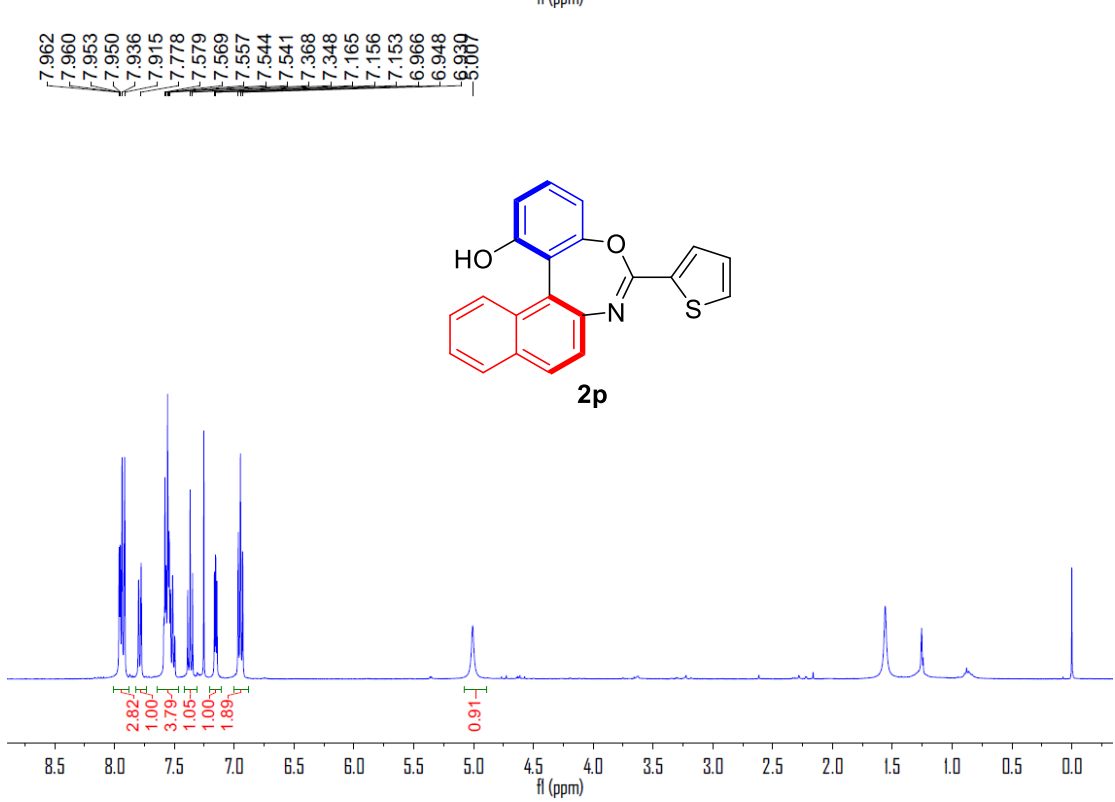
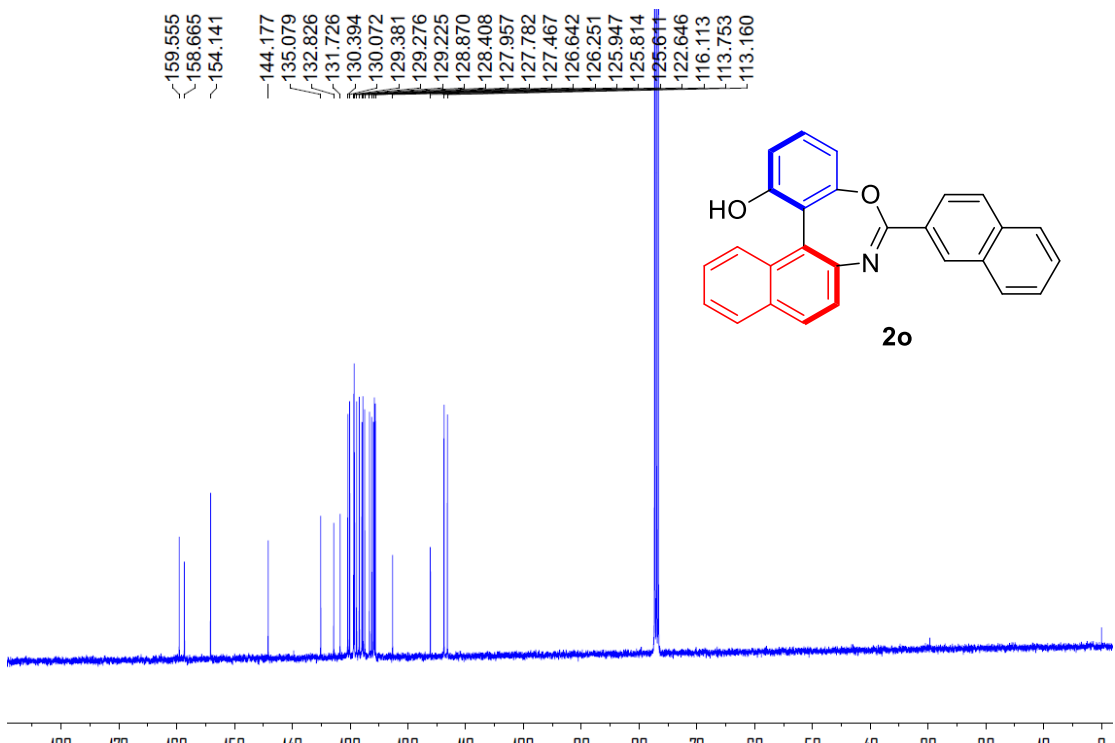


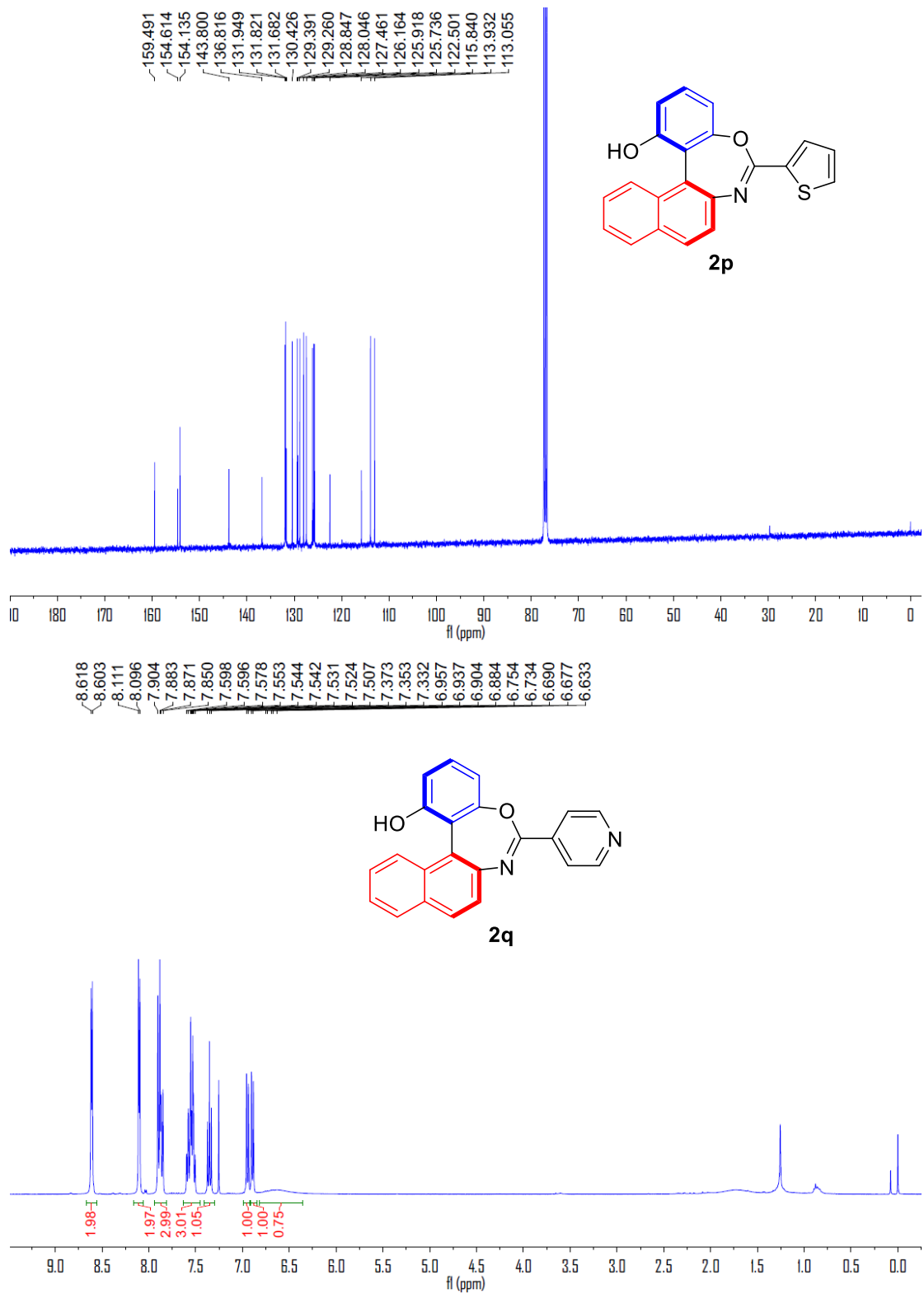


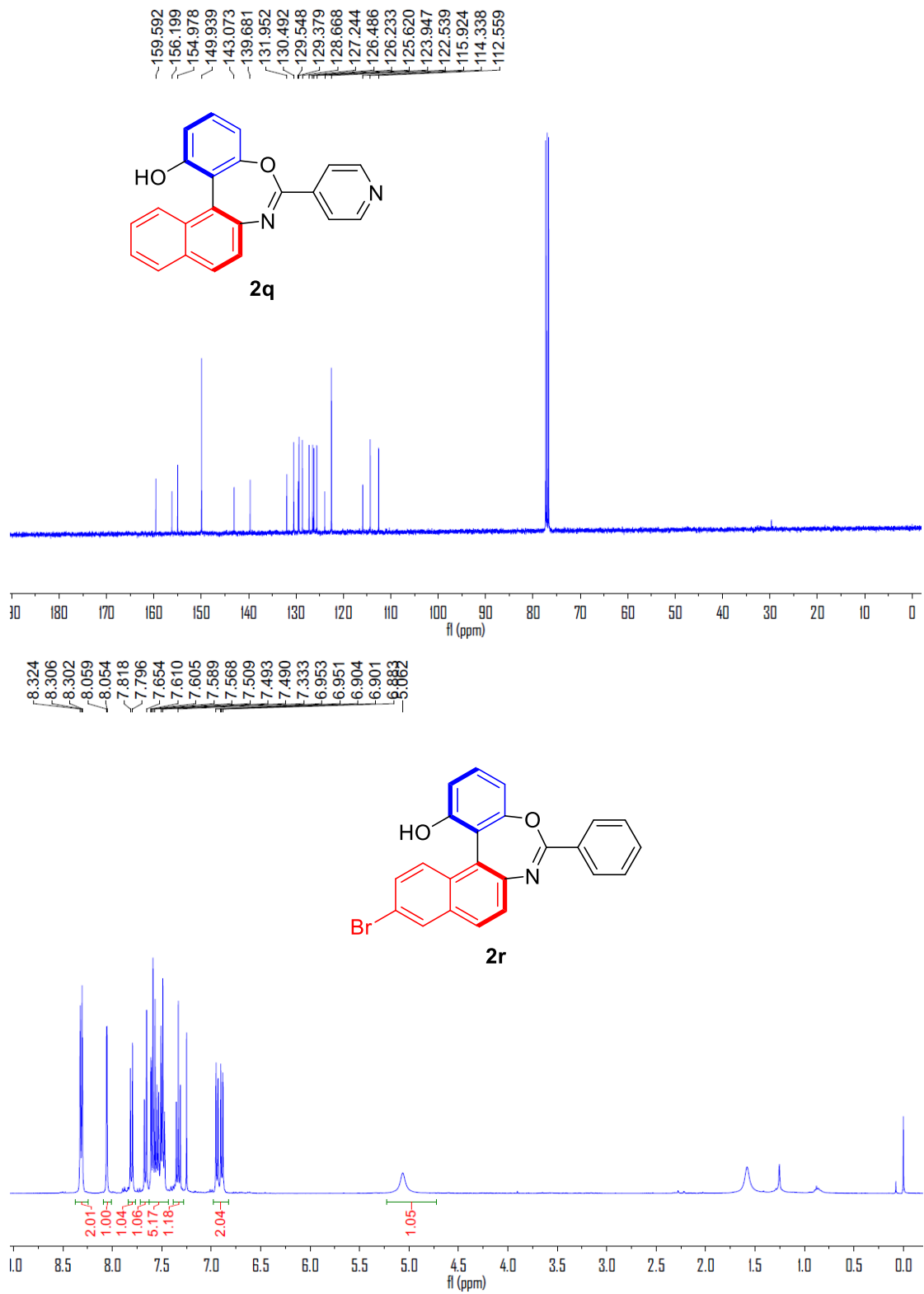


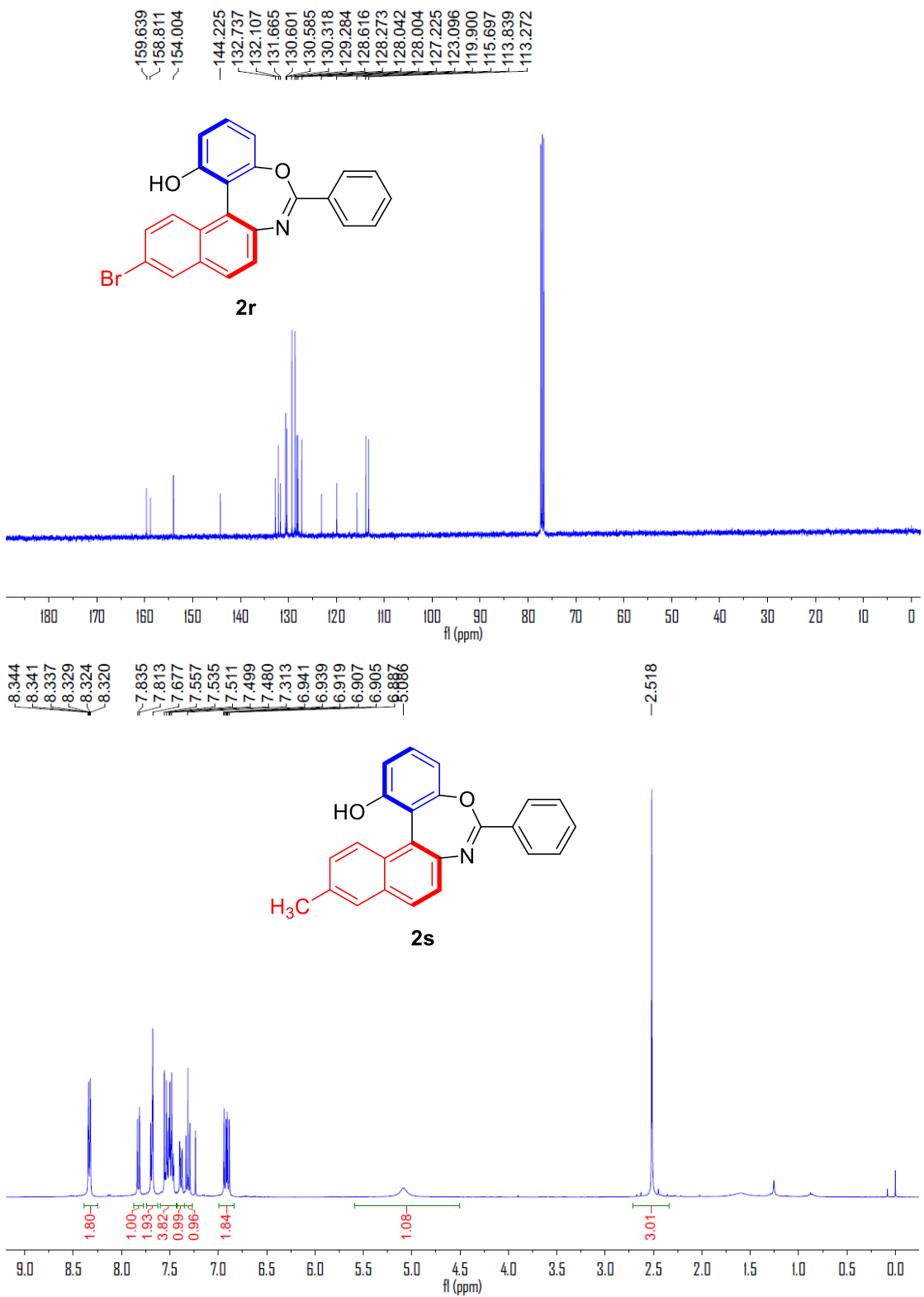


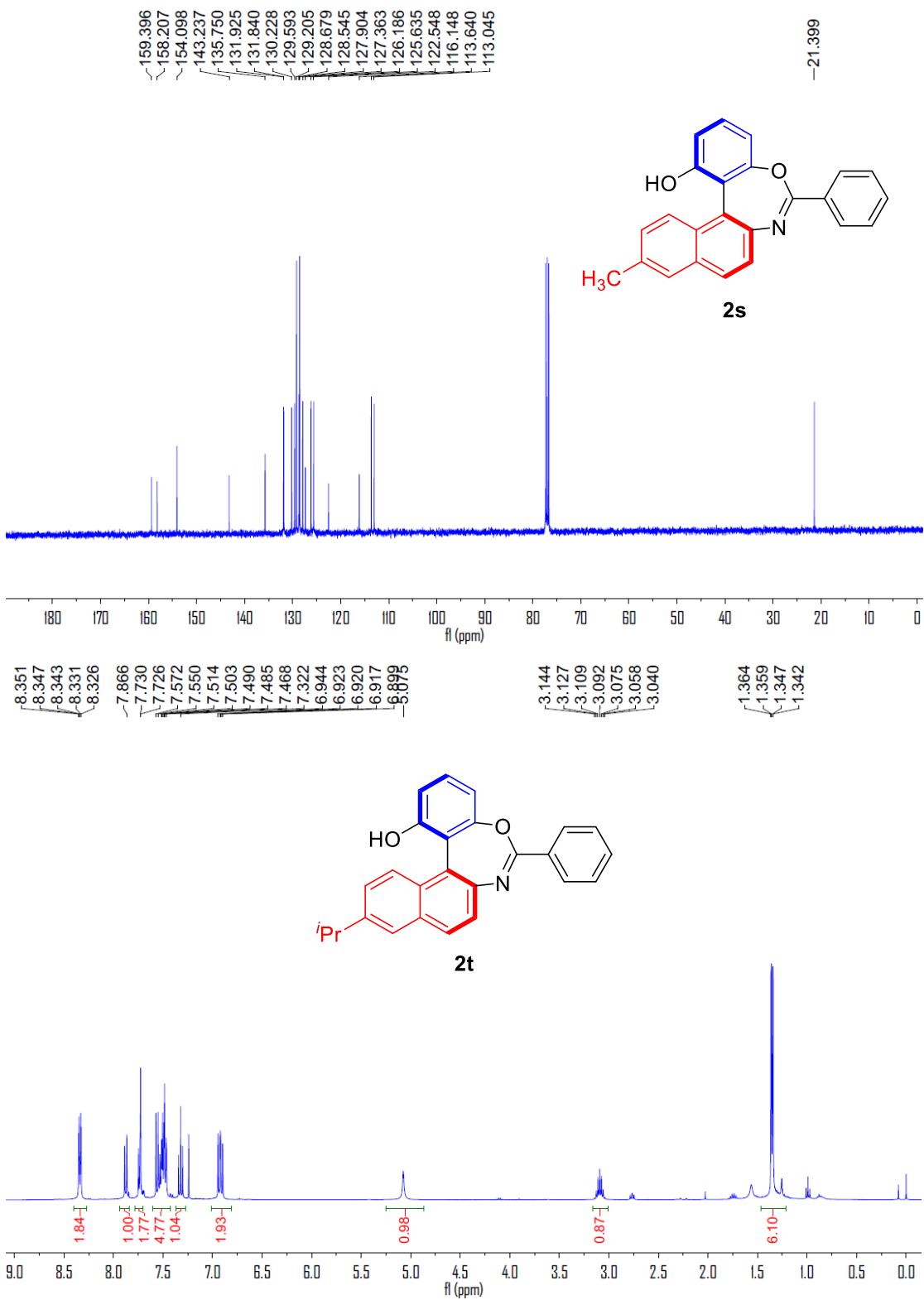


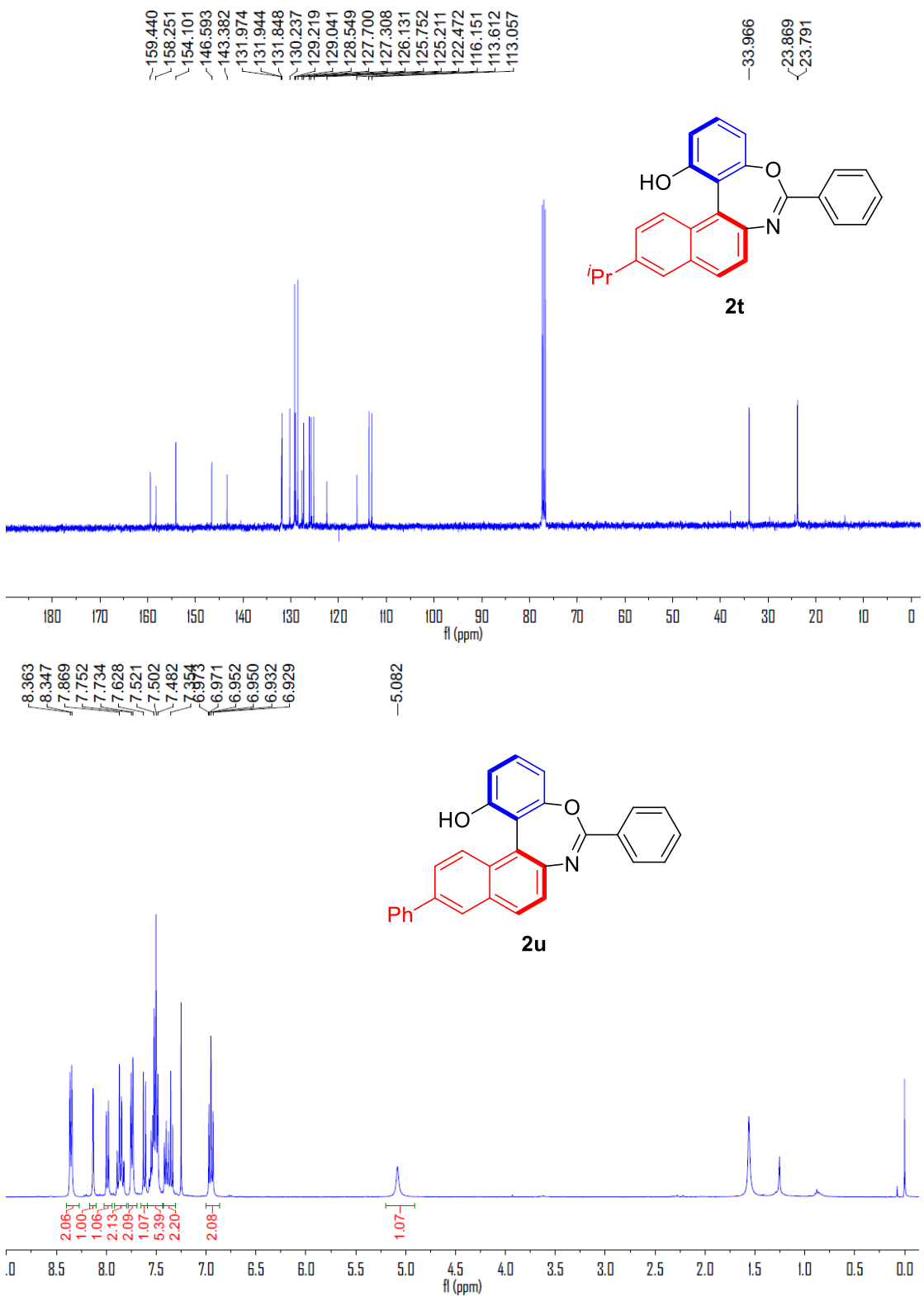


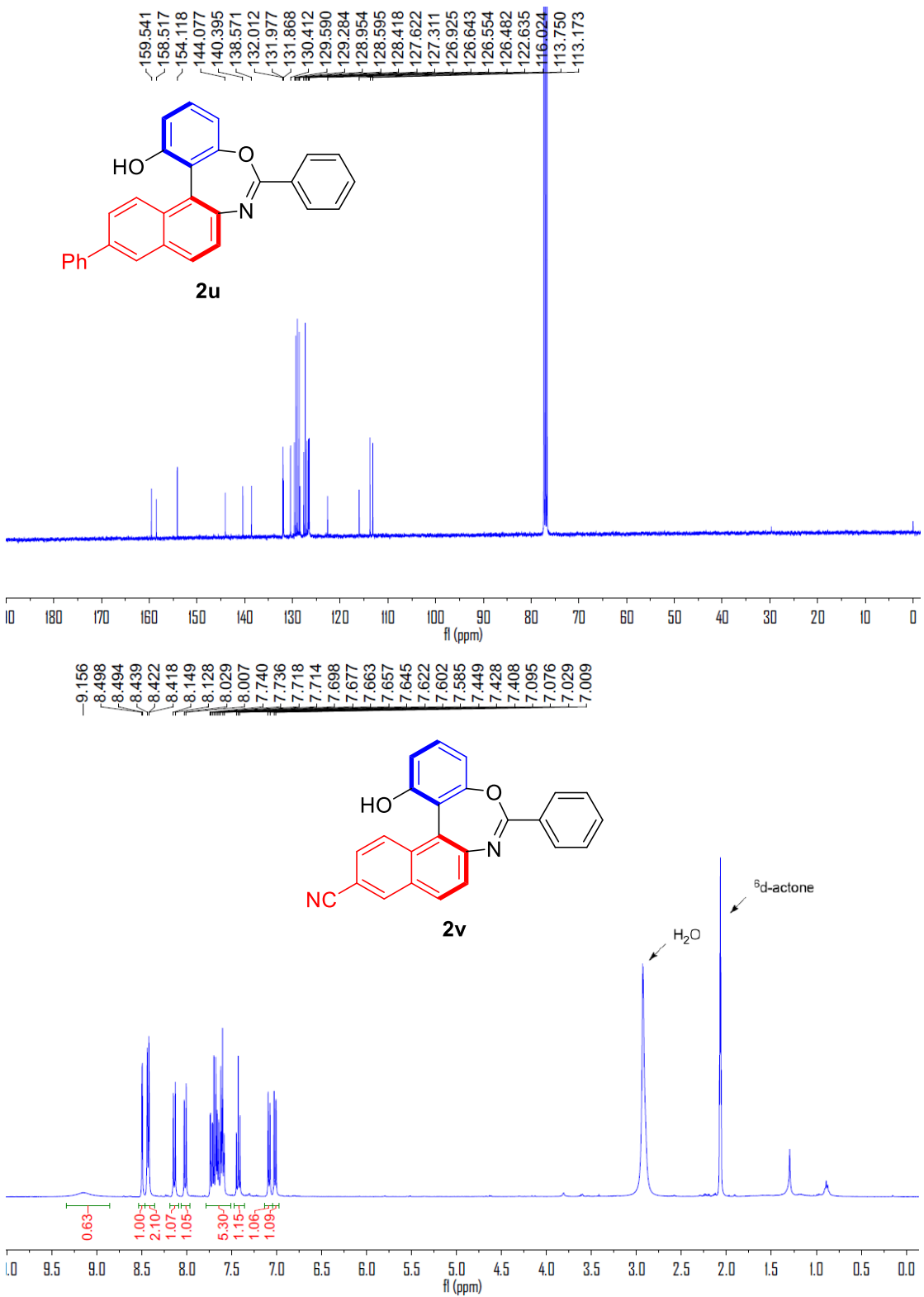


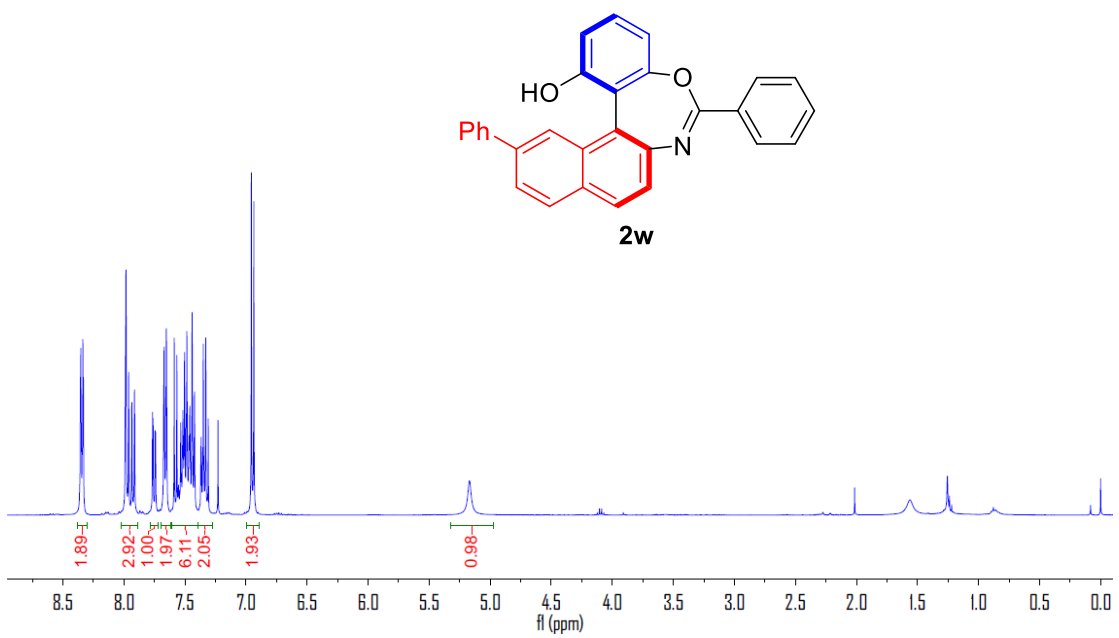
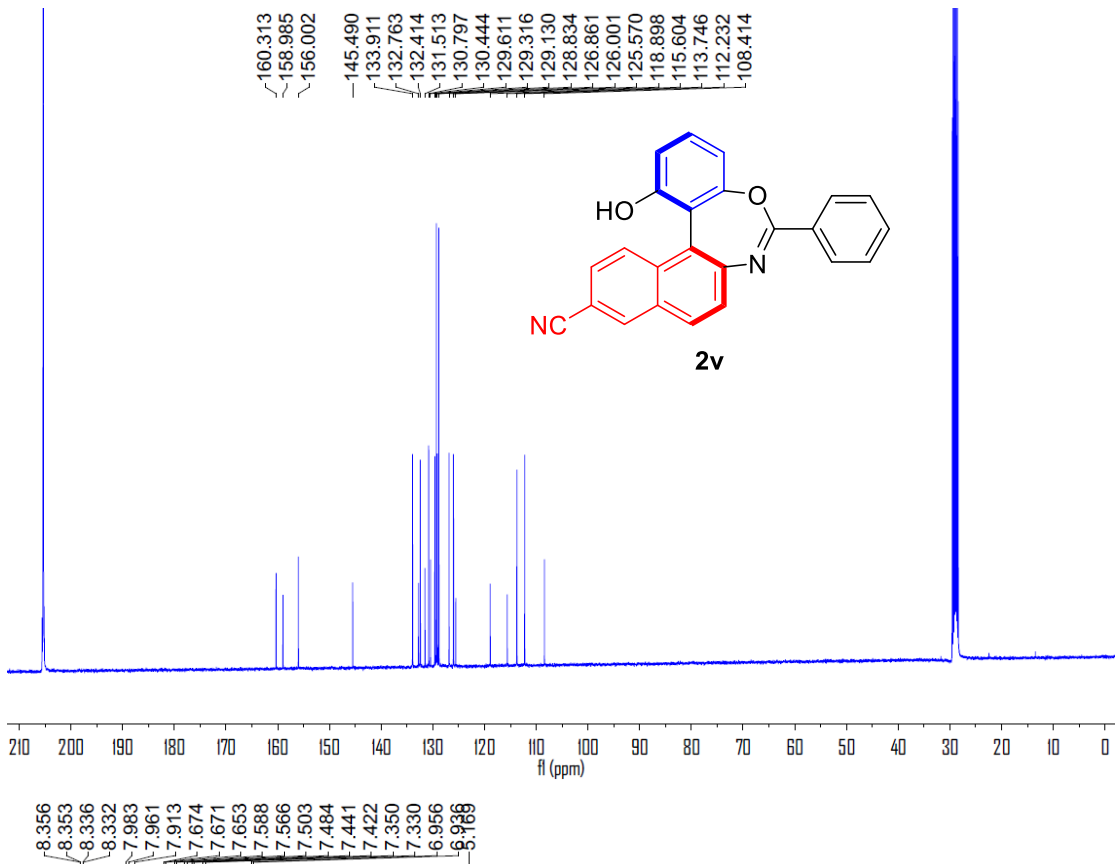


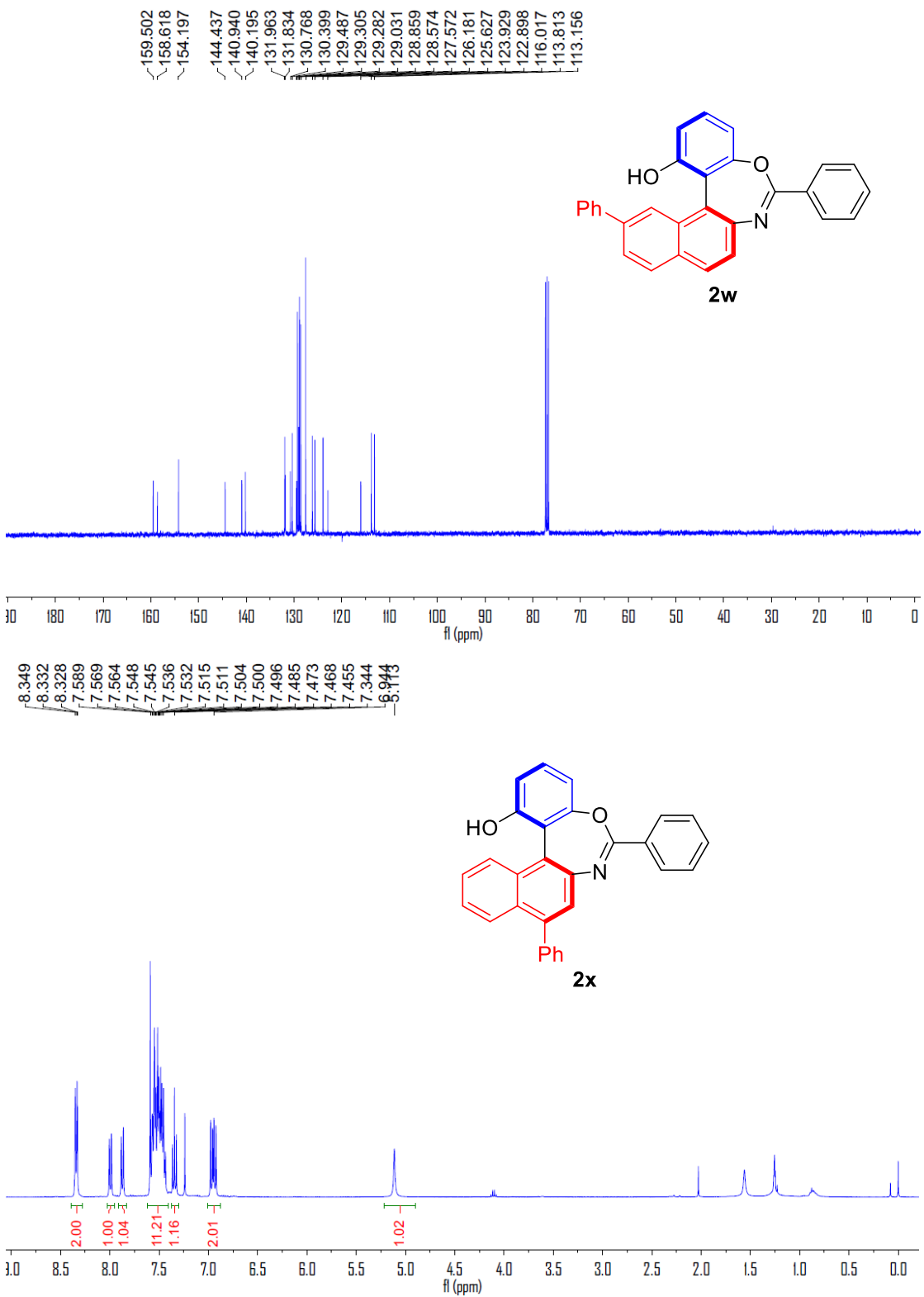


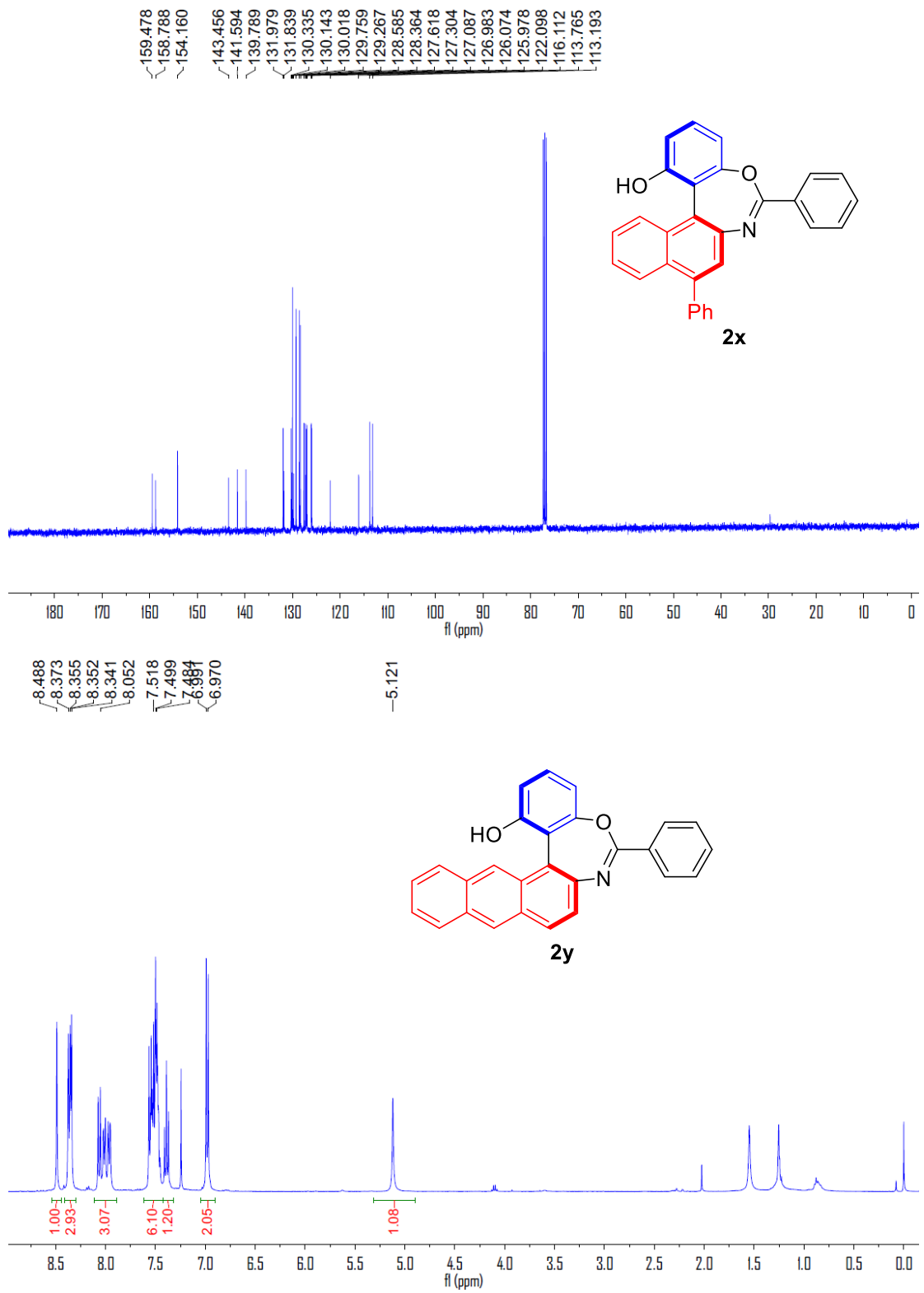


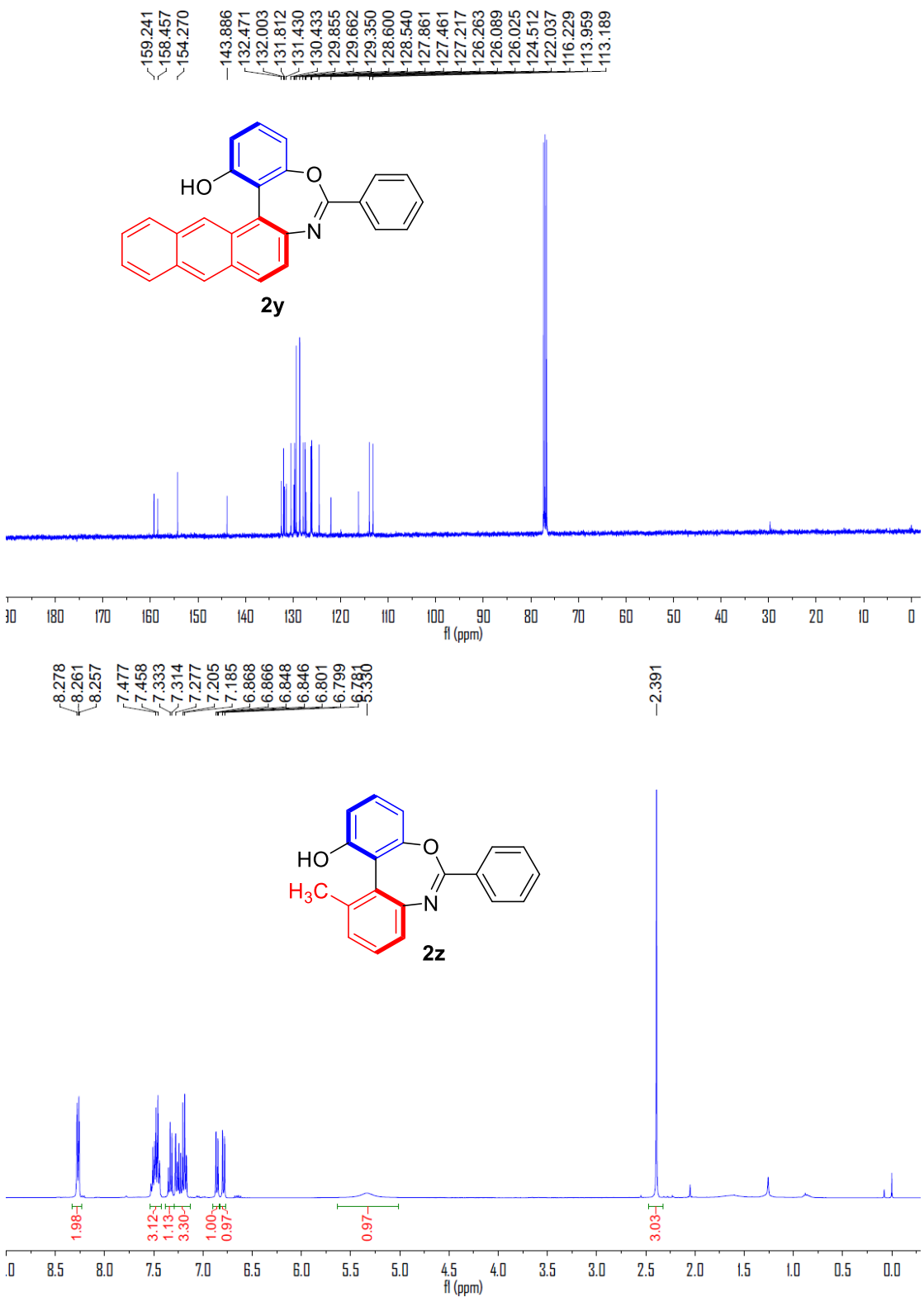


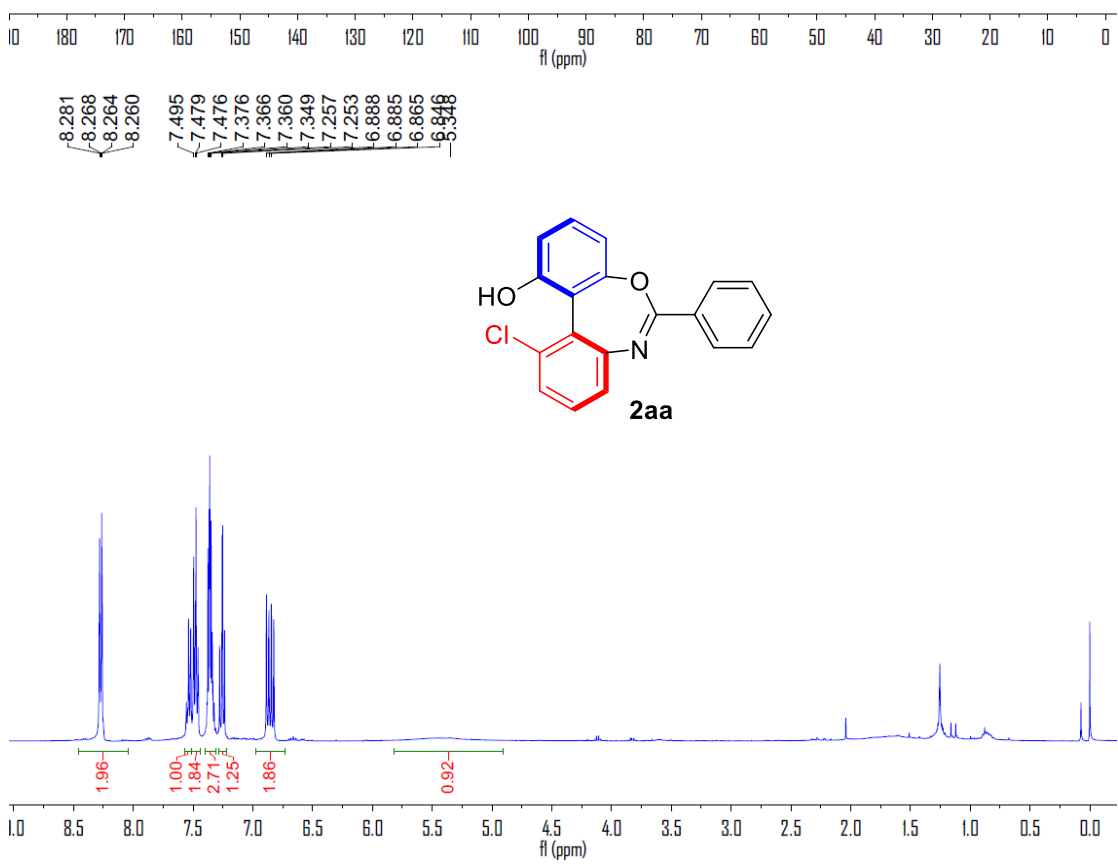
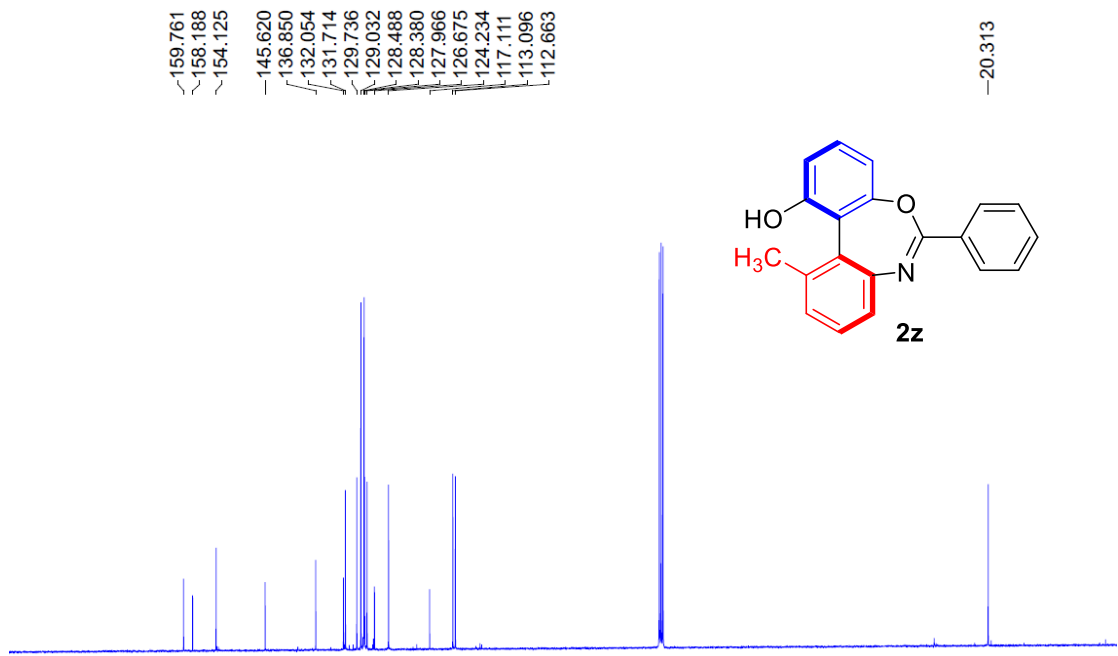


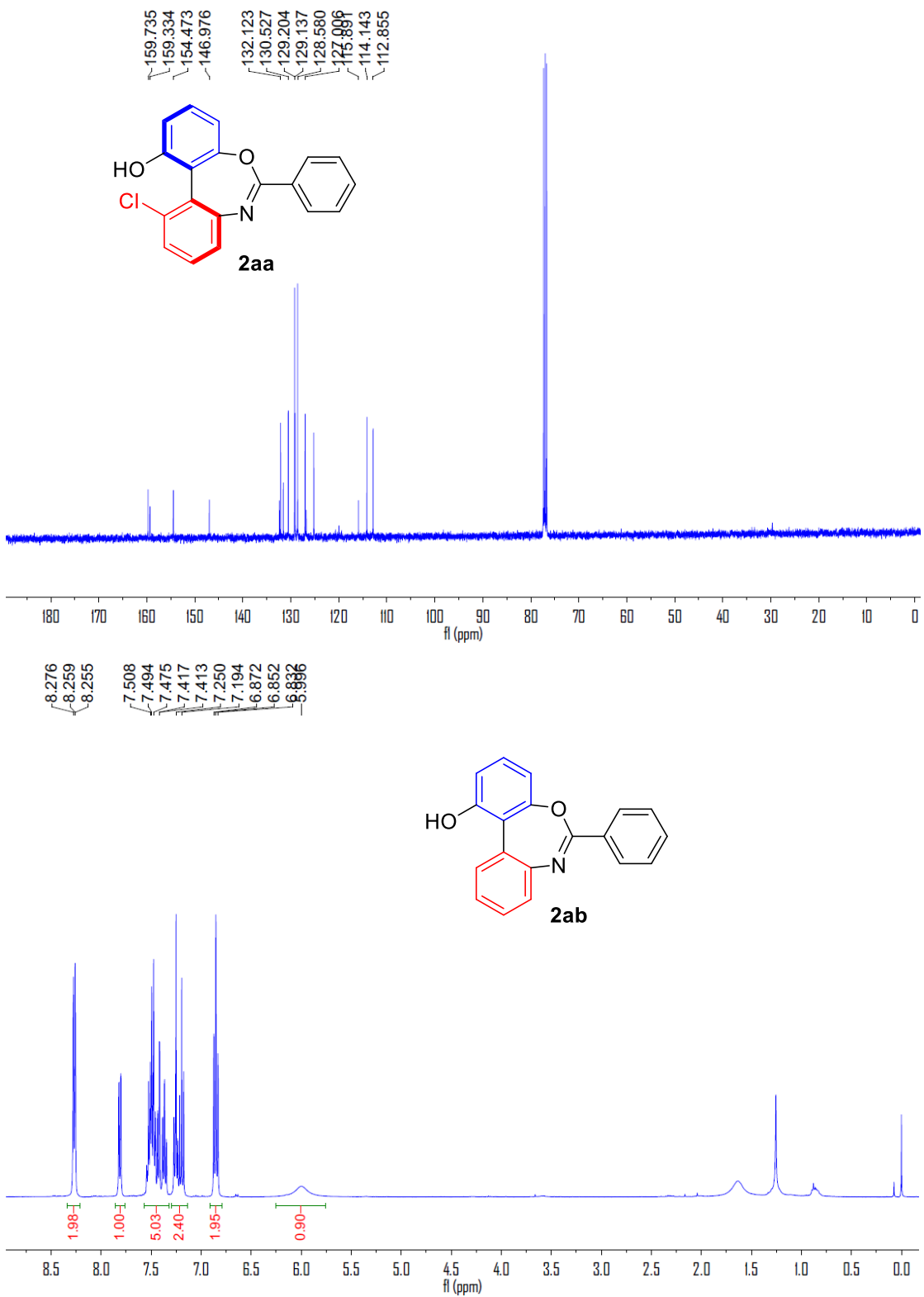


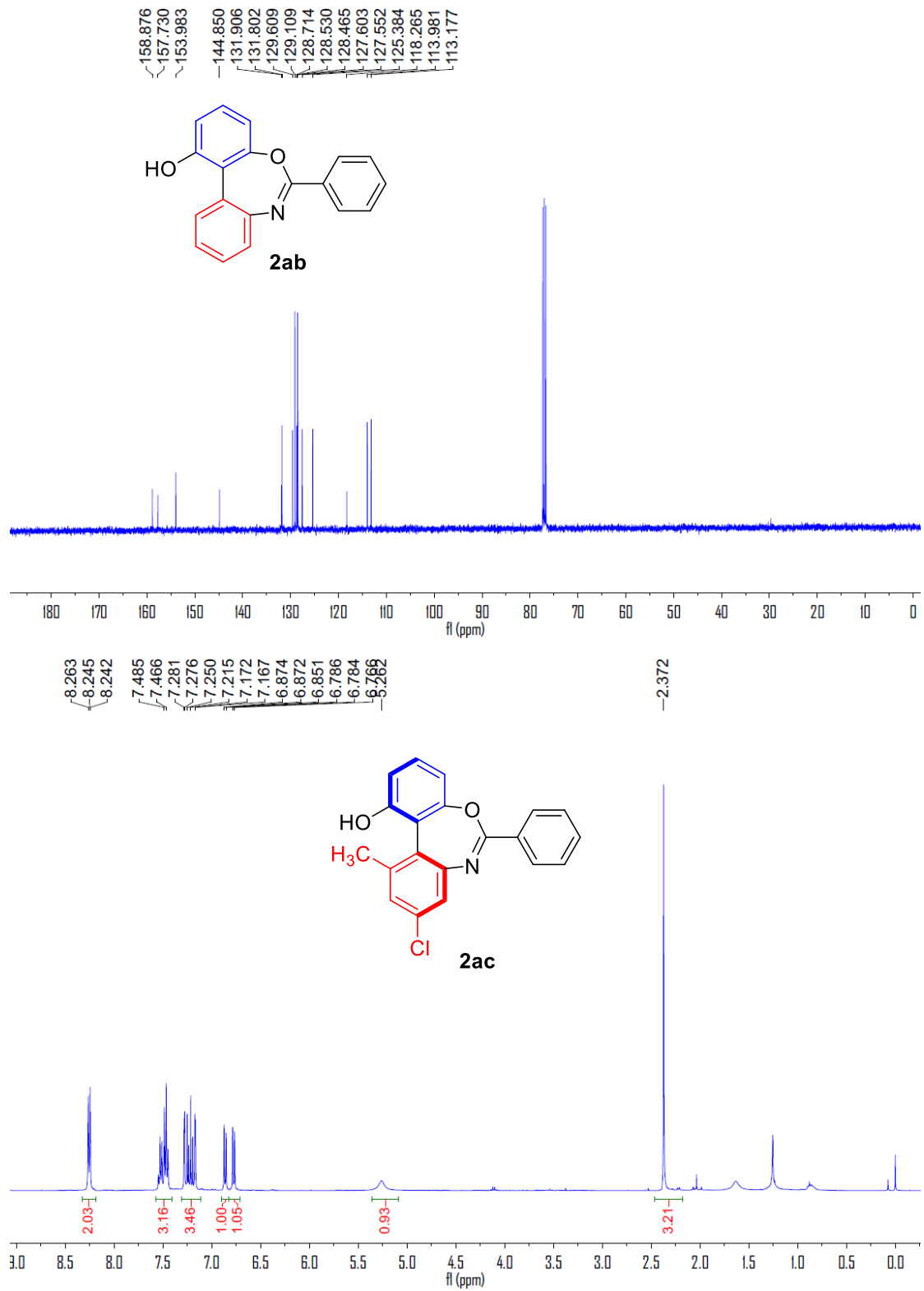


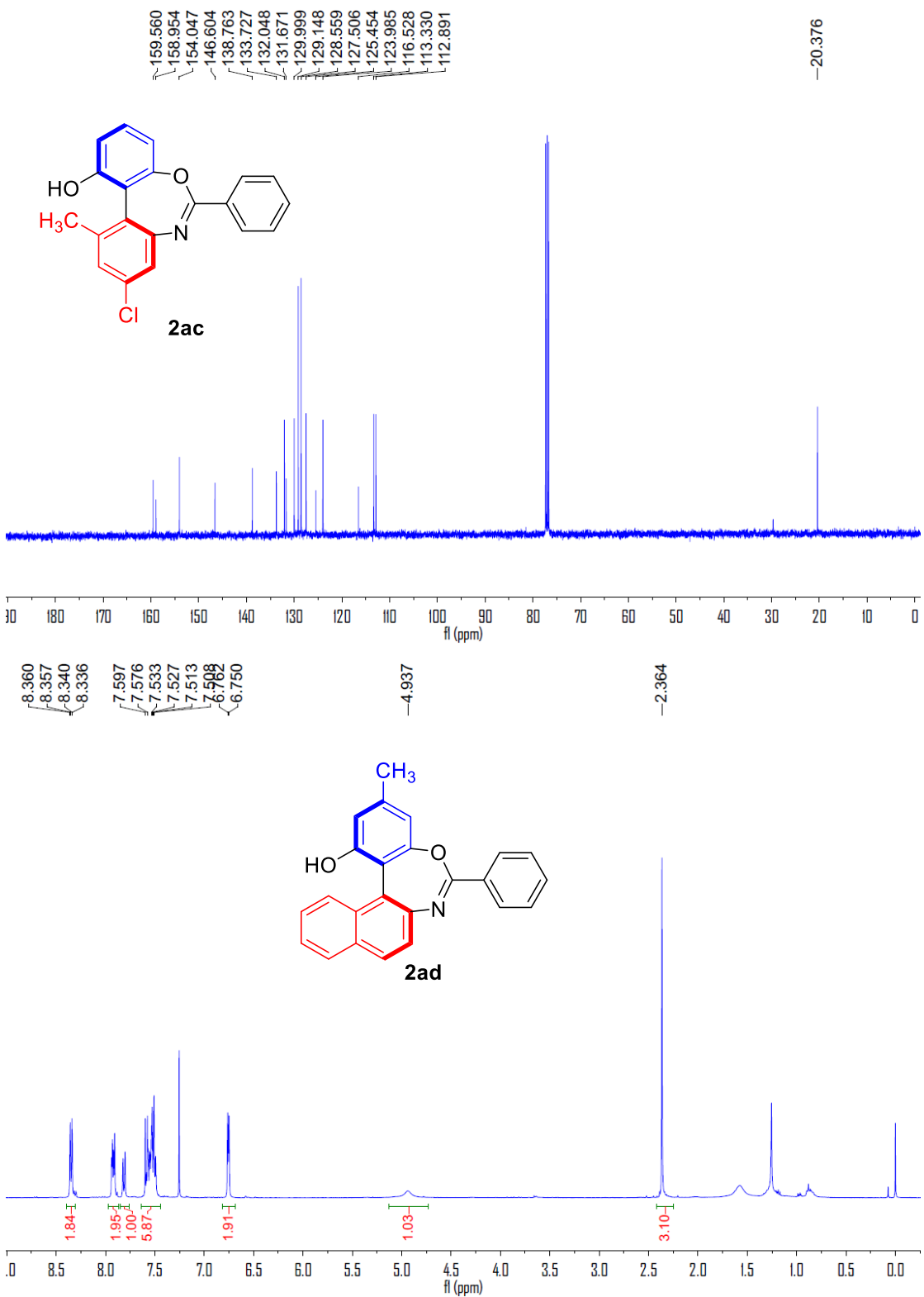


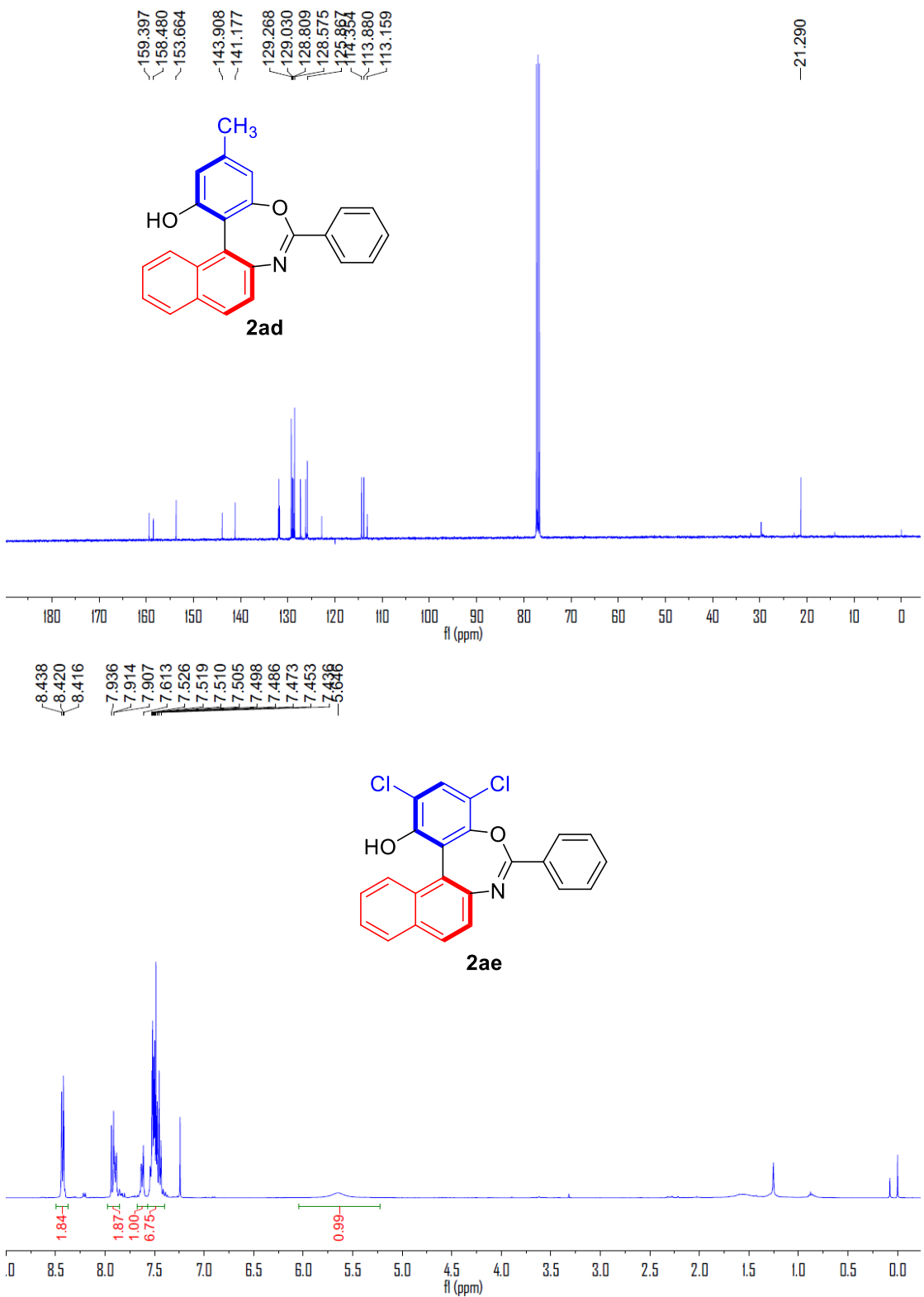


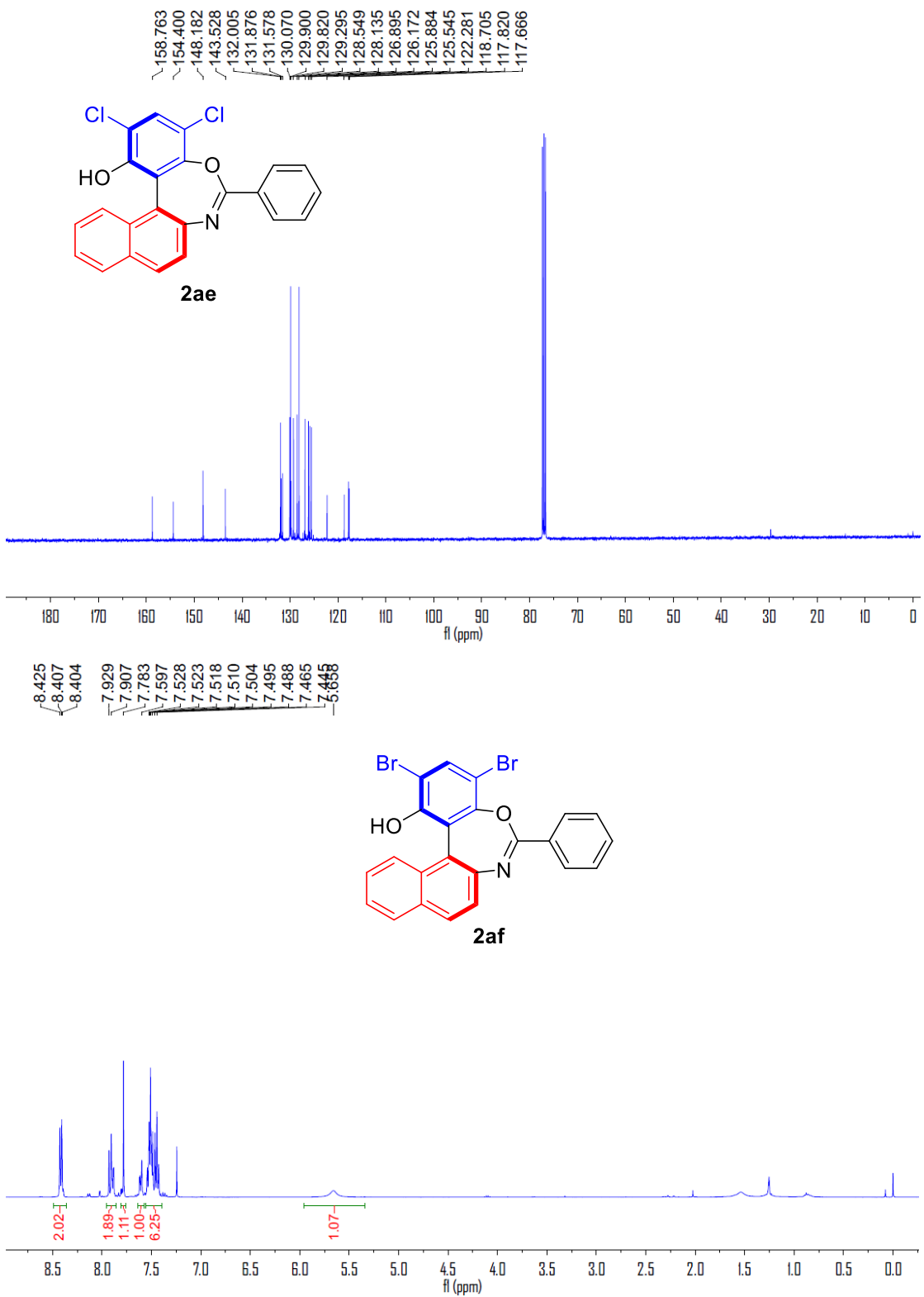


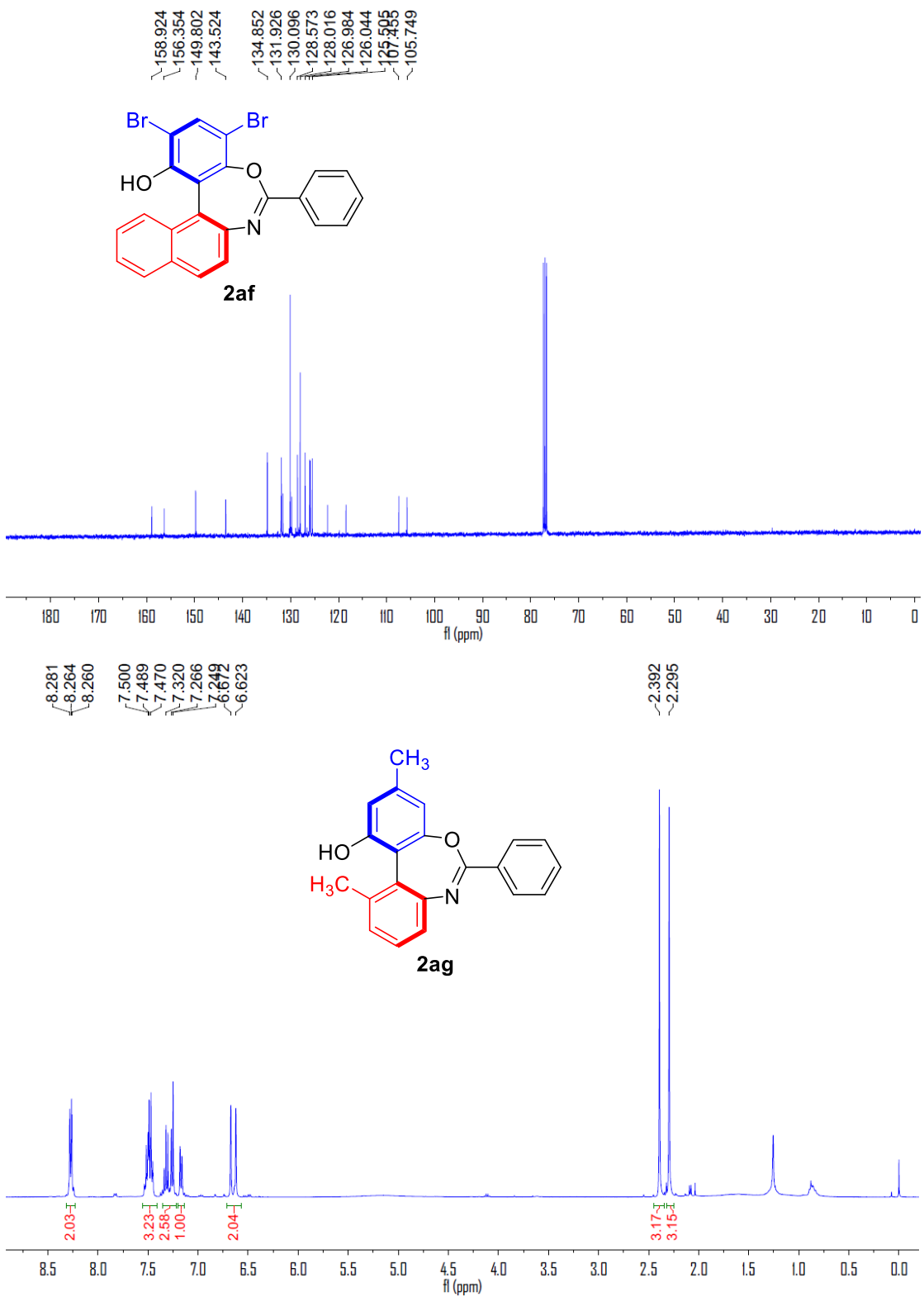


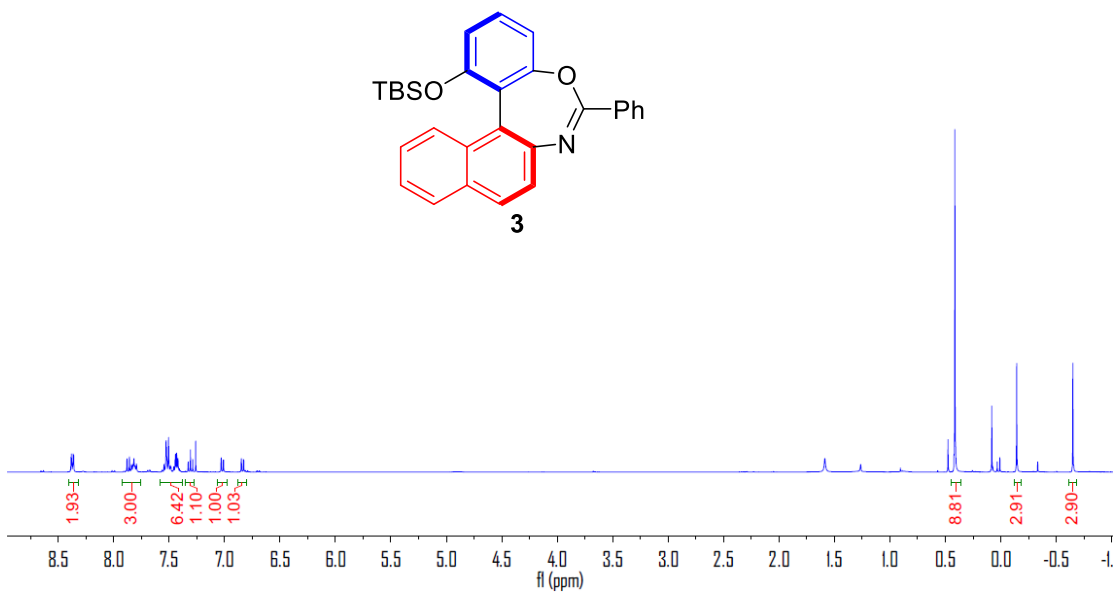
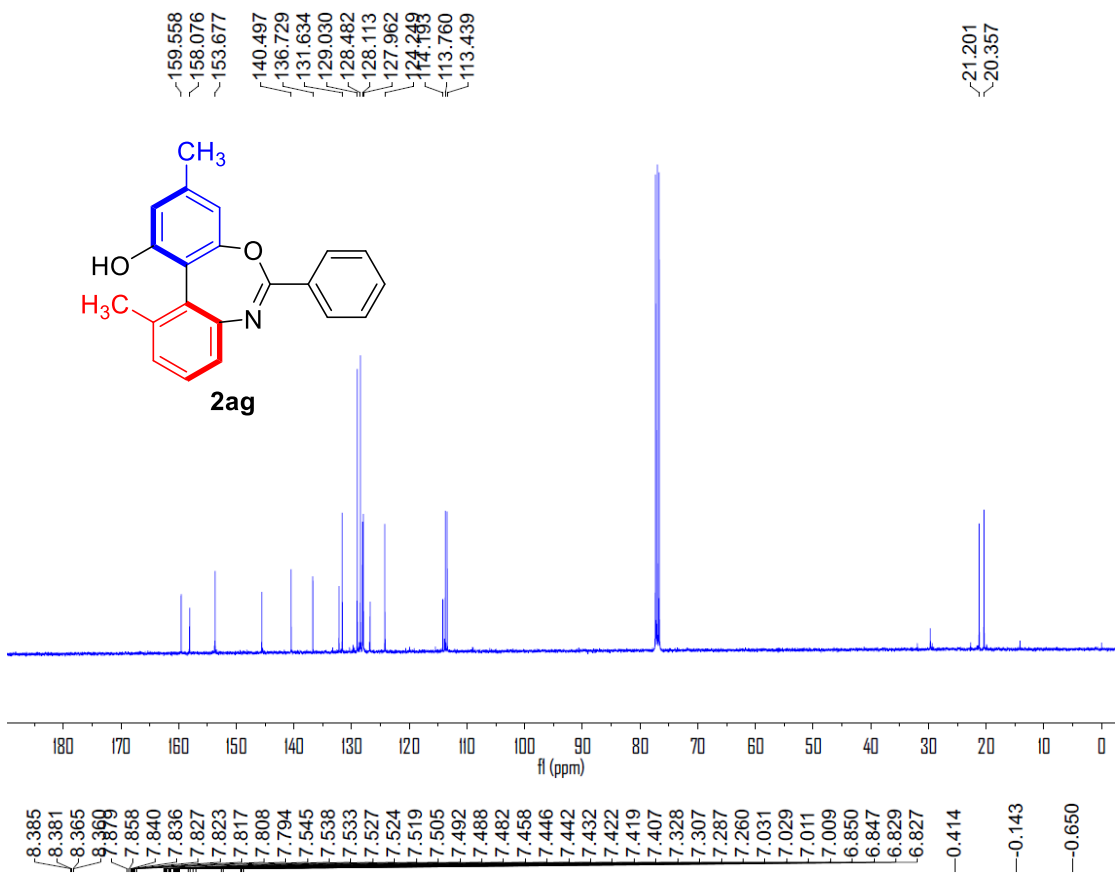


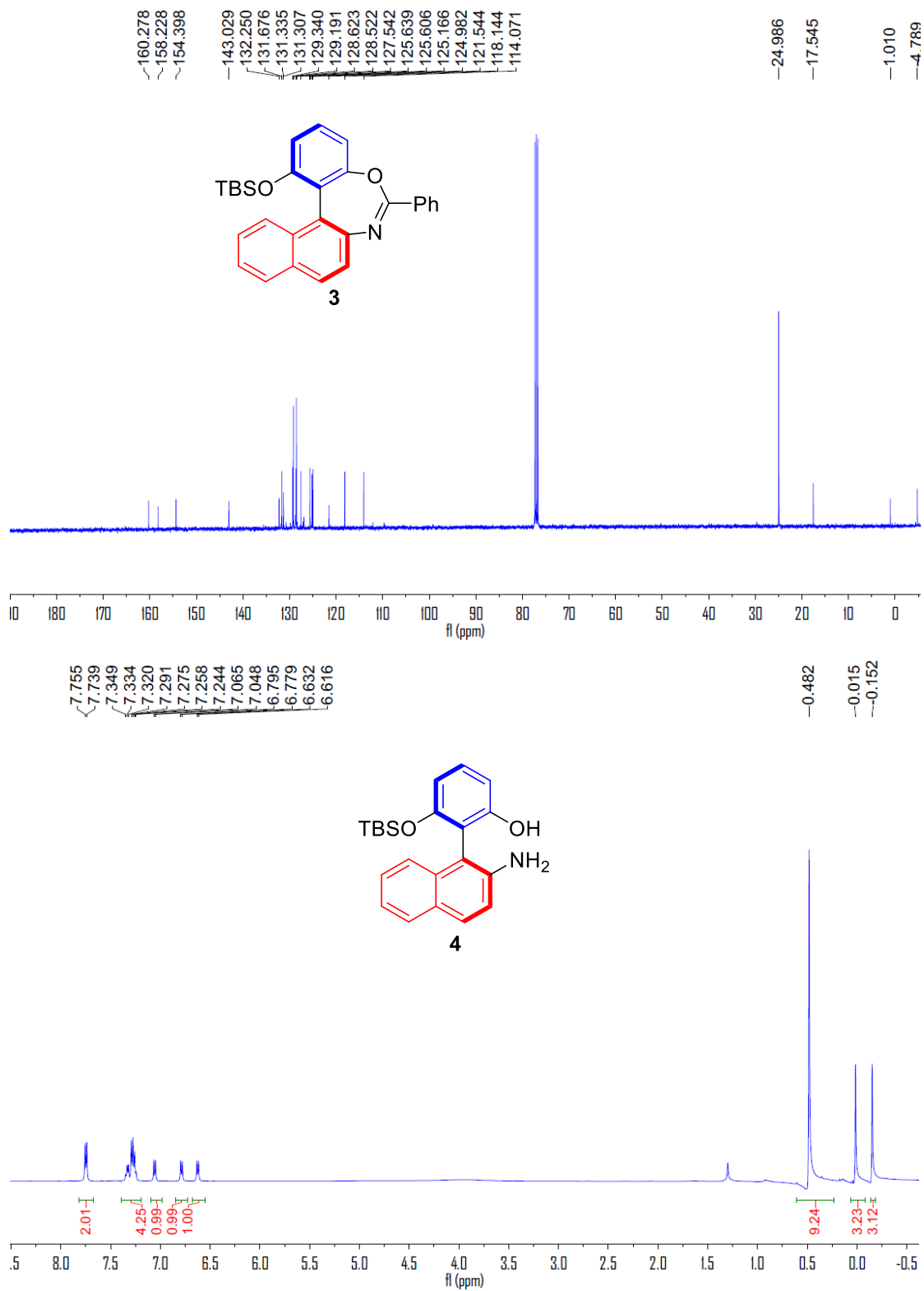


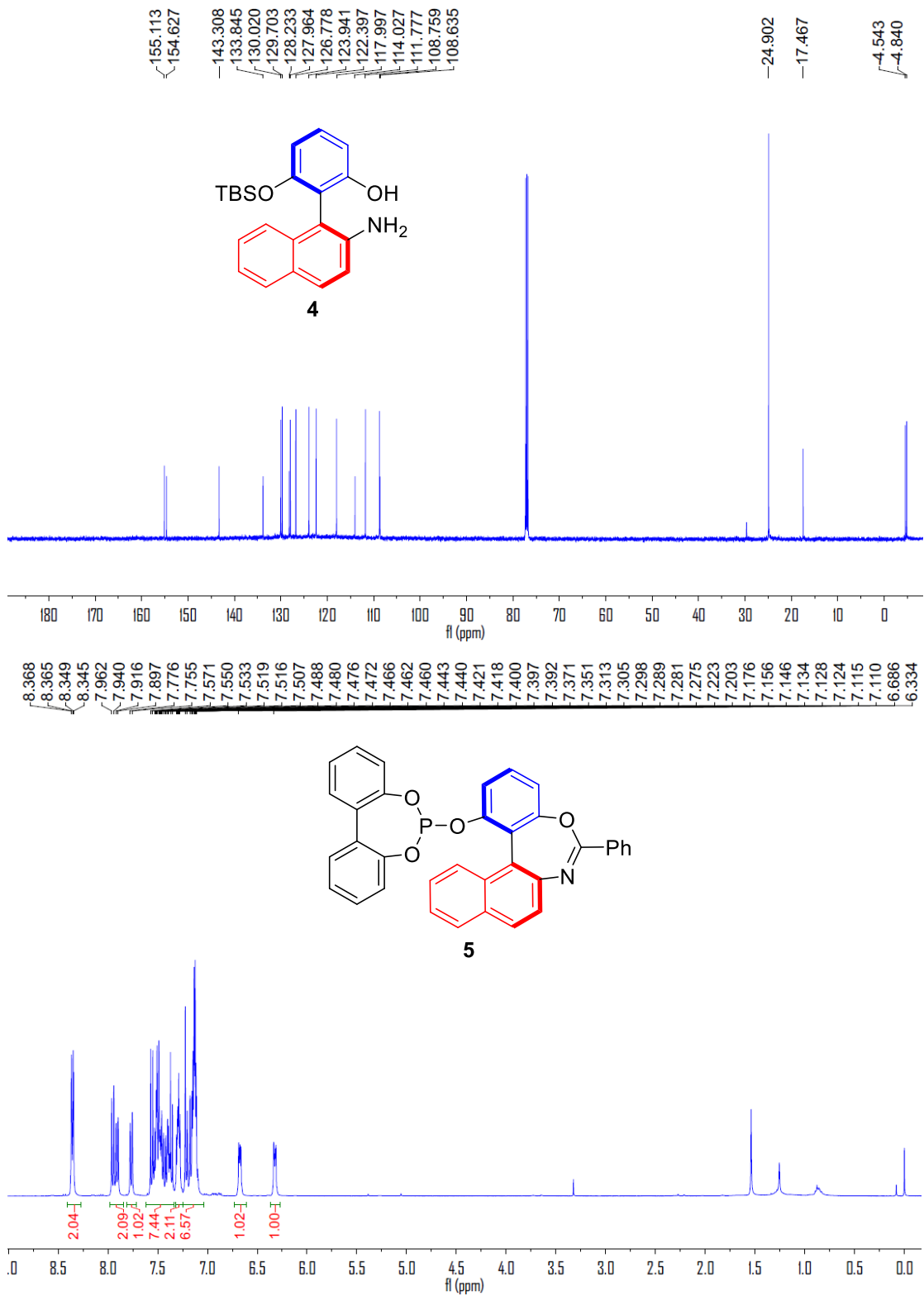


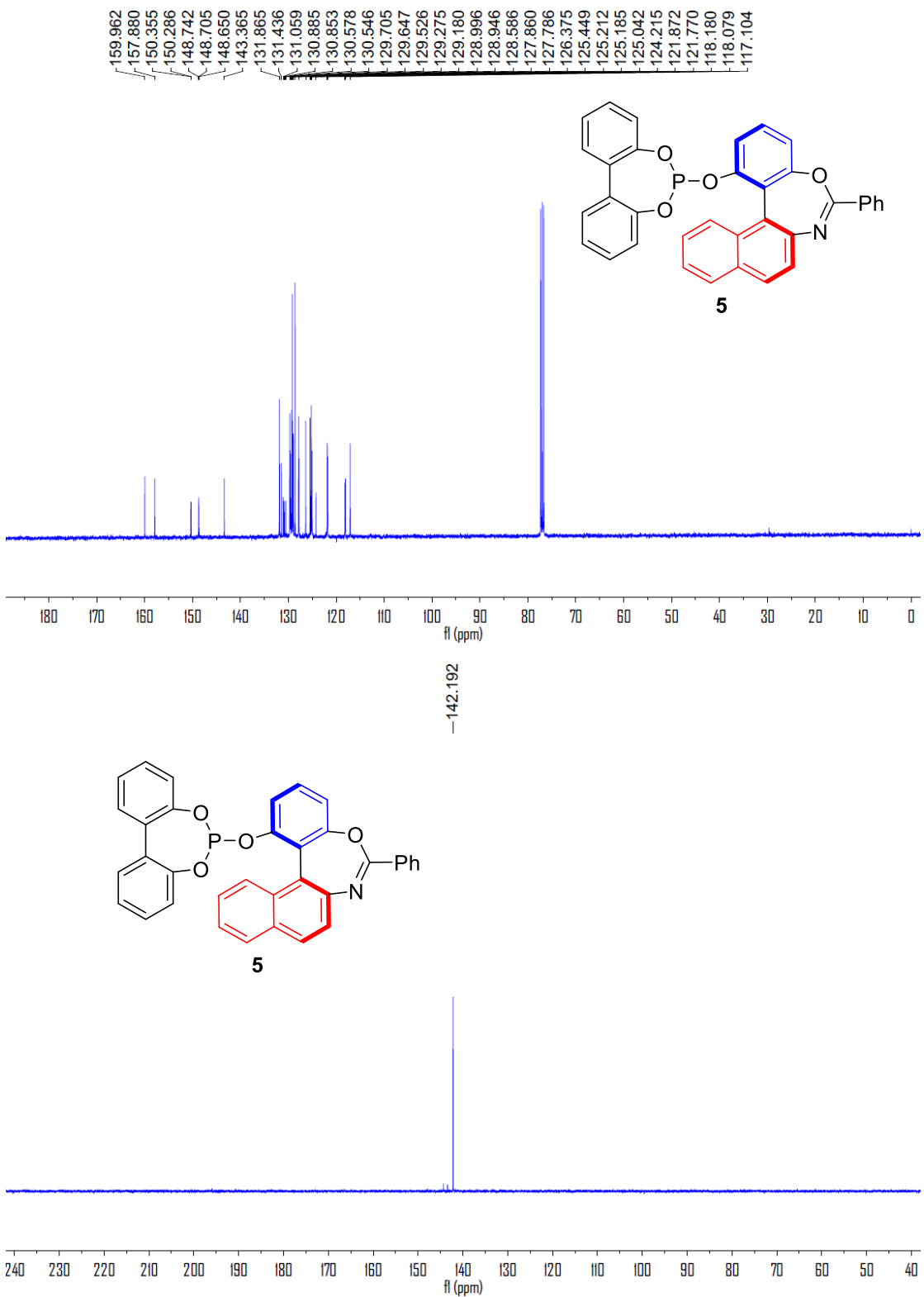




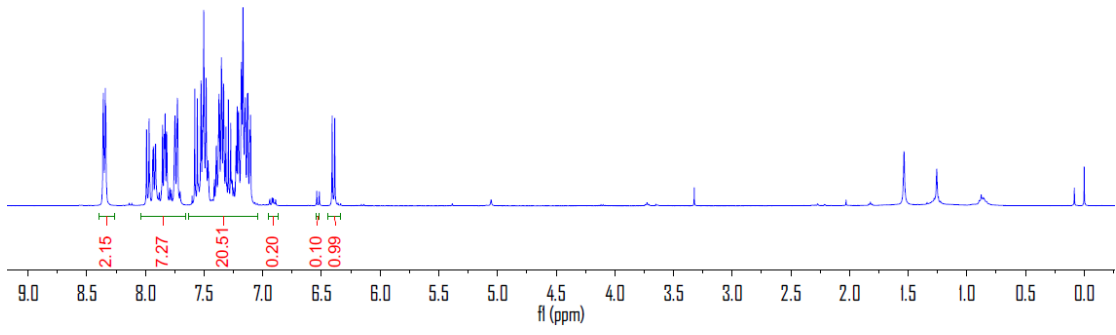
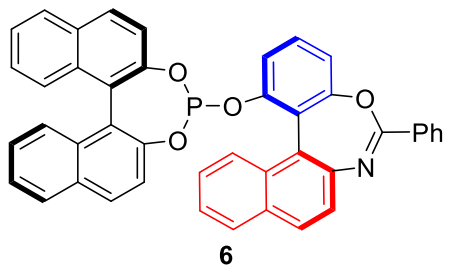




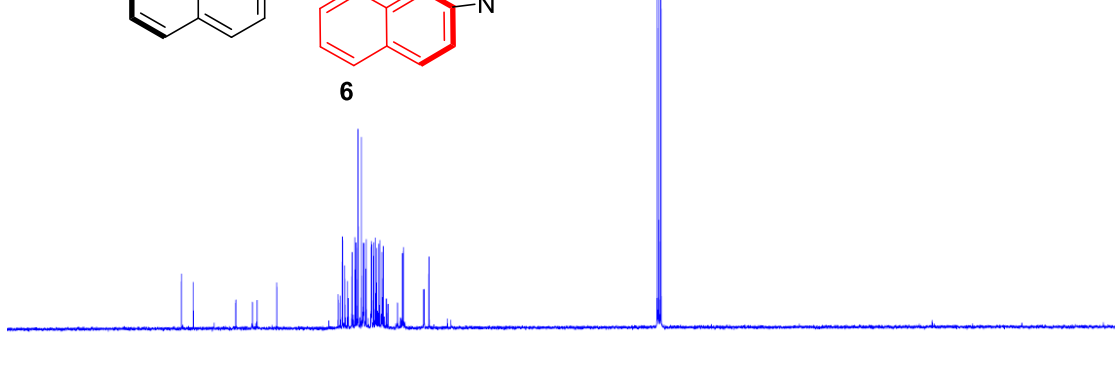
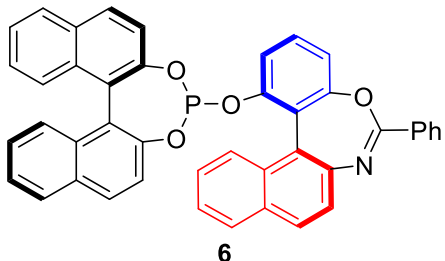


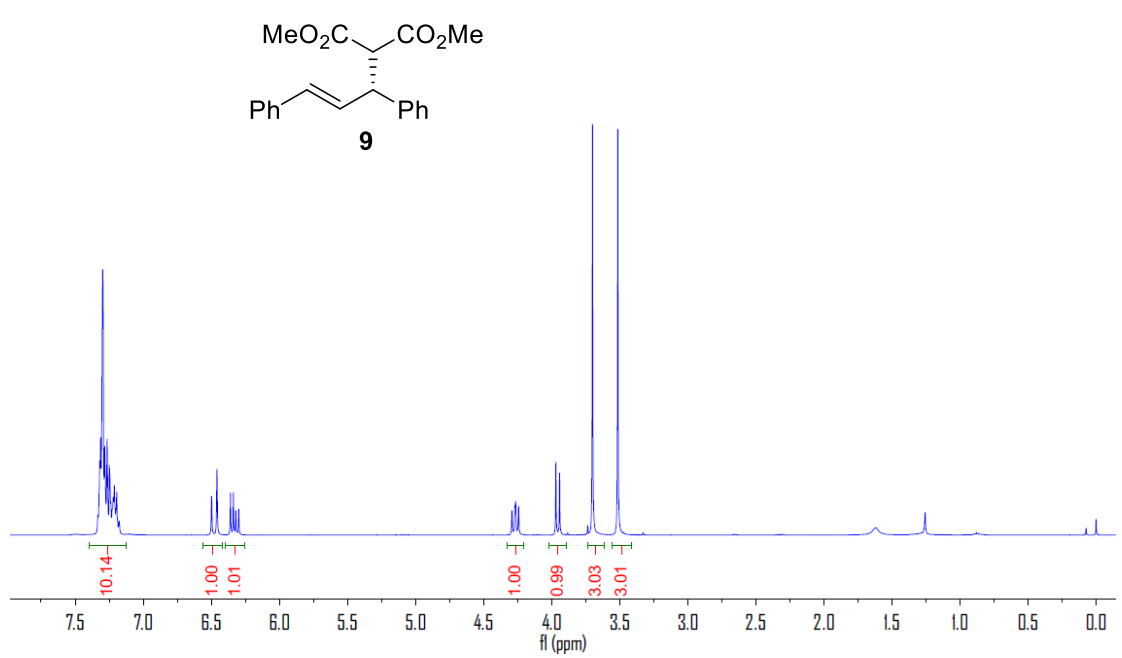
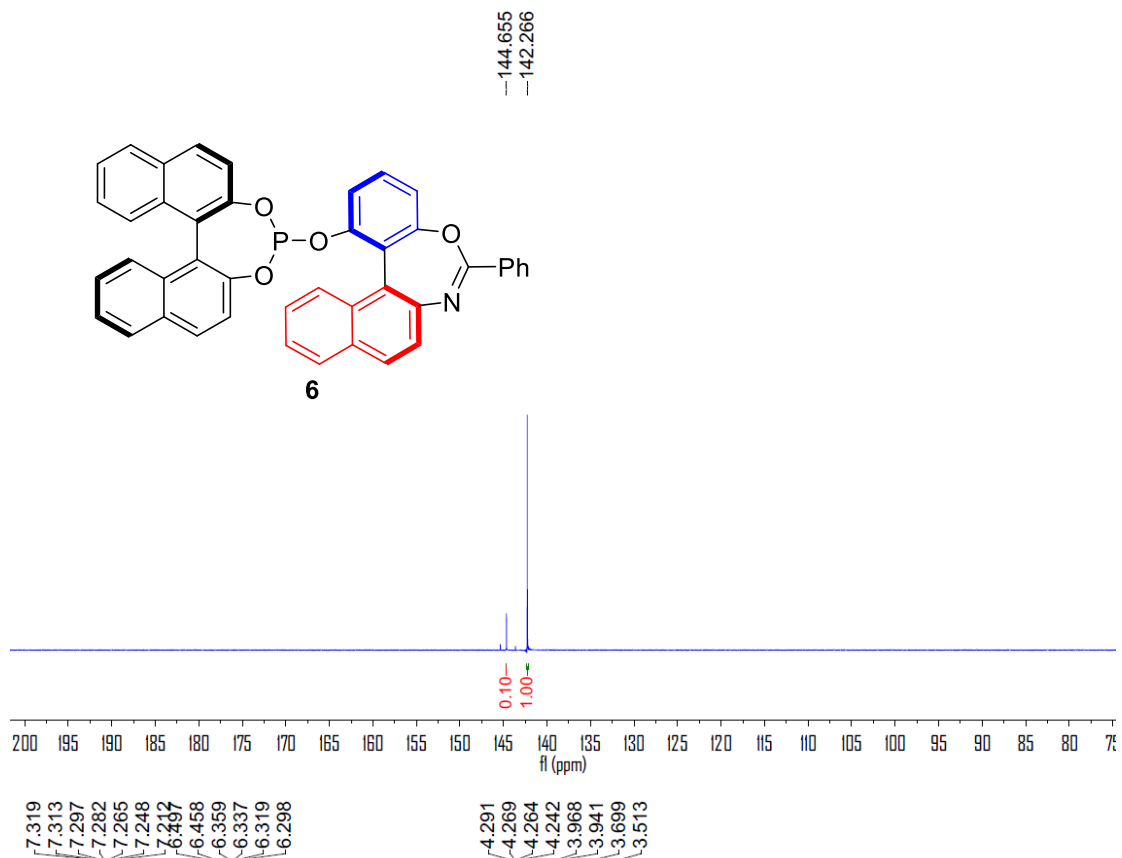


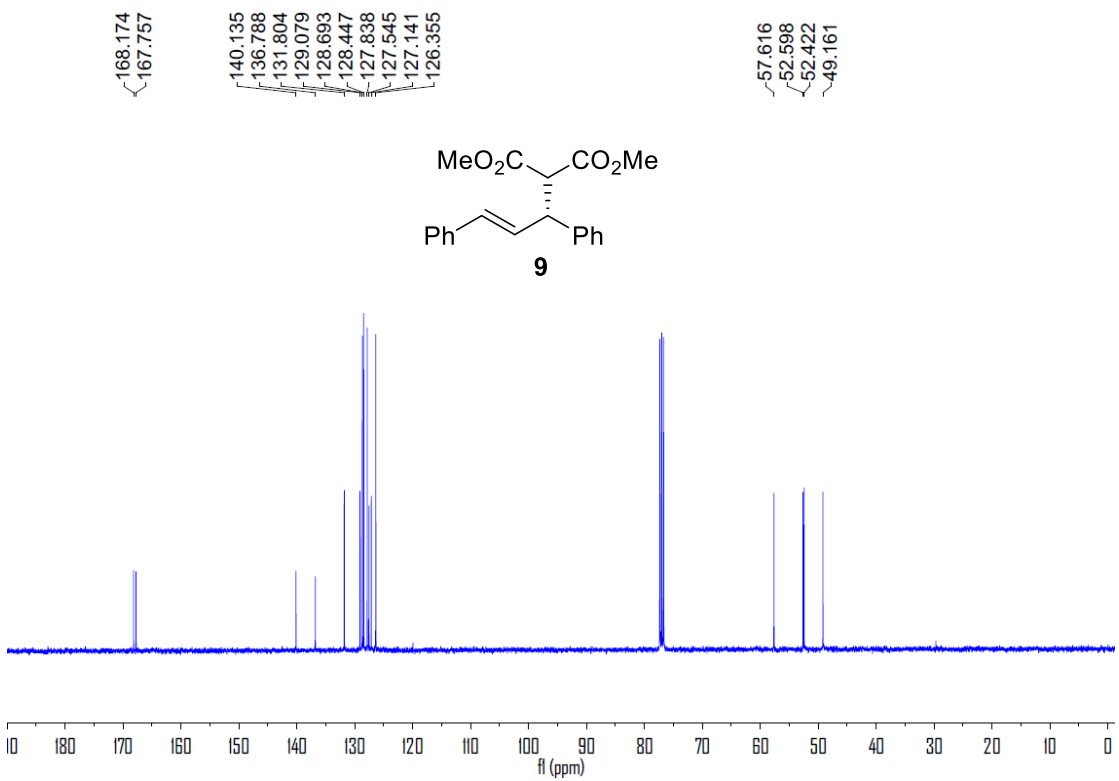
8.358
8.342
8.338
7.990
7.969
7.936
7.932
7.914
7.854
7.839
7.832
7.819
7.748
7.747
7.732
7.579
7.558
7.547
7.526
7.512
7.503
7.483
7.470
7.466
7.461
7.414
7.411
7.397
7.394
7.378
7.373
7.369
7.352
7.334
7.314
7.293
7.273
7.261
7.227
7.218
7.207
7.182
7.169
7.155
7.148
7.130
7.127
7.111
7.104
6.409
-6.387



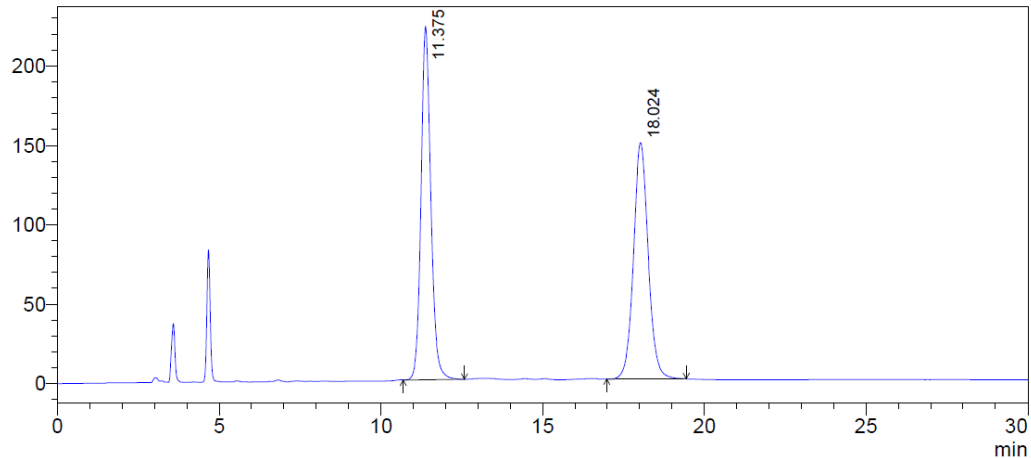
159.792
157.727
150.325
150.325
147.491
147.445
146.680
146.665
143.250
143.250
132.620
132.264
131.900
131.889
131.486
131.448
130.985
130.877
130.858
130.204
129.714
129.499
129.256
129.183
129.164
128.588
128.250
128.188
128.130
127.808
127.745
126.877
126.771
126.454
126.182
125.942
125.788
125.591
125.387
125.039
124.804
124.259
124.003
123.952
122.327
122.303
121.486
121.310
117.810
117.717
116.875





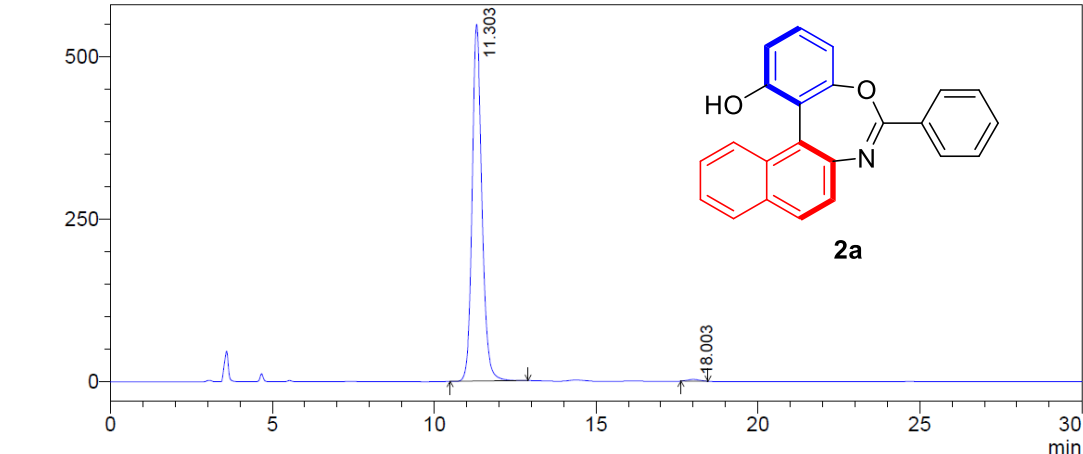


mV

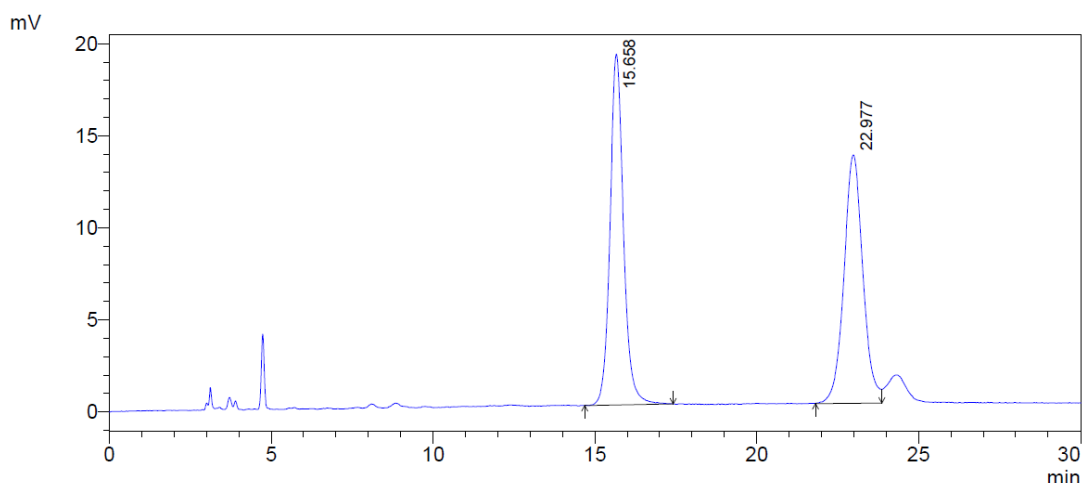


Peak#	Ret. Time	Area	Height	Area %	Height %
1	11.375	4704415	222475	49.998	59.937
2	18.024	4704733	148707	50.002	40.063
Total		9409148	371182	100.000	100.000

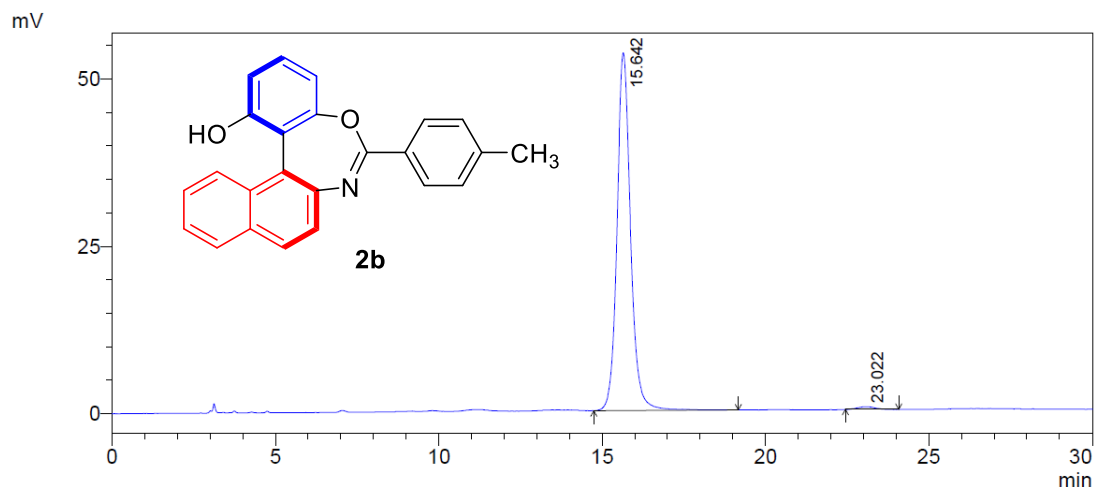
mV



Peak#	Ret. Time	Area	Height	Area %	Height %
1	11.303	11517925	548342	99.409	99.521
2	18.003	68530	2641	0.591	0.479
Total		11586456	550983	100.000	100.000

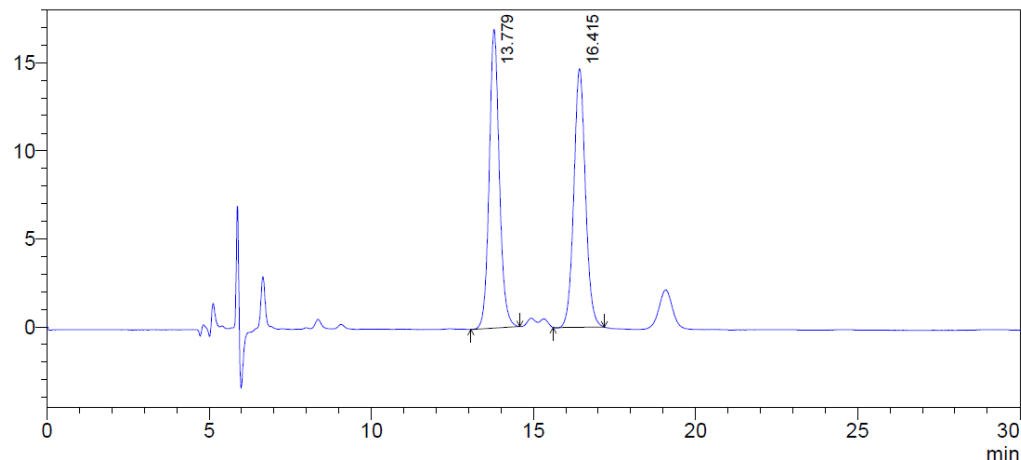


Peak#	Ret. Time	Area	Height	Area %	Height %
1	15.658	550273	19047	50.035	58.529
2	22.977	549507	13496	49.965	41.471
Total		1099781	32542	100.000	100.000



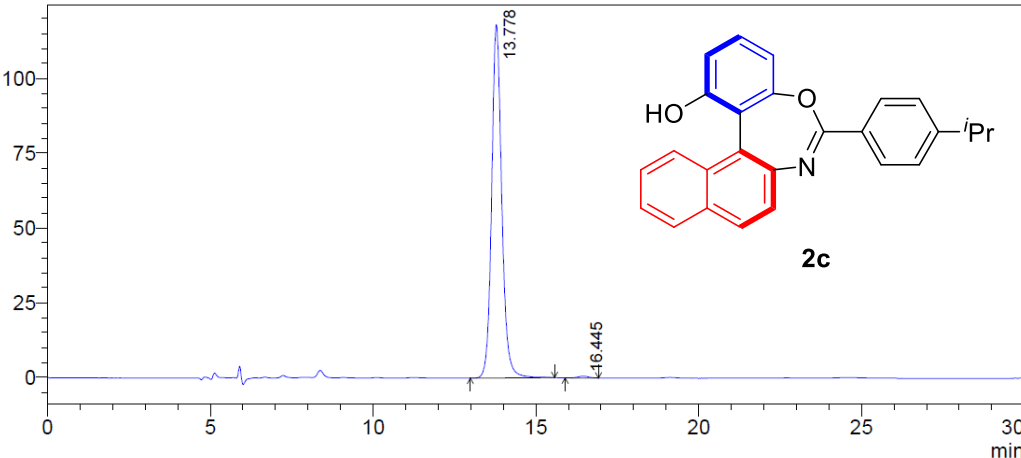
Peak#	Ret. Time	Area	Height	Area %	Height %
1	15.642	1540168	53411	99.022	99.237
2	23.022	15204	411	0.978	0.763
Total		1555372	53822	100.000	100.000

mAU

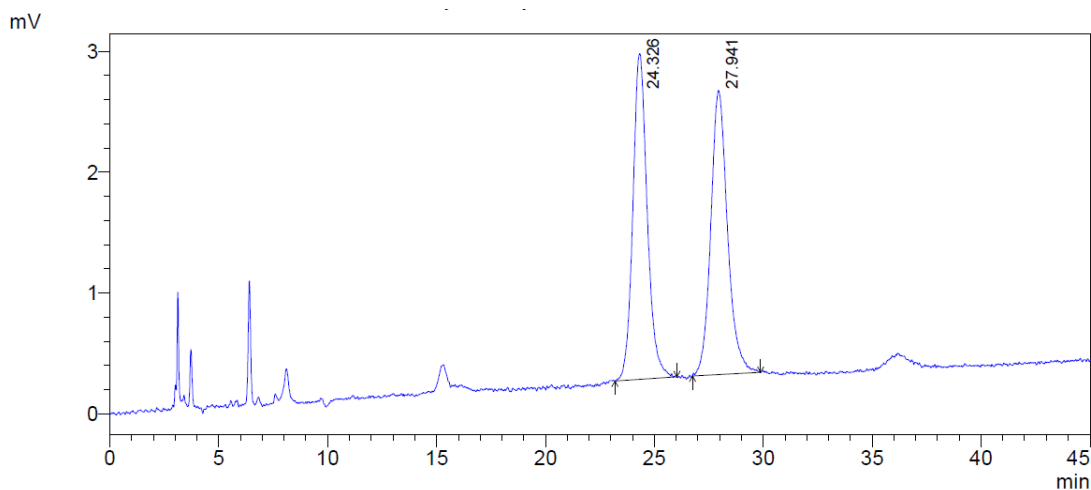


Peak#	Ret. Time	Area	Height	Area %	Height %
1	13.779	369106	16951	50.233	53.576
2	16.415	365685	14688	49.767	46.424
Total		734791	31639	100.000	100.000

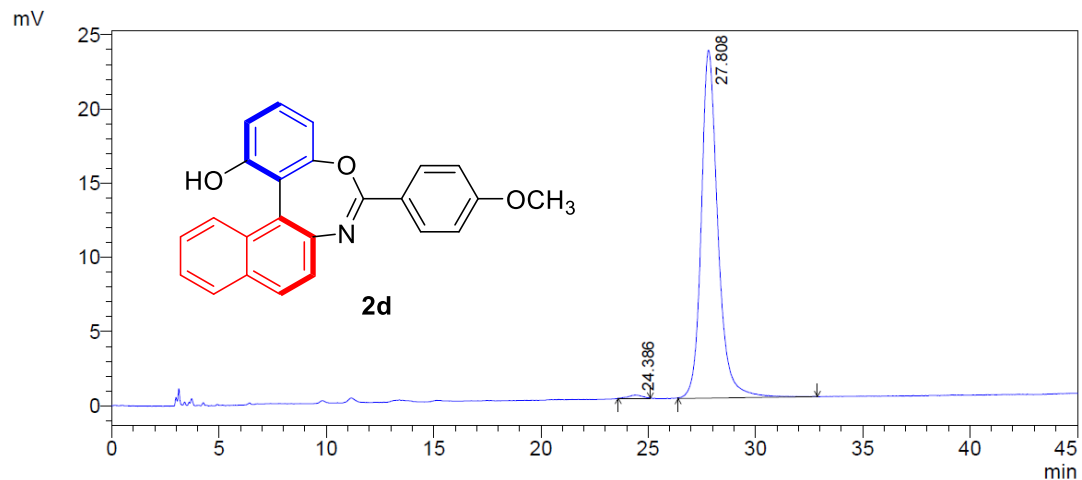
mAU



Peak#	Ret. Time	Area	Height	Area %	Height %
1	13.778	2557804	118187	99.452	99.490
2	16.445	14106	606	0.548	0.510
Total		2571911	118793	100.000	100.000

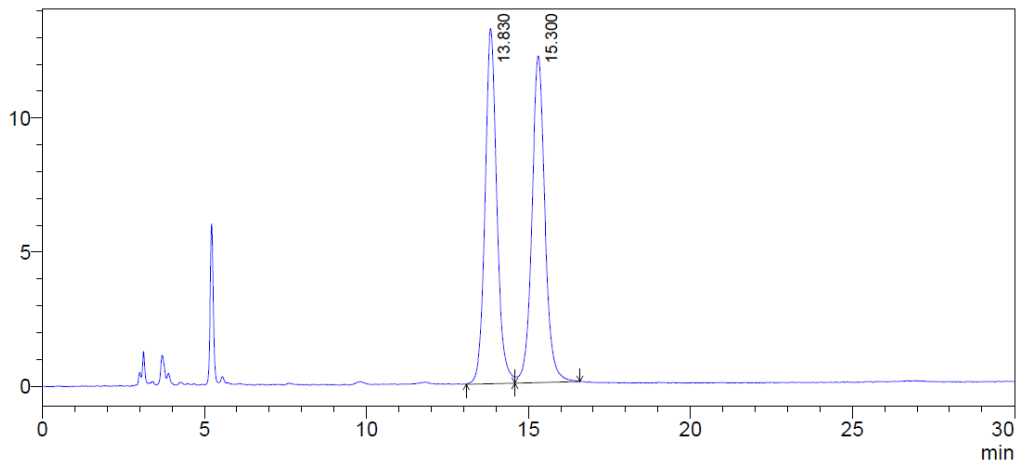


Peak#	Ret. Time	Area	Height	Area %	Height %
1	24.326	123697	2693	49.631	53.400
2	27.941	125536	2350	50.369	46.600
Total		249233	5043	100.000	100.000



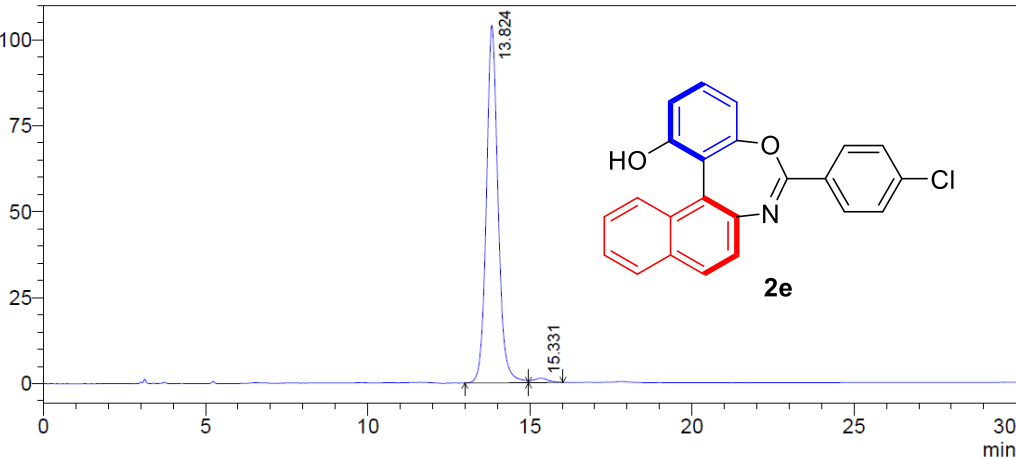
Peak#	Ret. Time	Area	Height	Area %	Height %
1	24.386	9320	216	0.731	0.913
2	27.808	1265553	23448	99.269	99.087
Total		1274872	23664	100.000	100.000

mV

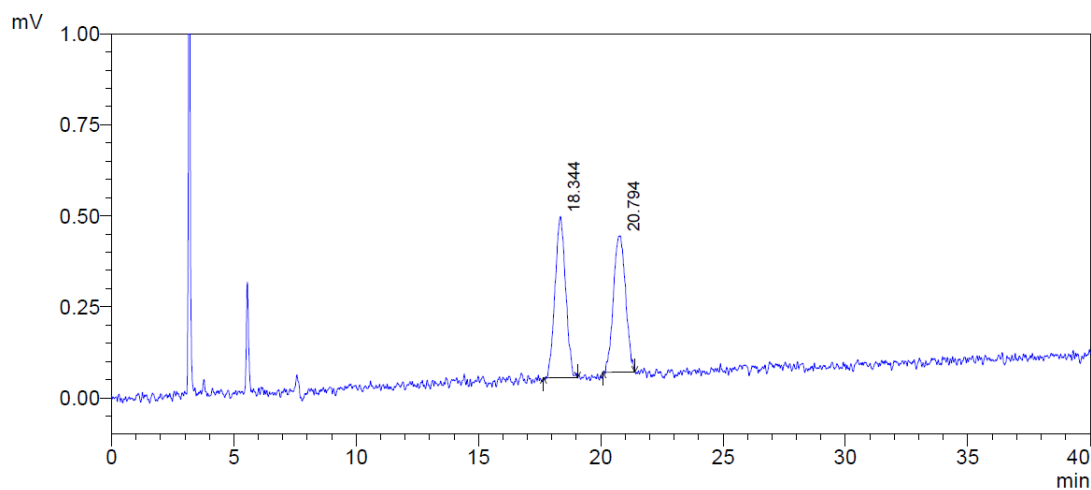


Peak#	Ret. Time	Area	Height	Area %	Height %
1	13.830	334591	13236	49.566	52.080
2	15.300	340444	12179	50.434	47.920
Total		675035	25416	100.000	100.000

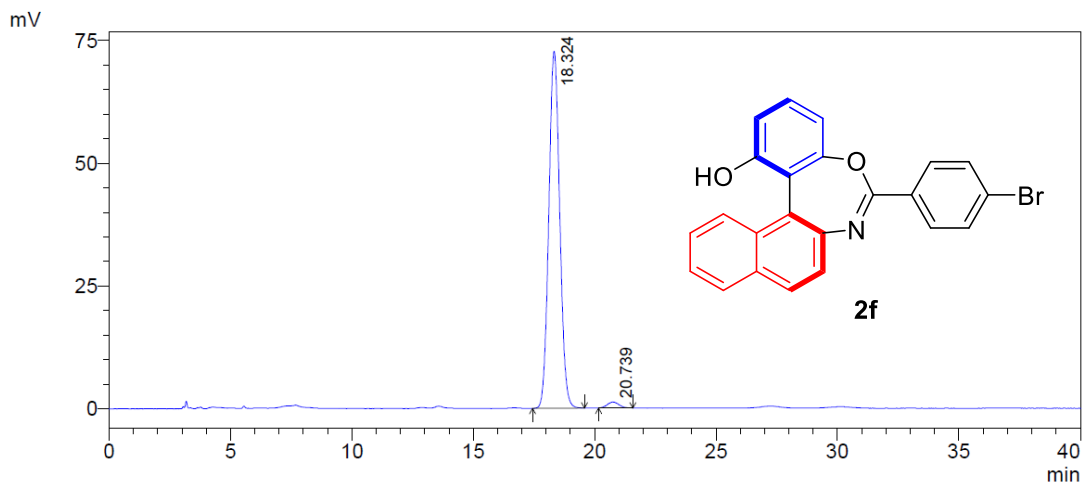
mV



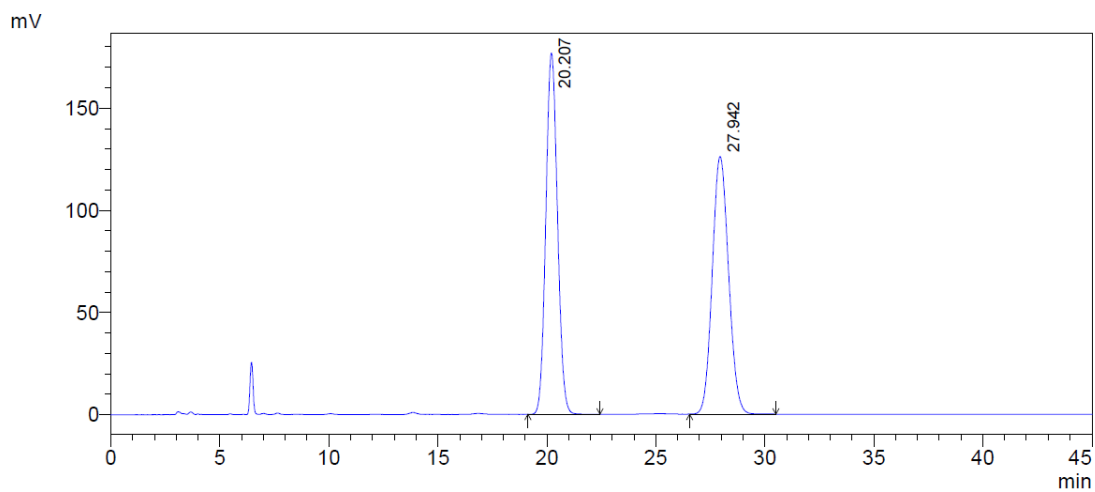
Peak#	Ret. Time	Area	Height	Area %	Height %
1	13.824	2606535	103996	98.496	98.802
2	15.331	39812	1261	1.504	1.198
Total		2646347	105257	100.000	100.000



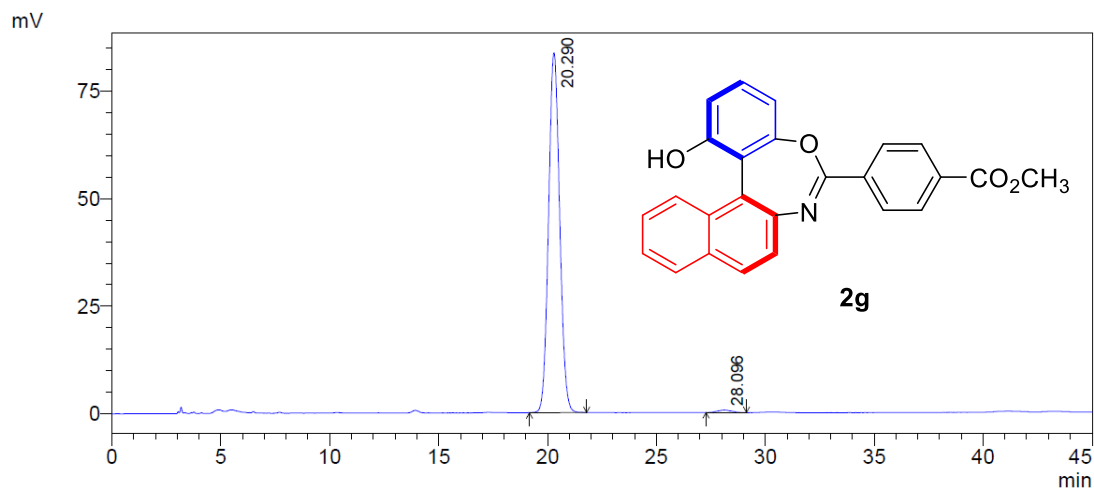
Peak#	Ret. Time	Area	Height	Area %	Height %
1	18.344	13313	444	50.725	54.254
2	20.794	12933	374	49.275	45.746
Total		26246	818	100.000	100.000



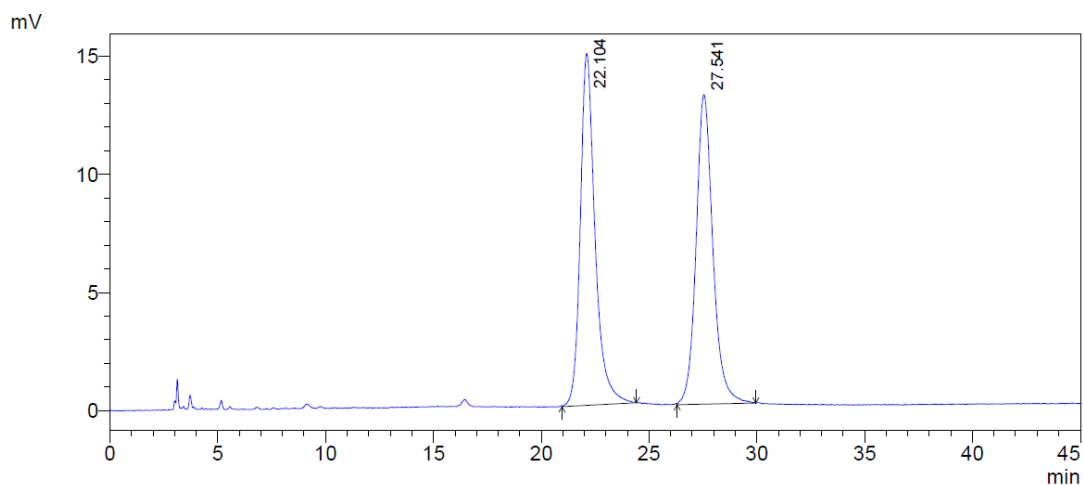
Peak#	Ret. Time	Area	Height	Area %	Height %
1	18.324	2274648	72684	98.247	98.370
2	20.739	40580	1205	1.753	1.630
Total		2315228	73889	100.000	100.000



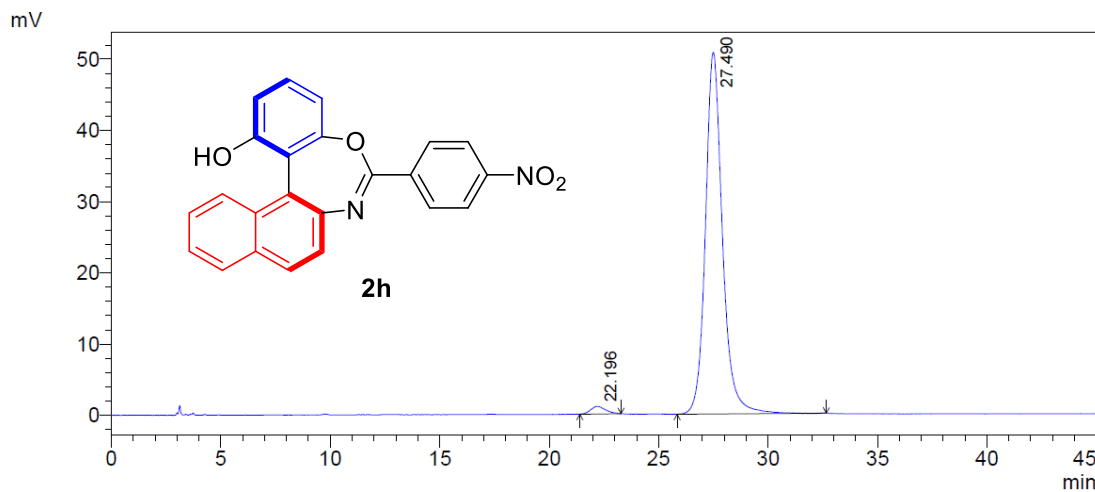
Peak#	Ret. Time	Area	Height	Area %	Height %
1	20.207	6552983	176795	49.971	58.357
2	27.942	6560648	126160	50.029	41.643
Total		13113632	302956	100.000	100.000



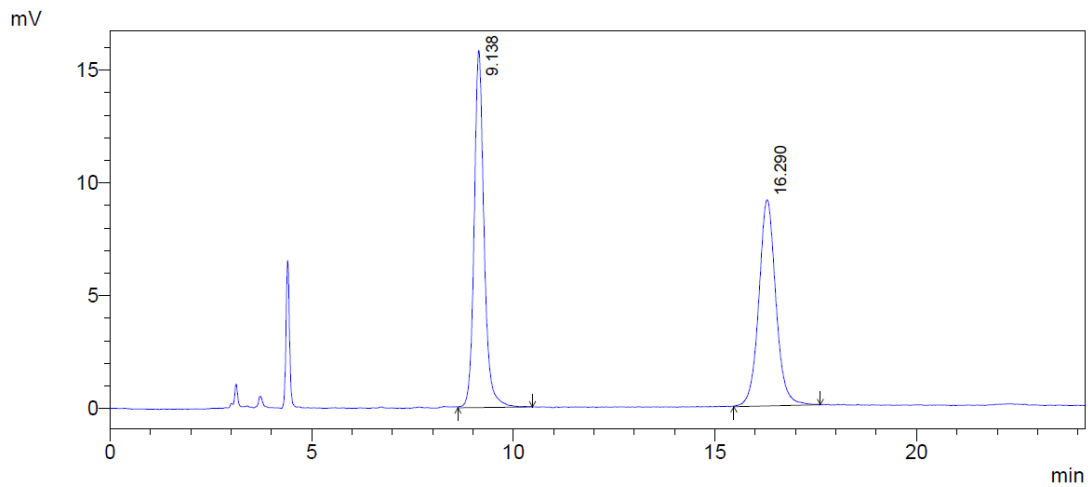
Peak#	Ret. Time	Area	Height	Area %	Height %
1	20.290	2963589	83612	99.098	99.319
2	28.096	26965	574	0.902	0.681
Total		2990554	84186	100.000	100.000



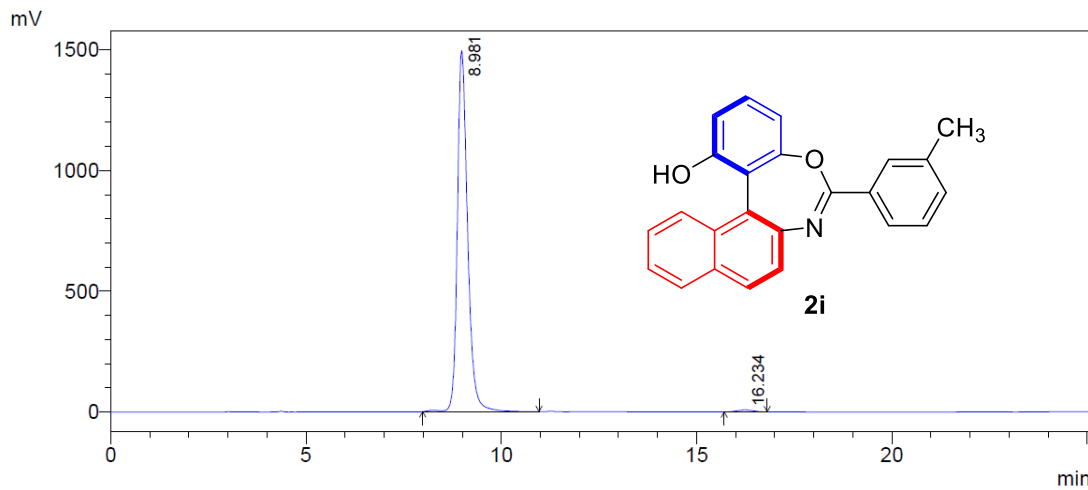
Peak#	Ret. Time	Area	Height	Area %	Height %
1	22.104	706482	14881	49.859	53.199
2	27.541	710483	13092	50.141	46.801
Total		1416965	27973	100.000	100.000



Peak#	Ret. Time	Area	Height	Area %	Height %
1	22.196	50499	1079	1.807	2.080
2	27.490	2743786	50816	98.193	97.920
Total		2794285	51895	100.000	100.000

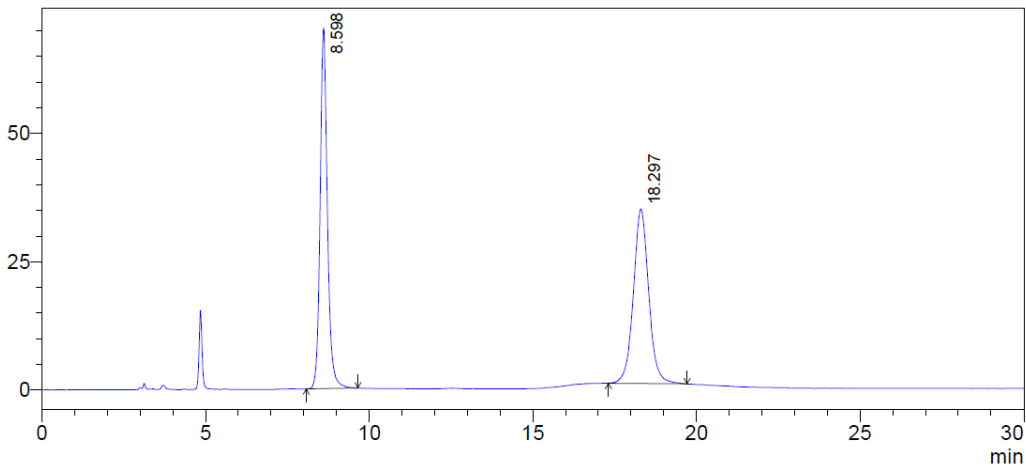


Peak#	Ret. Time	Area	Height	Area %	Height %
1	9.138	270577	15827	50.175	63.390
2	16.290	268691	9141	49.825	36.610
Total		539267	24968	100.000	100.000



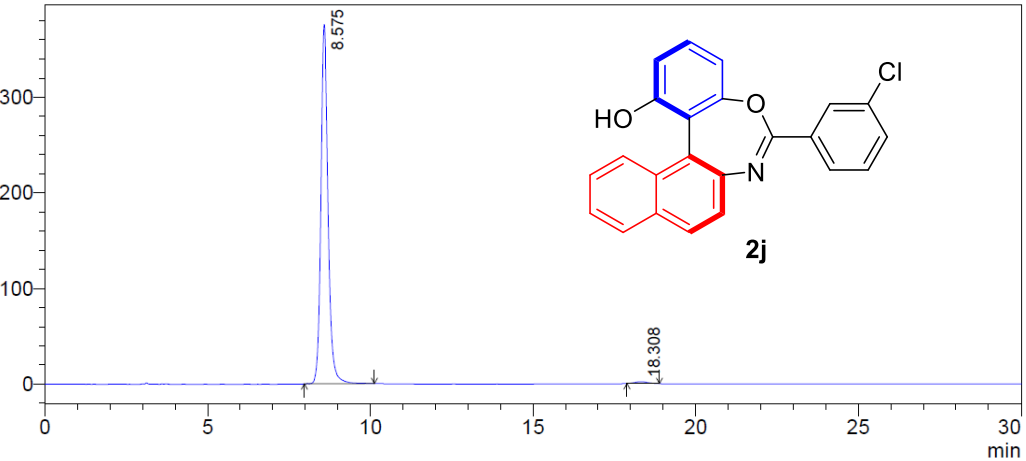
Peak#	Ret. Time	Area	Height	Area %	Height %
1	8.981	27332667	1494100	99.195	99.465
2	16.234	221725	8043	0.805	0.535
Total		27554392	1502144	100.000	100.000

mV



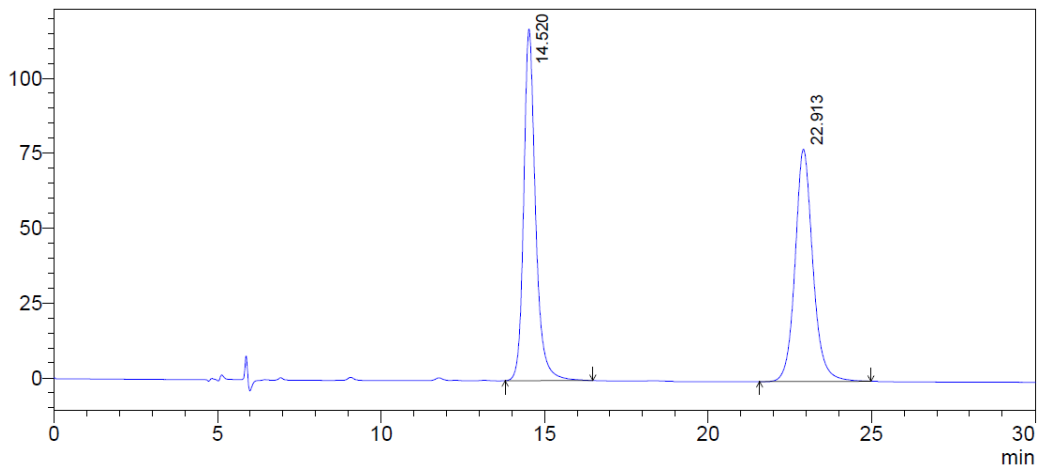
Peak#	Ret. Time	Area	Height	Area %	Height %
1	8.598	1092625	70318	49.584	67.378
2	18.297	1110975	34045	50.416	32.622
Total		2203600	104363	100.000	100.000

mV



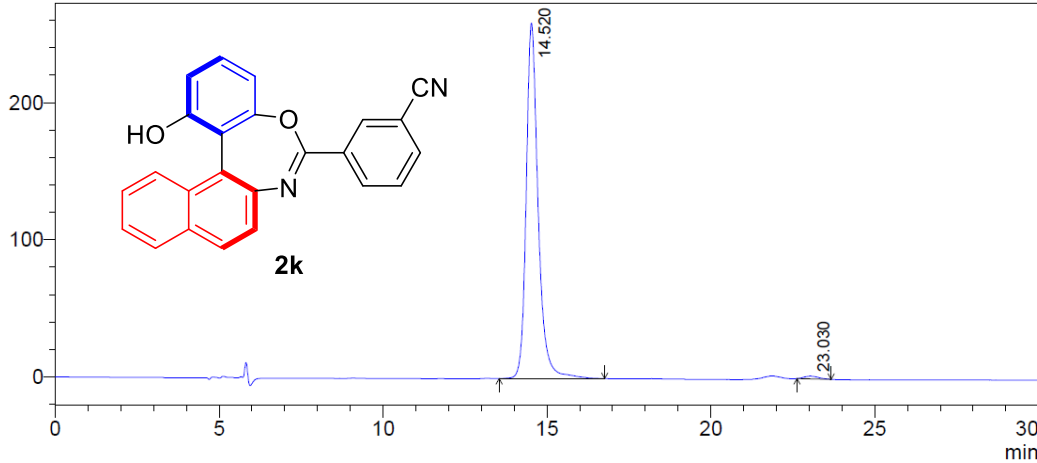
Peak#	Ret. Time	Area	Height	Area %	Height %
1	8.575	5755496	375723	99.094	99.505
2	18.308	52643	1871	0.906	0.495
Total		5808139	377593	100.000	100.000

mAU

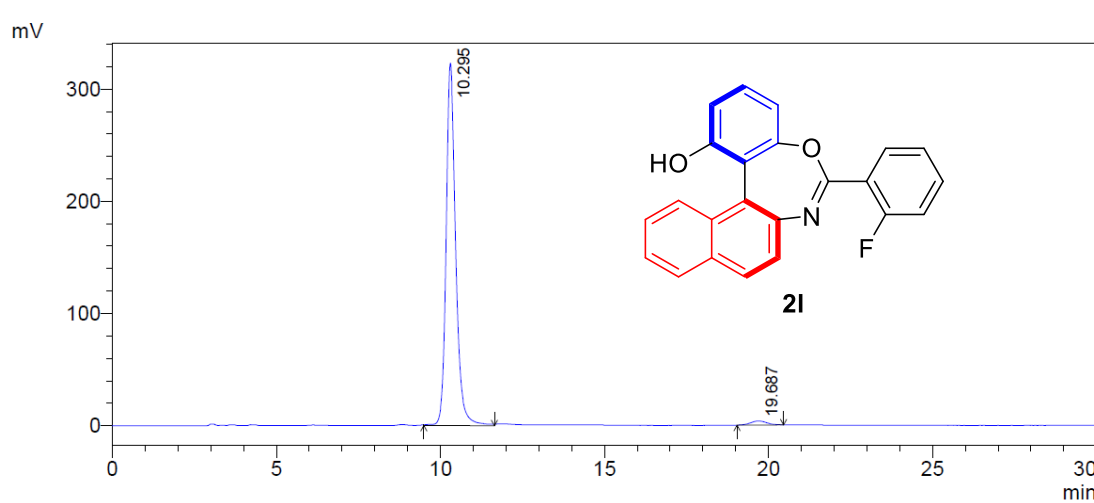
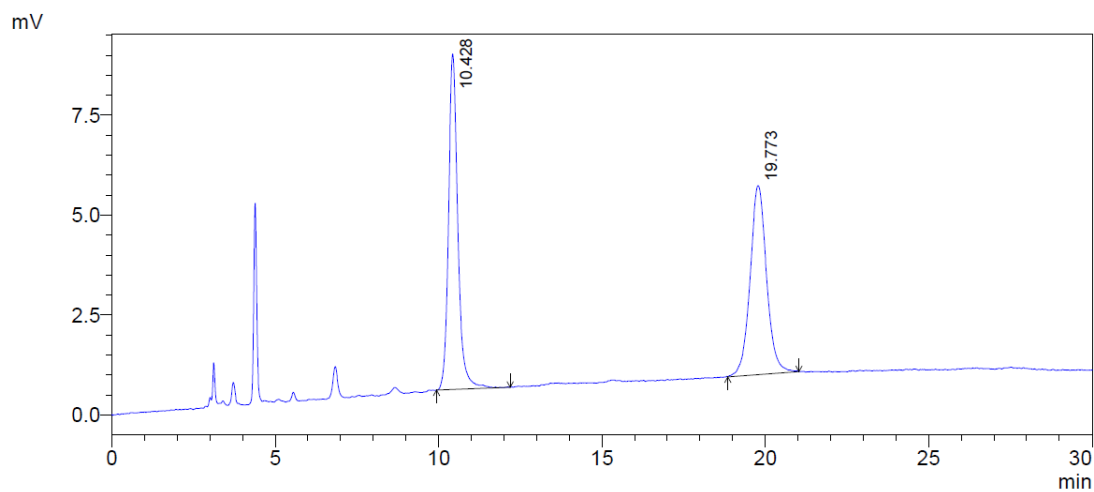


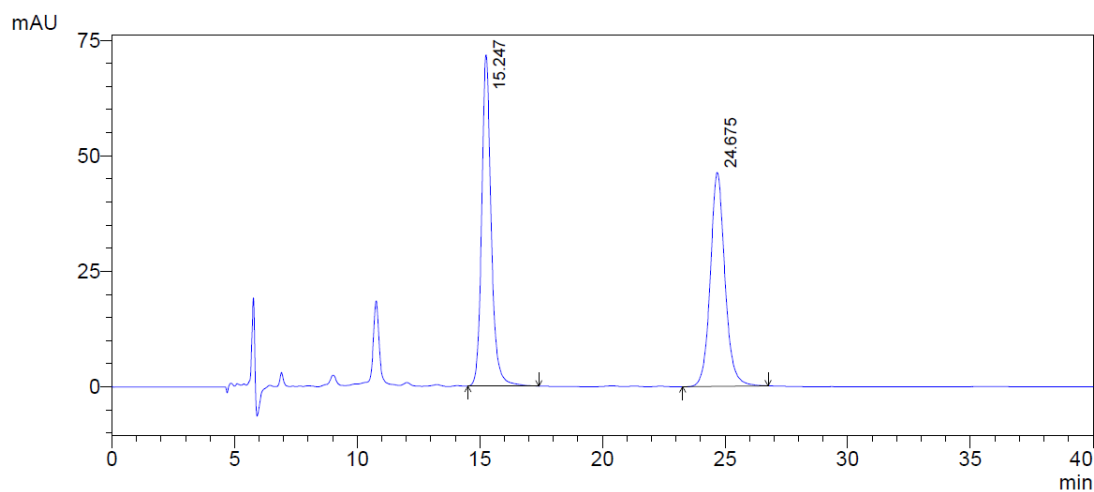
Peak#	Ret. Time	Area	Height	Area %	Height %
1	14.520	2959066	117365	50.153	60.225
2	22.913	2940990	77513	49.847	39.775
Total		5900056	194878	100.000	100.000

mAU

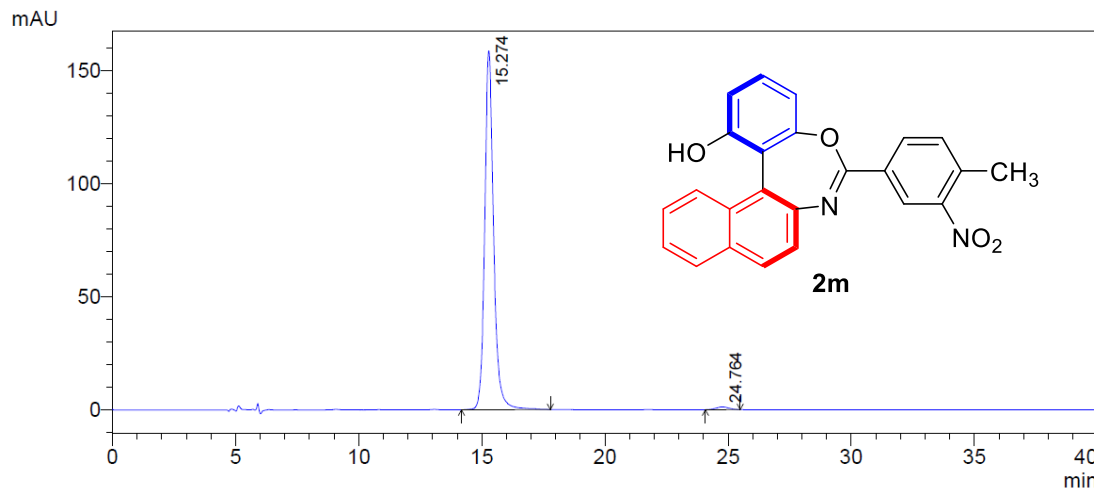


Peak#	Ret. Time	Area	Height	Area %	Height %
1	14.520	6598038	259365	99.077	99.230
2	23.030	61495	2012	0.923	0.770
Total		6659533	261377	100.000	100.000



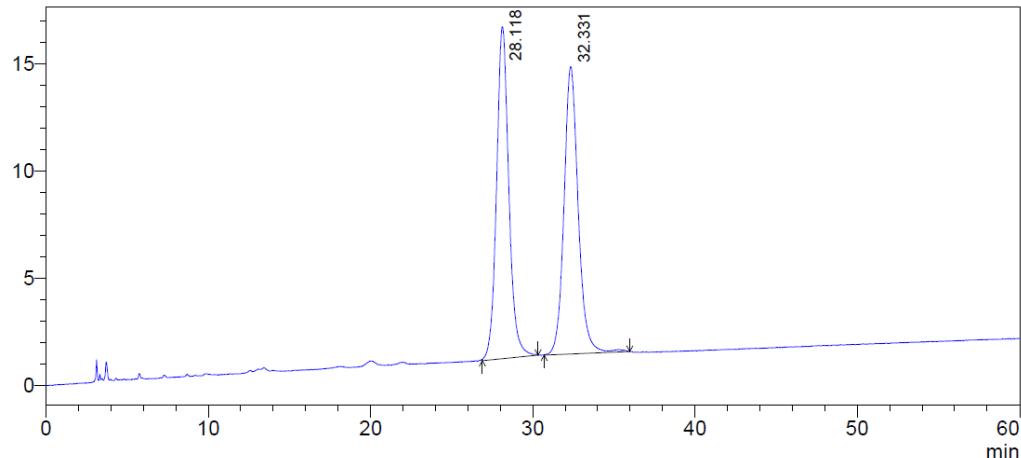


Peak#	Ret. Time	Area	Height	Area %	Height %
1	15.247	1935435	71717	50.155	60.758
2	24.675	1923467	46320	49.845	39.242
Total		3858902	118037	100.000	100.000



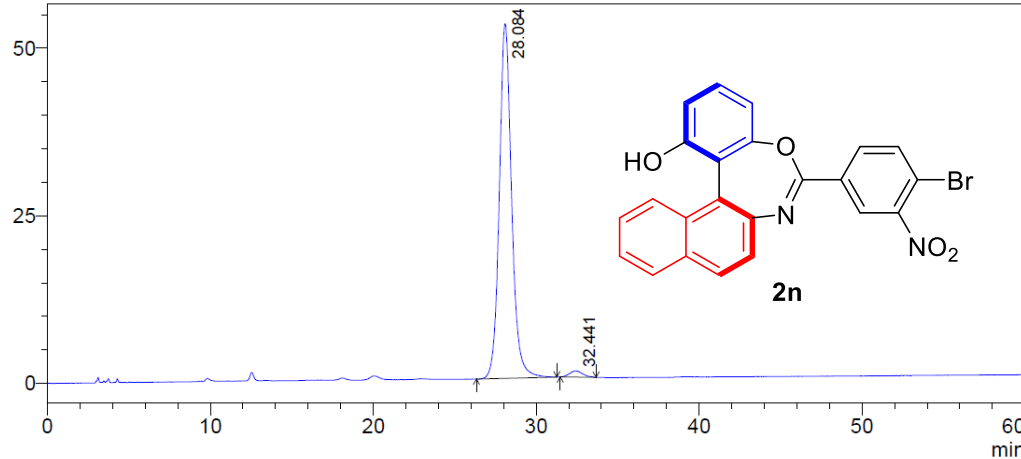
Peak#	Ret. Time	Area	Height	Area %	Height %
1	15.274	4005449	158635	98.910	99.258
2	24.764	44129	1186	1.090	0.742
Total		4049578	159821	100.000	100.000

mV

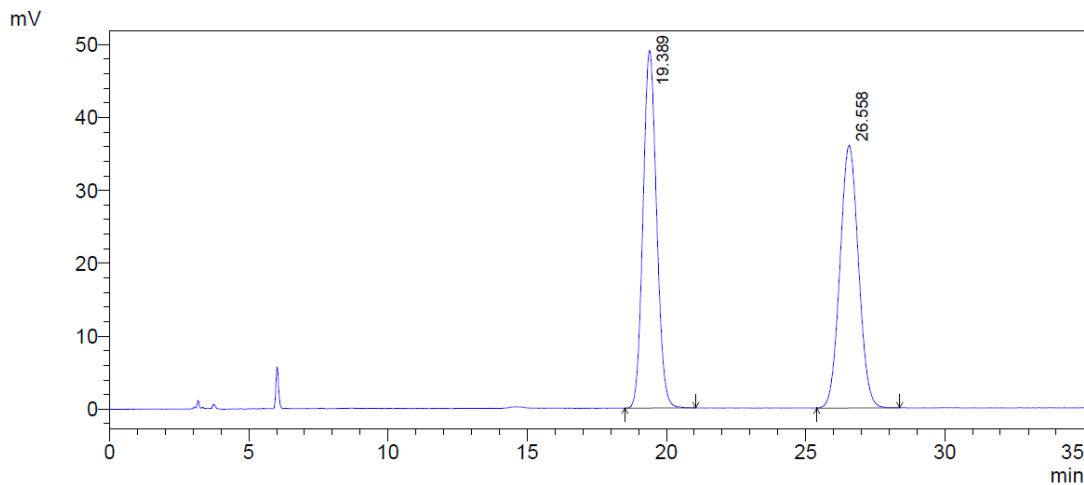


Peak#	Ret. Time	Area	Height	Area %	Height %
1	28.118	813295	15477	49.990	53.583
2	32.331	813632	13407	50.010	46.417
Total		1626927	28884	100.000	100.000

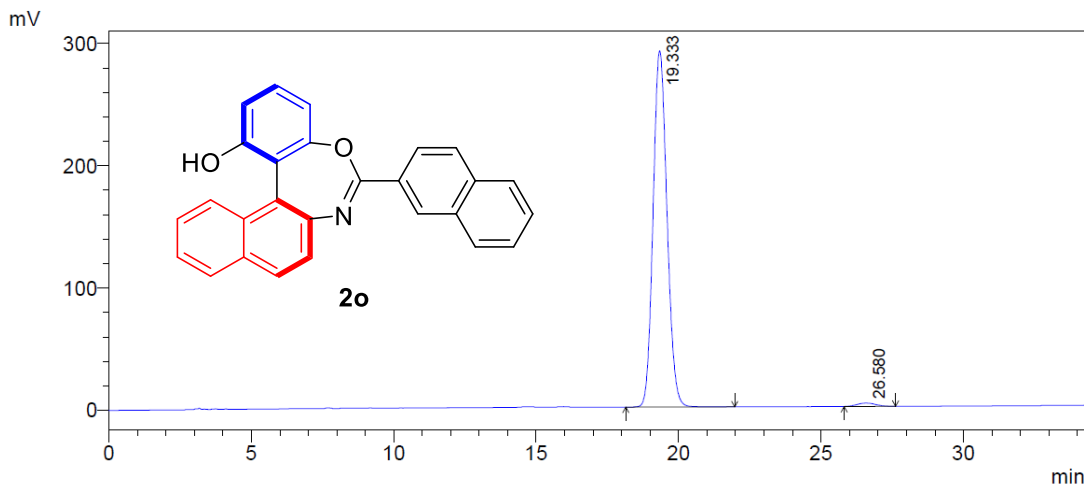
mV



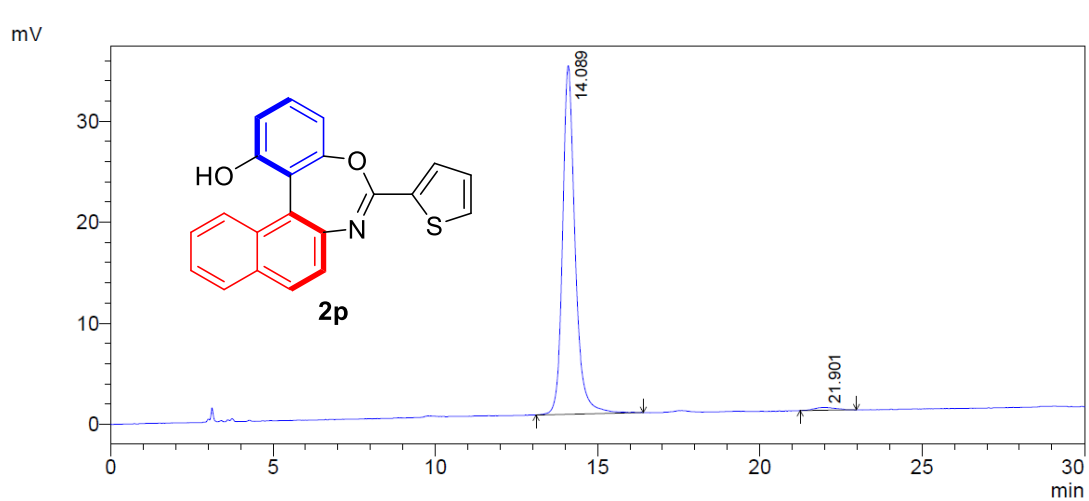
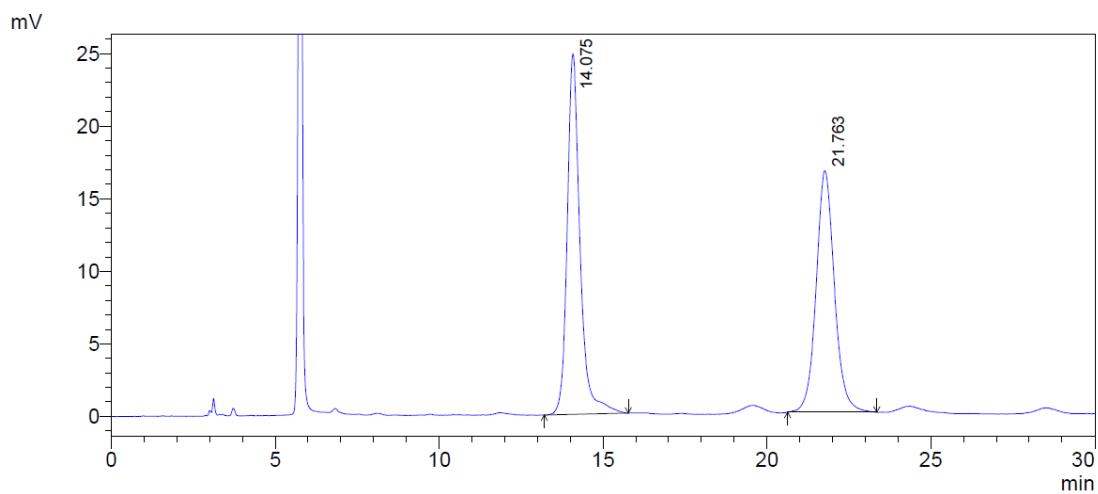
Peak#	Ret. Time	Area	Height	Area %	Height %
1	28.084	2784211	52892	98.228	98.302
2	32.441	50215	913	1.772	1.698
Total		2834426	53805	100.000	100.000

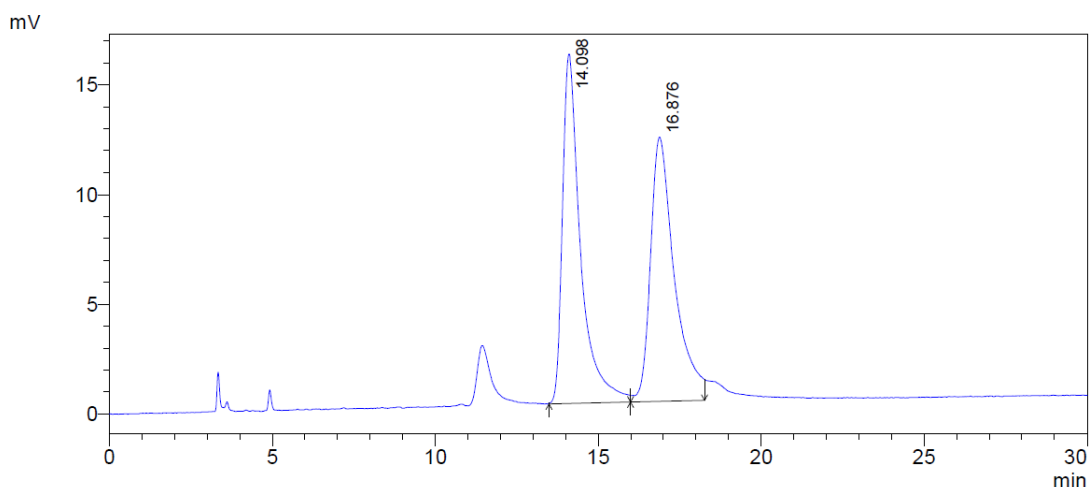


Peak#	Ret. Time	Area	Height	Area %	Height %
1	19.389	1663102	49044	49.969	57.685
2	26.558	1665194	35977	50.031	42.315
Total		3328295	85022	100.000	100.000

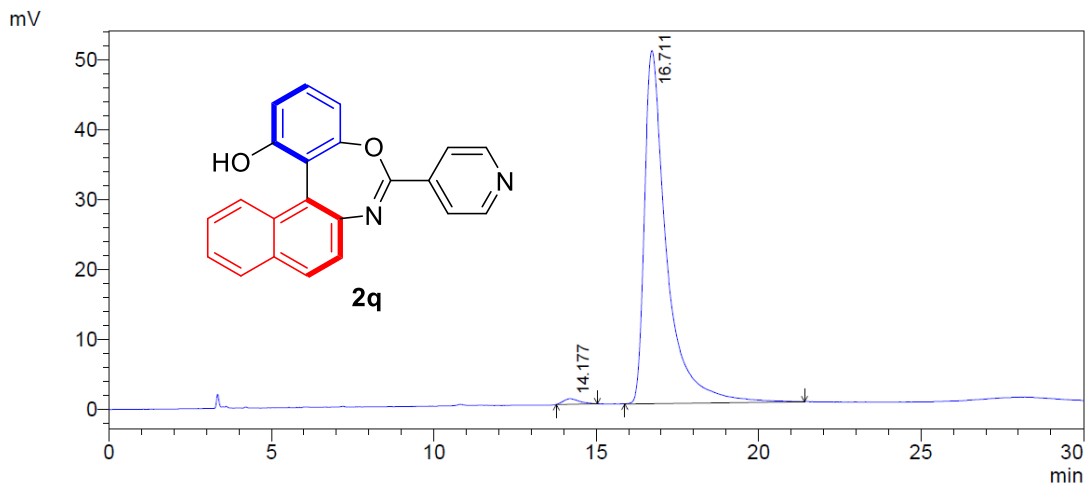


Peak#	Ret. Time	Area	Height	Area %	Height %
1	19.333	9880094	291393	98.764	99.067
2	26.580	123695	2744	1.236	0.933
Total		10003789	294137	100.000	100.000



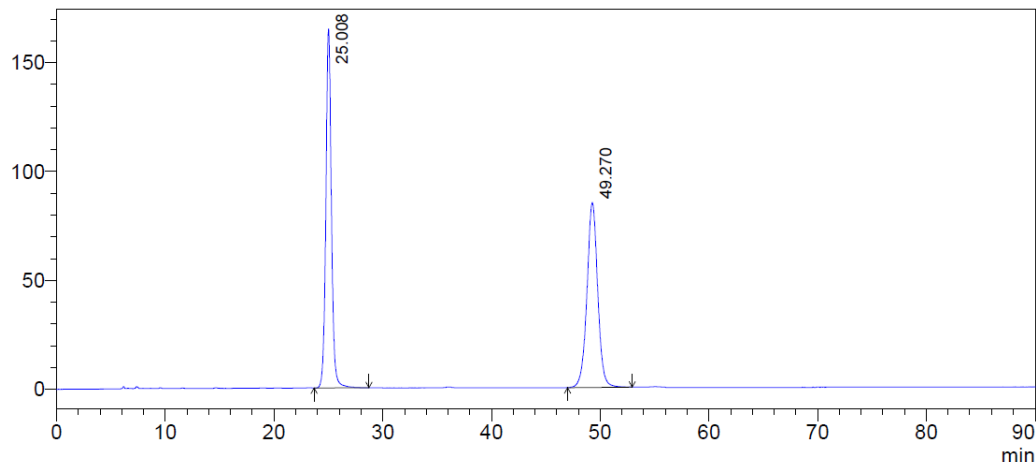


Peak#	Ret. Time	Area	Height	Area %	Height %
1	14.098	614580	15935	49.972	56.925
2	16.876	615263	12058	50.028	43.075
Total		1229844	27994	100.000	100.000



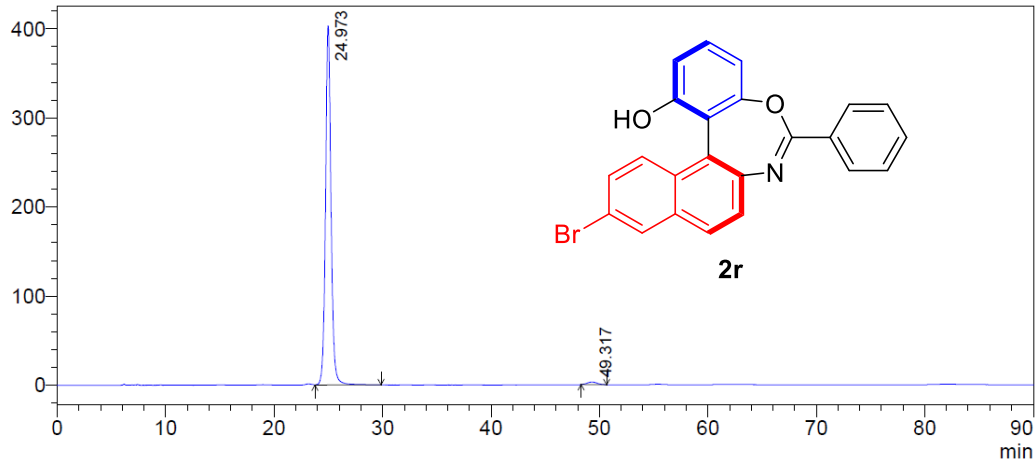
Peak#	Ret. Time	Area	Height	Area %	Height %
1	14.177	27017	783	1.116	1.526
2	16.711	2393261	50500	98.884	98.474
Total		2420279	51283	100.000	100.000

mV

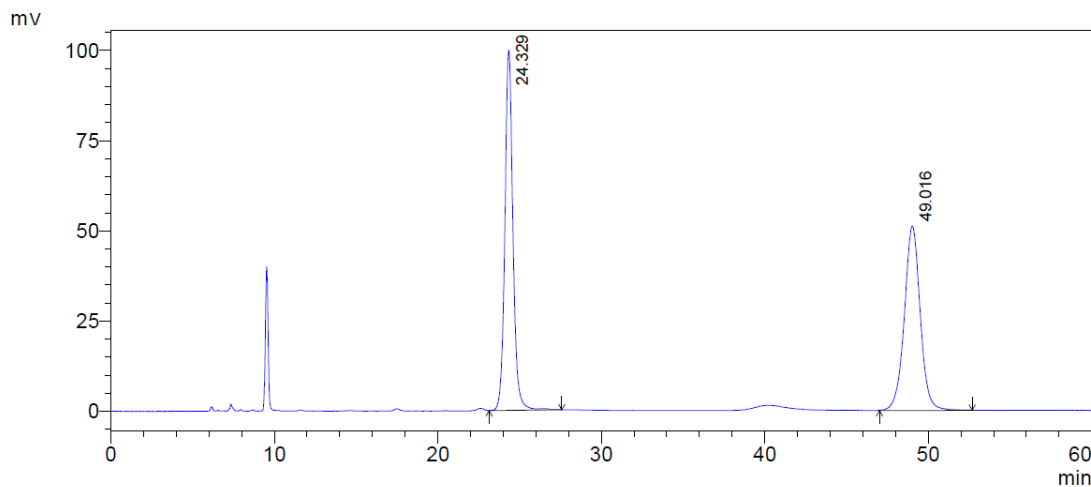


Peak#	Ret. Time	Area	Height	Area %	Height %
1	25.008	5858487	164897	50.075	66.007
2	49.270	5840850	84920	49.925	33.993
Total		11699336	249817	100.000	100.000

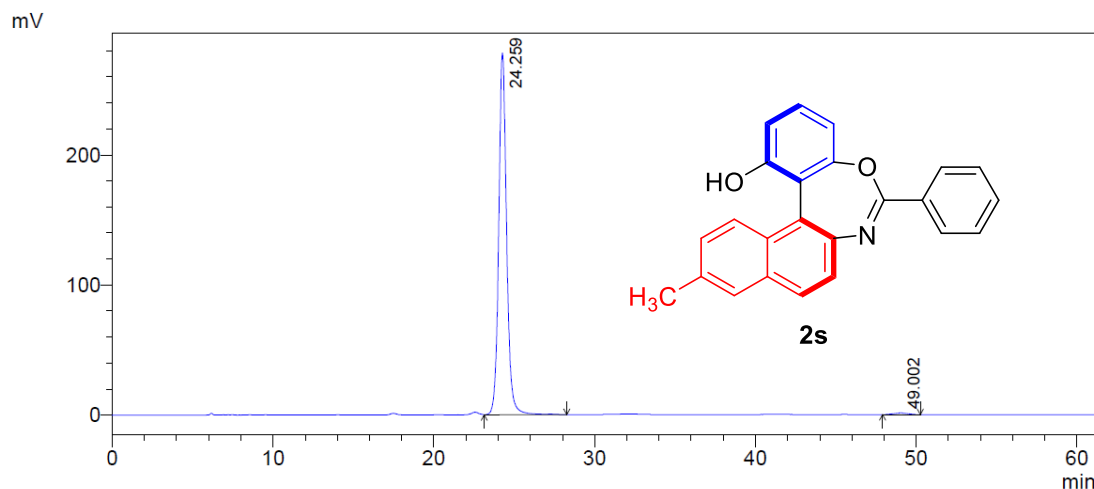
mV



Peak#	Ret. Time	Area	Height	Area %	Height %
1	24.973	14313736	403111	98.738	99.267
2	49.317	183007	2978	1.262	0.733
Total		14496744	406089	100.000	100.000

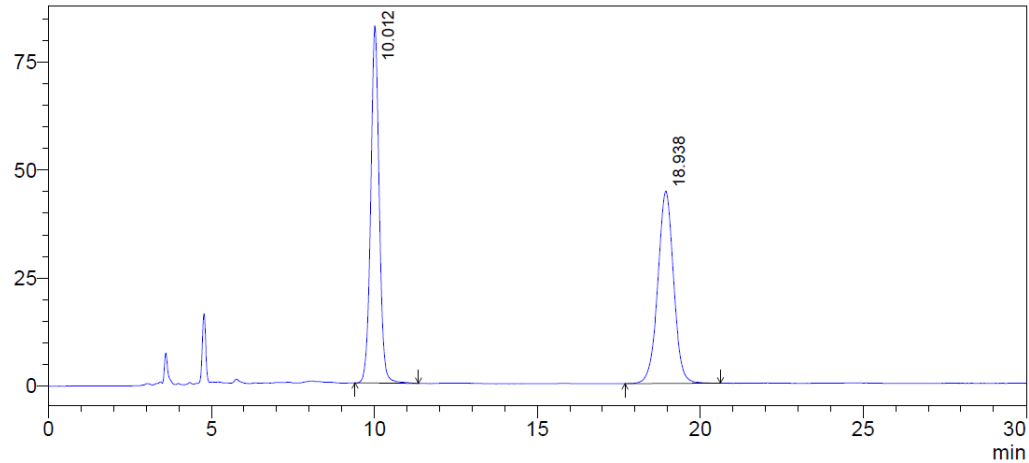


Peak#	Ret. Time	Area	Height	Area %	Height %
1	24.329	3420889	99825	49.773	66.136
2	49.016	3452027	51113	50.227	33.864
Total		6872916	150938	100.000	100.000



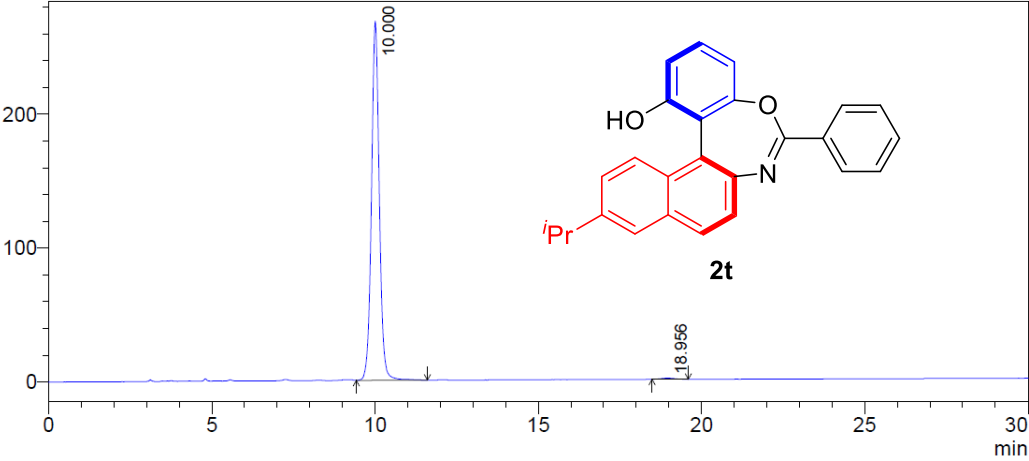
Peak#	Ret. Time	Area	Height	Area %	Height %
1	24.259	9502978	278046	99.218	99.563
2	49.002	74934	1219	0.782	0.437
Total		9577913	279266	100.000	100.000

mV

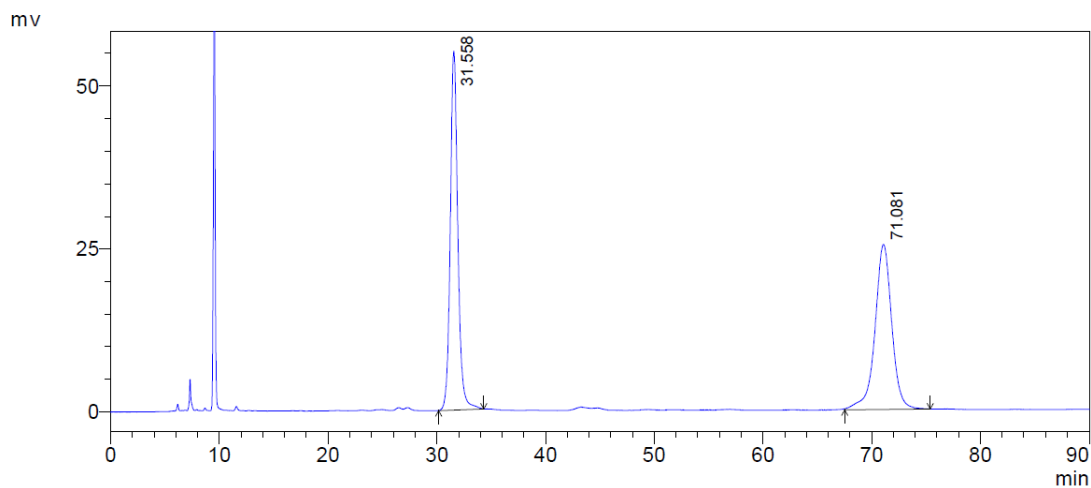


Peak#	Ret. Time	Area	Height	Area %	Height %
1	10.012	1506828	82717	50.084	64.998
2	18.938	1501780	44544	49.916	35.002
Total		3008607	127260	100.000	100.000

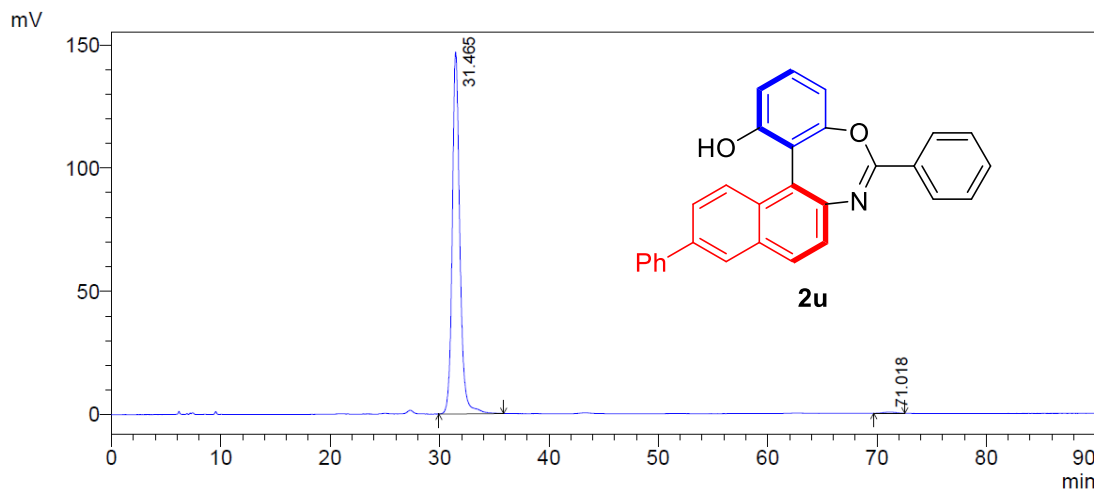
mV



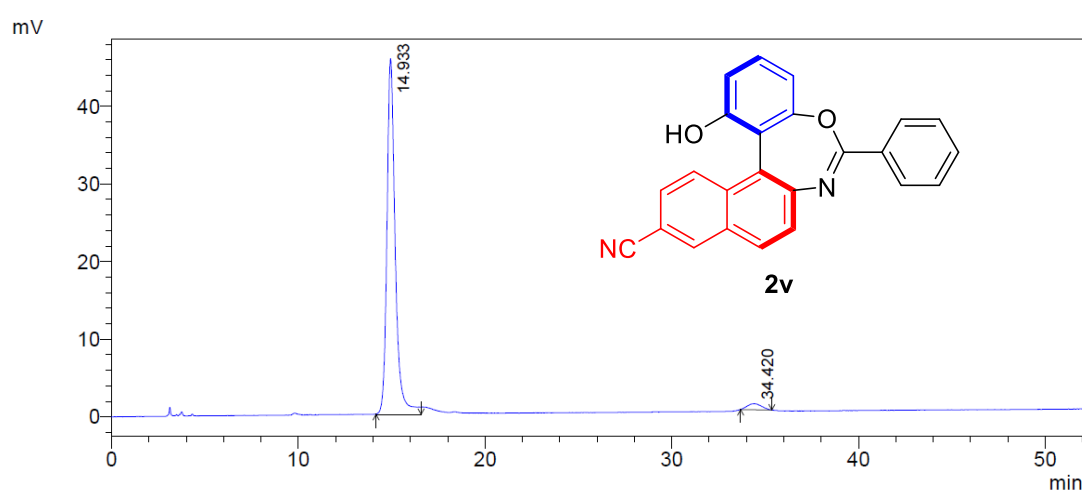
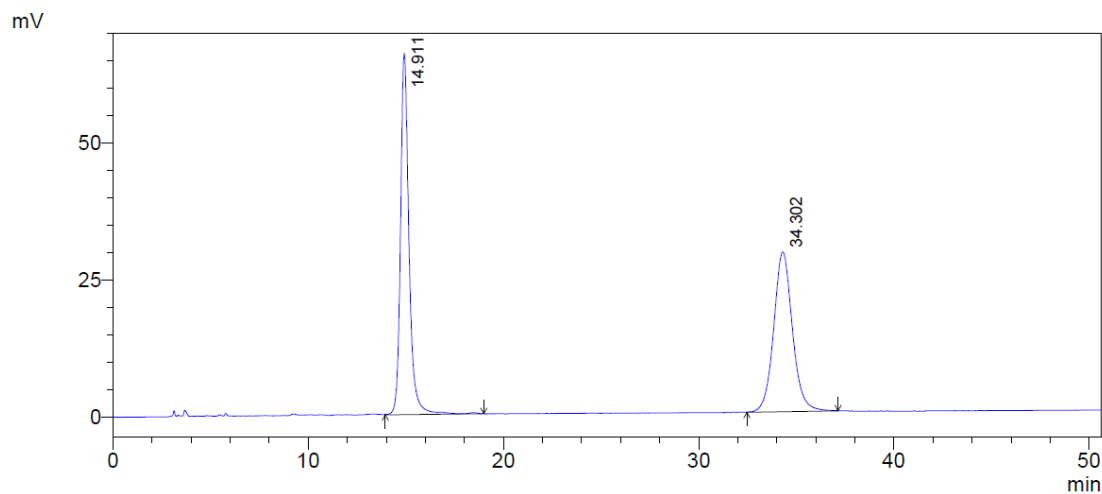
Peak#	Ret. Time	Area	Height	Area %	Height %
1	10.000	4499666	268186	99.467	99.702
2	18.956	24090	801	0.533	0.298
Total		4523756	268987	100.000	100.000



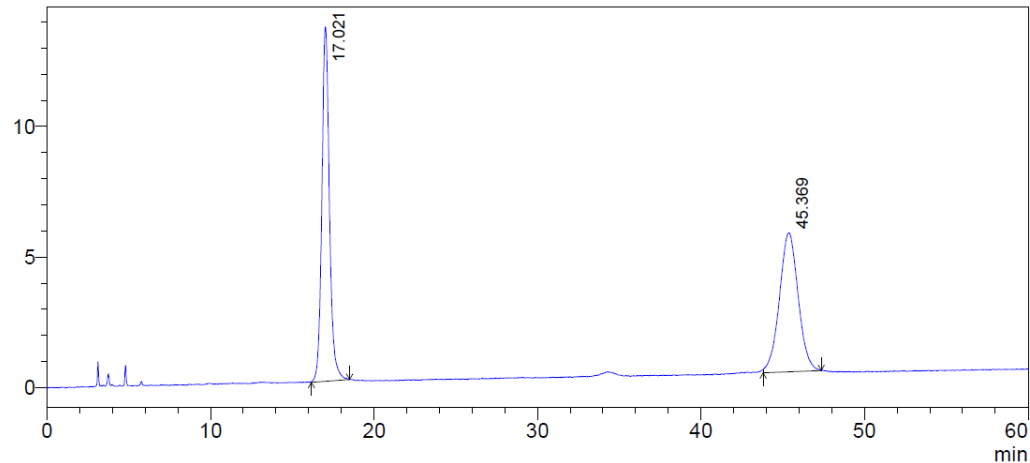
Peak#	Ret. Time	Area	Height	Area %	Height %
1	31.558	2654562	55061	49.389	68.500
2	71.081	2720213	25319	50.611	31.500
Total		5374774	80380	100.000	100.000



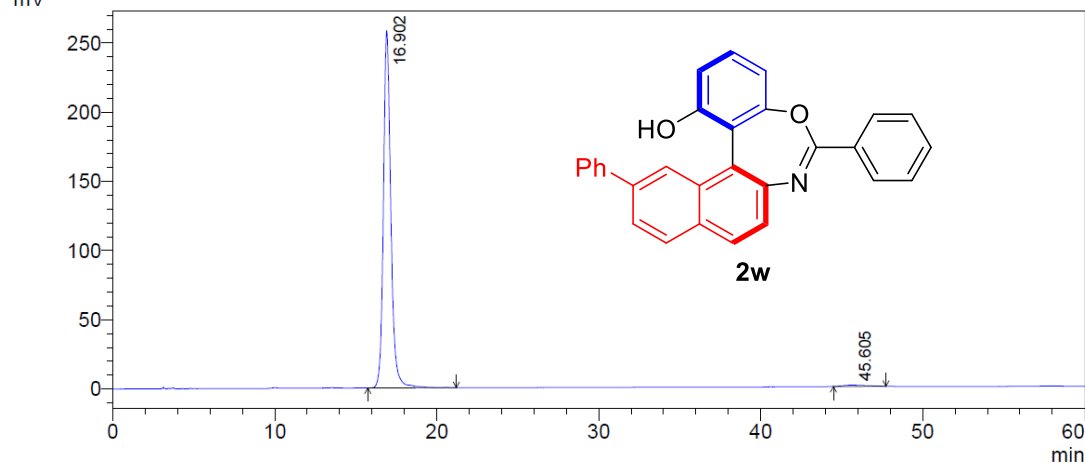
Peak#	Ret. Time	Area	Height	Area %	Height %
1	31.465	7094384	146790	99.481	99.699
2	71.018	37028	443	0.519	0.301
Total		7131411	147232	100.000	100.000



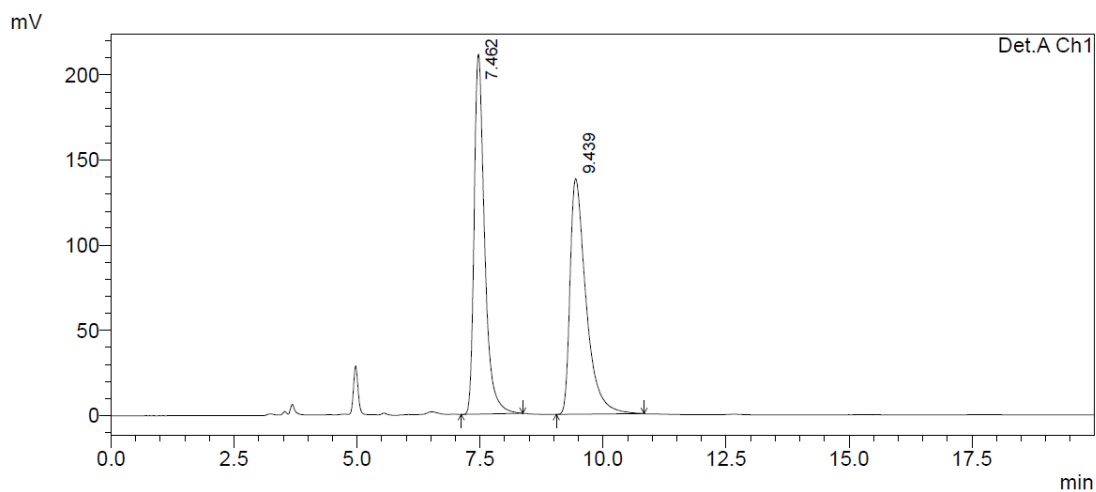
mV



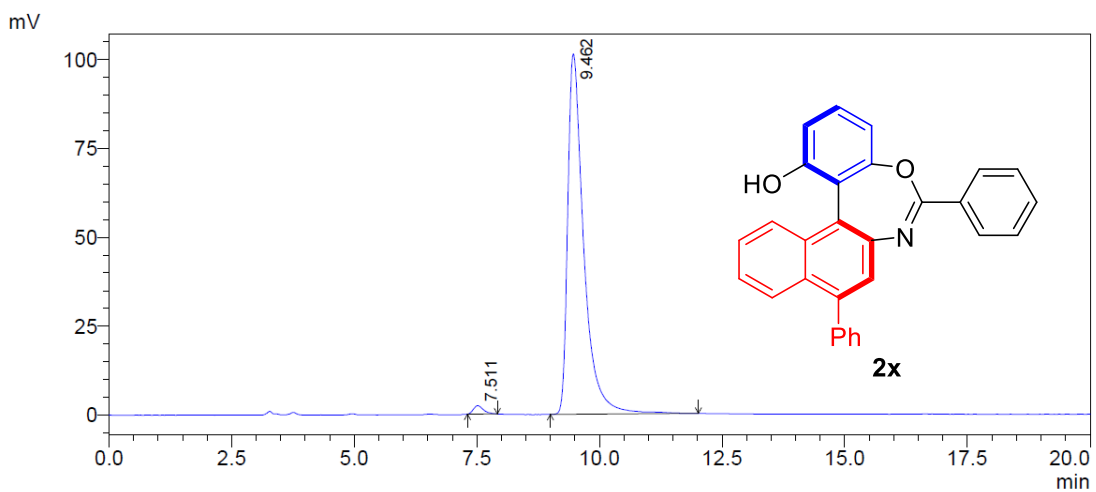
mV



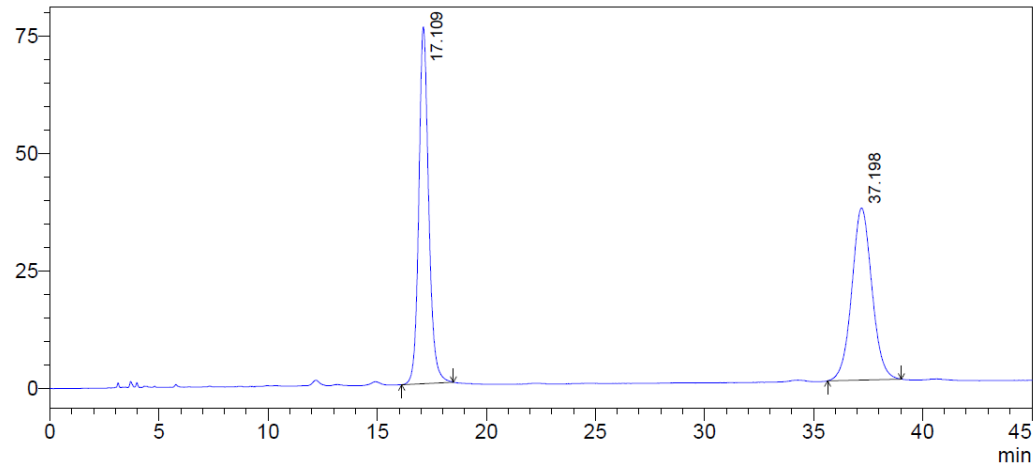
Peak#	Ret. Time	Area	Height	Area %	Height %
1	16.902	8238917	258180	98.944	99.668
2	45.605	87943	861	1.056	0.332
Total		8326860	259041	100.000	100.000



Peak#	Ret. Time	Area	Height	Area %	Height %
1	7.462	3124111	211338	49.971	60.433
2	9.439	3127693	138368	50.029	39.567
Total		6251804	349706	100.000	100.000

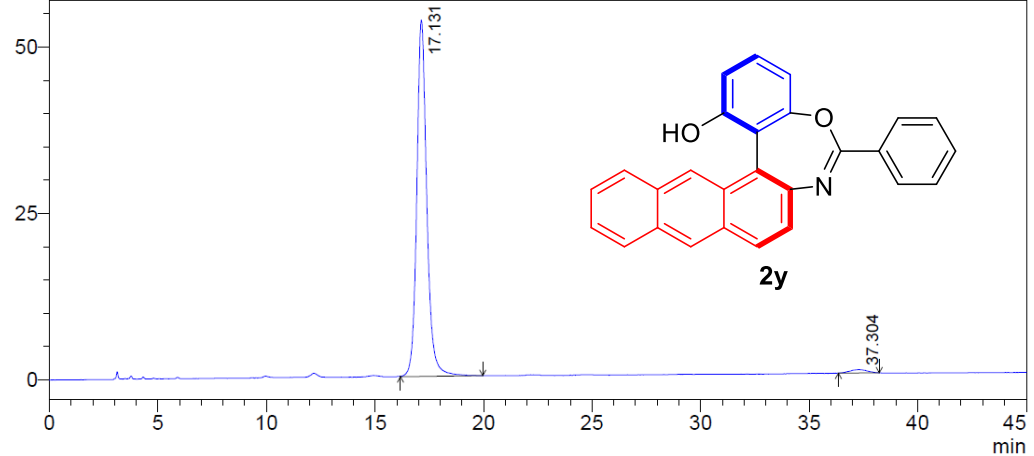


mV

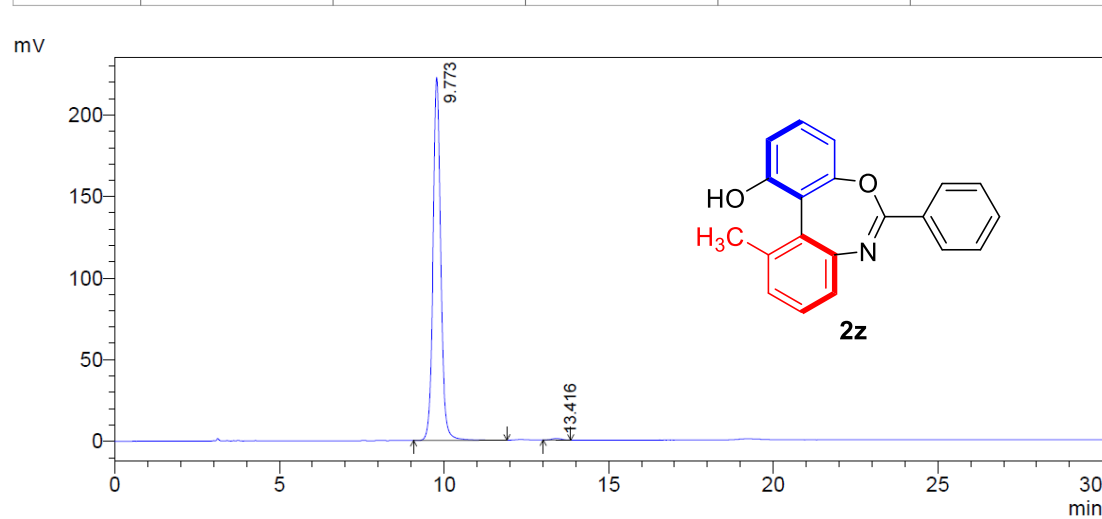
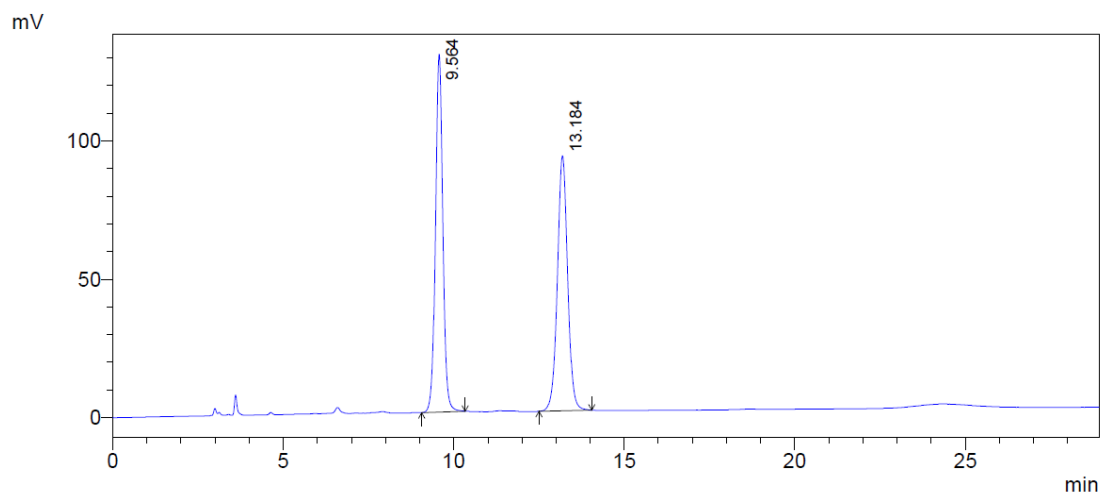


Peak#	Ret. Time	Area	Height	Area %	Height %
1	17.109	2388839	75938	50.424	67.461
2	37.198	2348700	36627	49.576	32.539
Total		4737539	112565	100.000	100.000

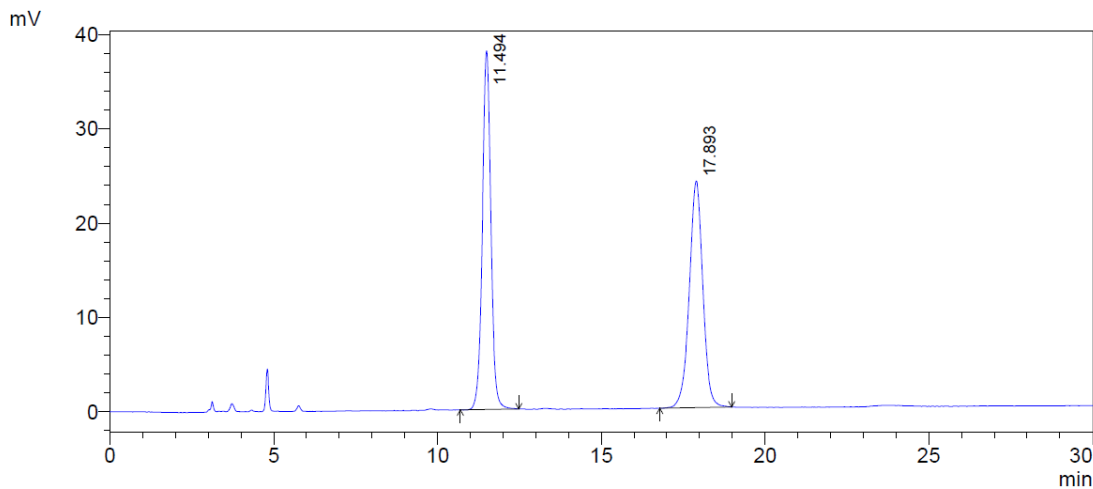
mV



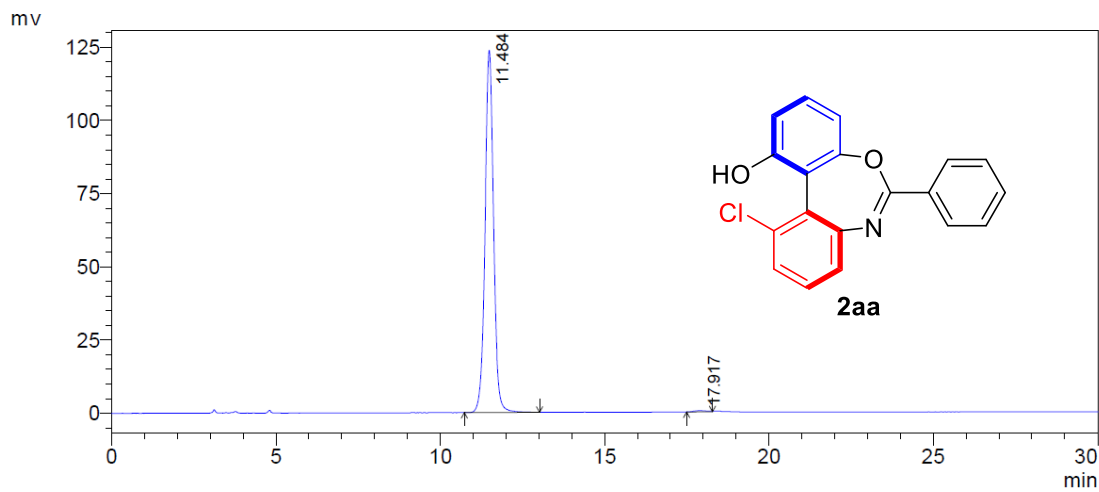
Peak#	Ret. Time	Area	Height	Area %	Height %
1	17.131	1724562	53536	98.430	99.057
2	37.304	27500	509	1.570	0.943
Total		1752062	54046	100.000	100.000



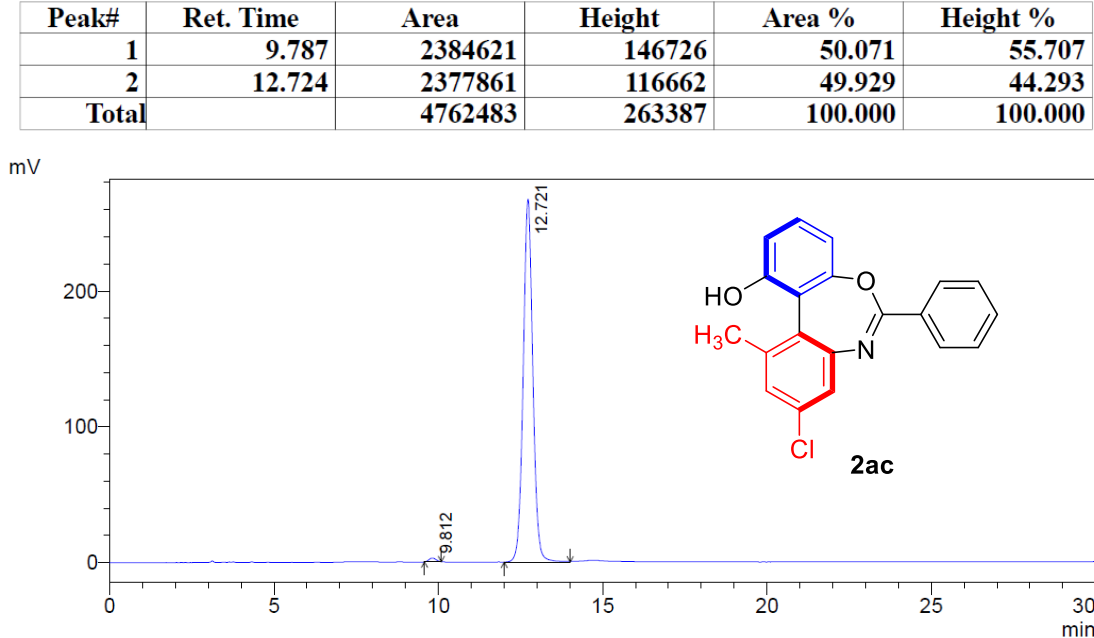
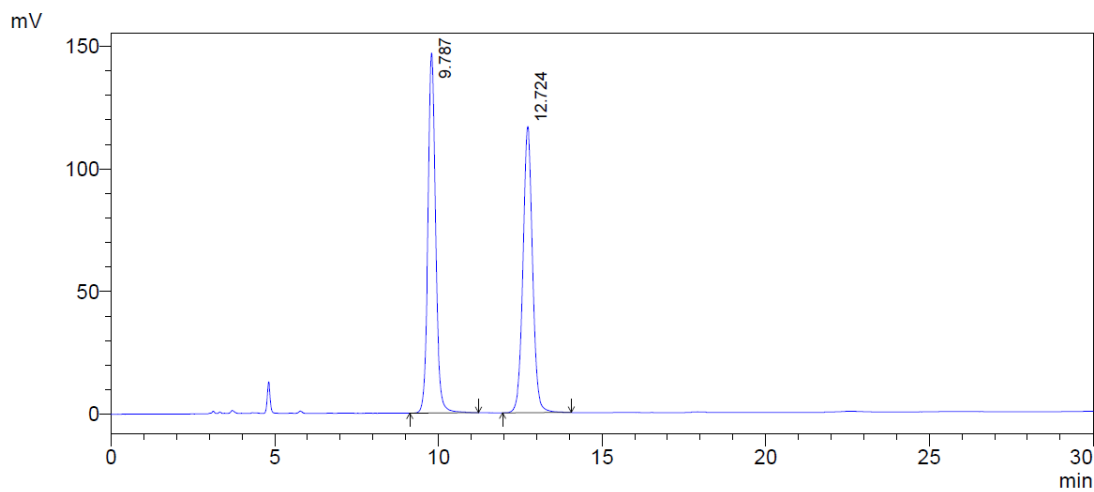
Peak#	Ret. Time	Area	Height	Area %	Height %
1	9.773	3628022	222589	99.452	99.581
2	13.416	19985	937	0.548	0.419
Total		3648008	223526	100.000	100.000

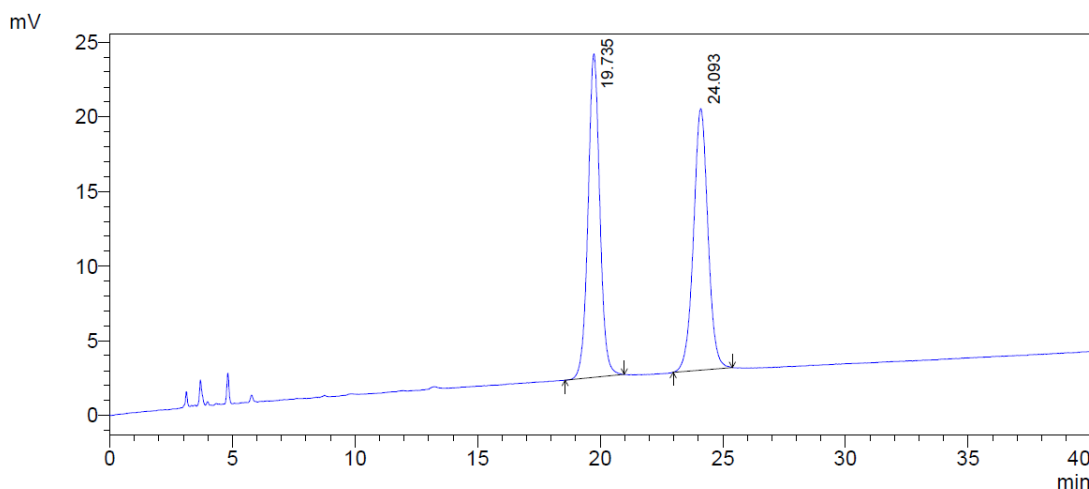


Peak#	Ret. Time	Area	Height	Area %	Height %
1	11.494	688150	38061	49.907	61.272
2	17.893	690713	24058	50.093	38.728
Total		1378864	62119	100.000	100.000

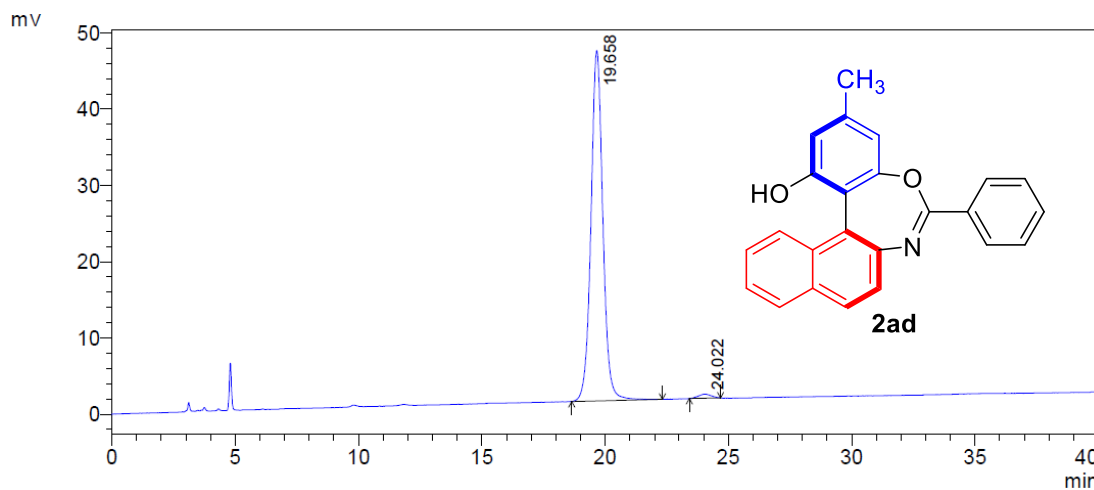


Peak#	Ret. Time	Area	Height	Area %	Height %
1	11.484	2226921	123624	99.459	99.661
2	17.917	12117	420	0.541	0.339
Total		2239038	124044	100.000	100.000

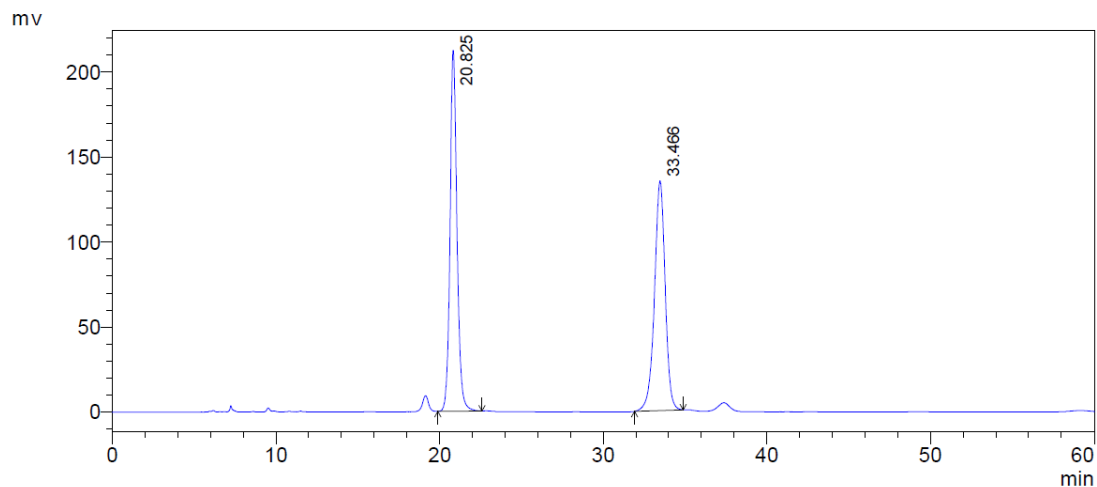




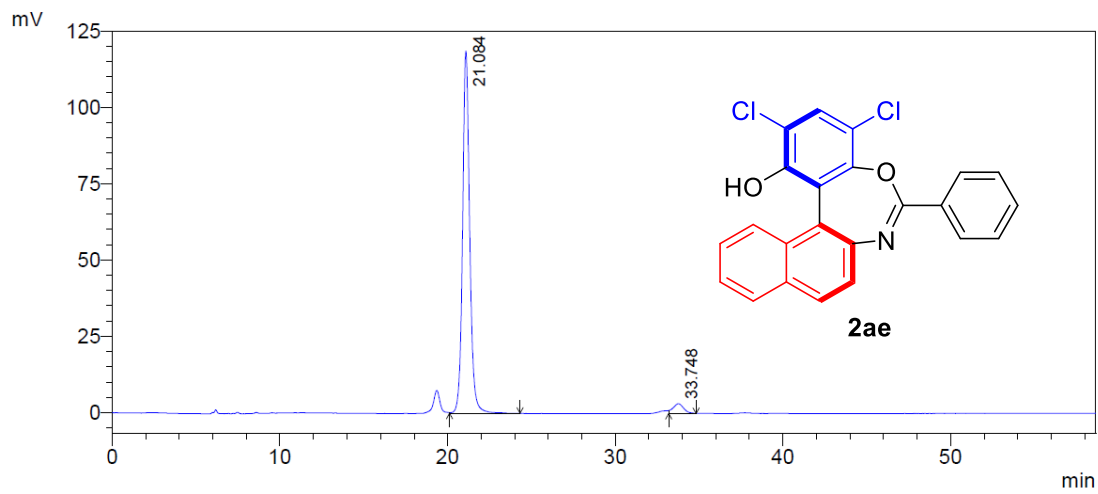
Peak#	Ret. Time	Area	Height	Area %	Height %
1	19.735	723485	21675	50.240	55.319
2	24.093	716583	17507	49.760	44.681
Total		1440069	39182	100.000	100.000



Peak#	Ret. Time	Area	Height	Area %	Height %
1	19.658	1545718	45948	98.770	98.848
2	24.022	19253	535	1.230	1.152
Total		1564971	46484	100.000	100.000

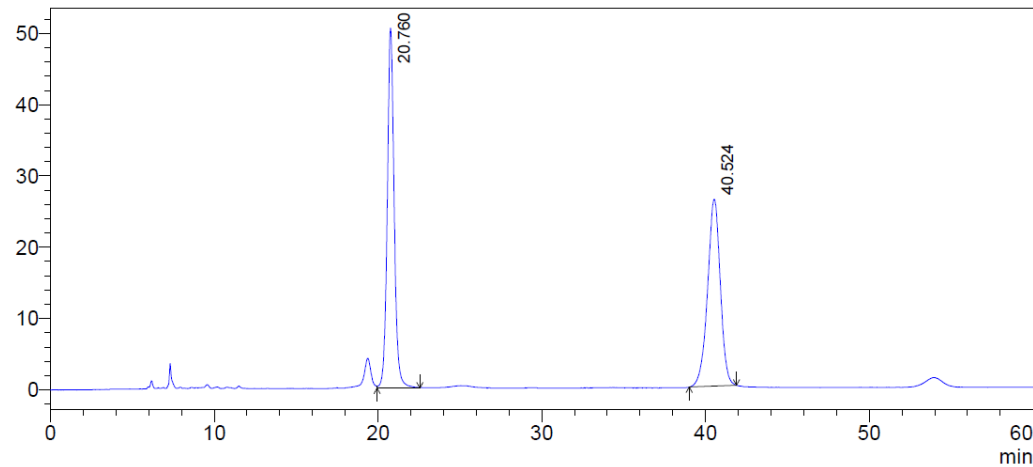


Peak#	Ret. Time	Area	Height	Area %	Height %
1	20.825	6268606	212338	50.452	61.109
2	33.466	6156314	135138	49.548	38.891
Total		12424920	347477	100.000	100.000



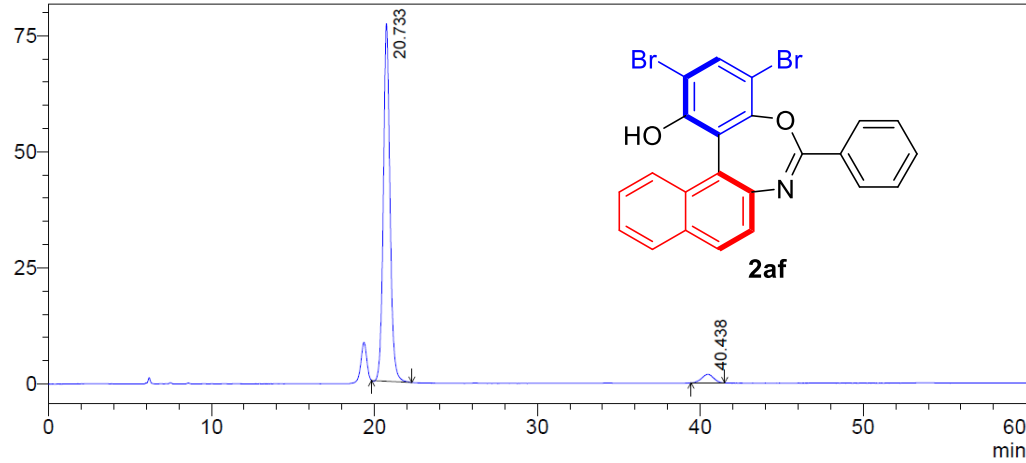
Peak#	Ret. Time	Area	Height	Area %	Height %
1	21.084	3503747	118545	96.037	97.366
2	33.748	144602	3207	3.963	2.634
Total		3648349	121752	100.000	100.000

mV



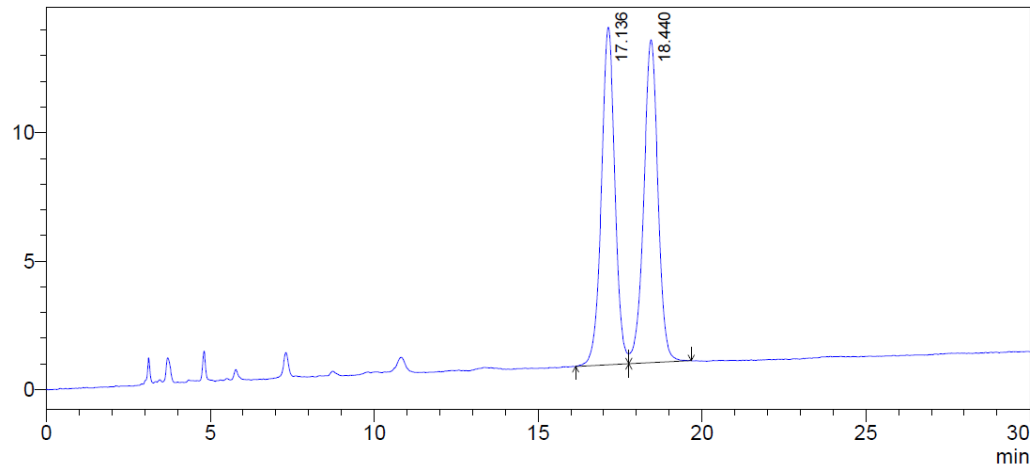
Peak#	Ret. Time	Area	Height	Area %	Height %
1	20.760	1474386	50494	50.946	65.807
2	40.524	1419644	26237	49.054	34.193
Total		2894030	76731	100.000	100.000

mV

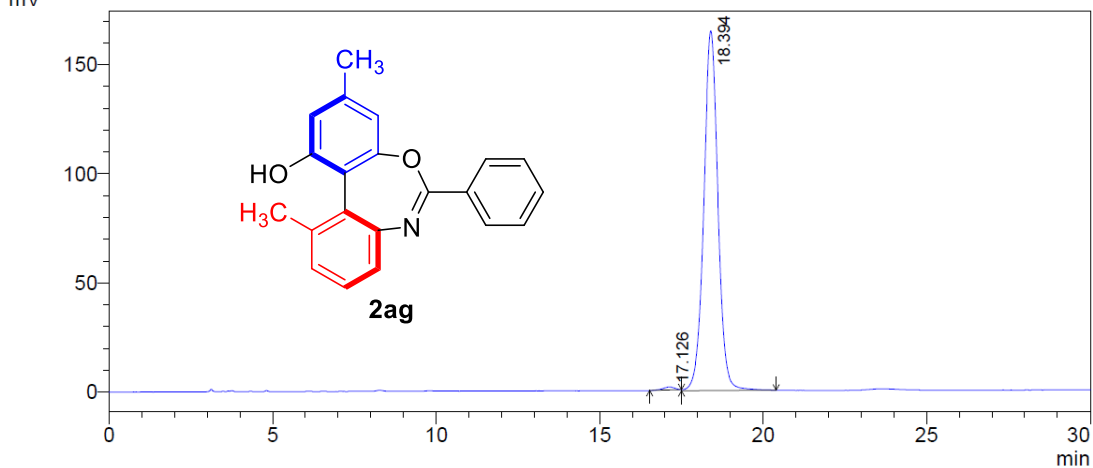


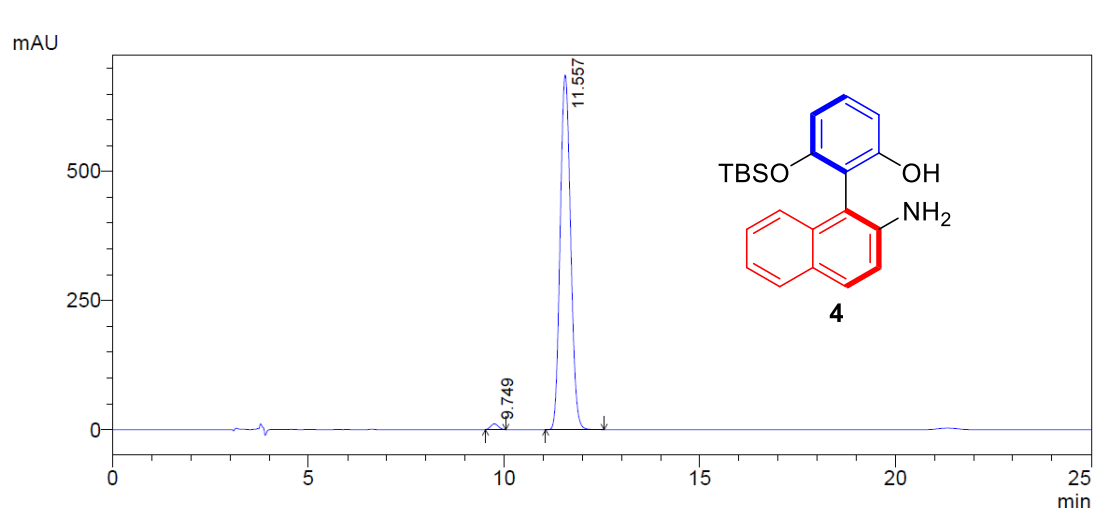
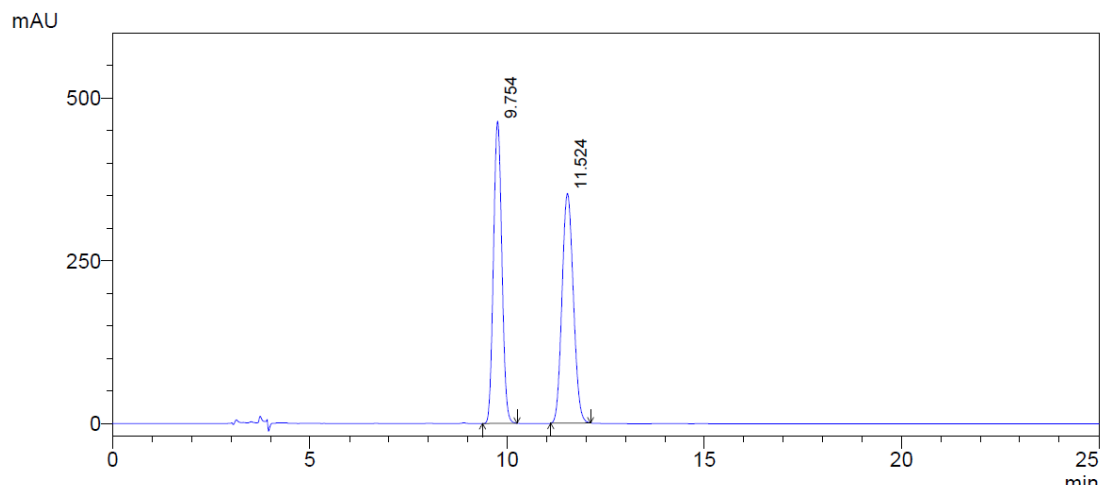
Peak#	Ret. Time	Area	Height	Area %	Height %
1	20.733	2188262	76923	95.911	97.679
2	40.438	93283	1828	4.089	2.321
Total		2281545	78751	100.000	100.000

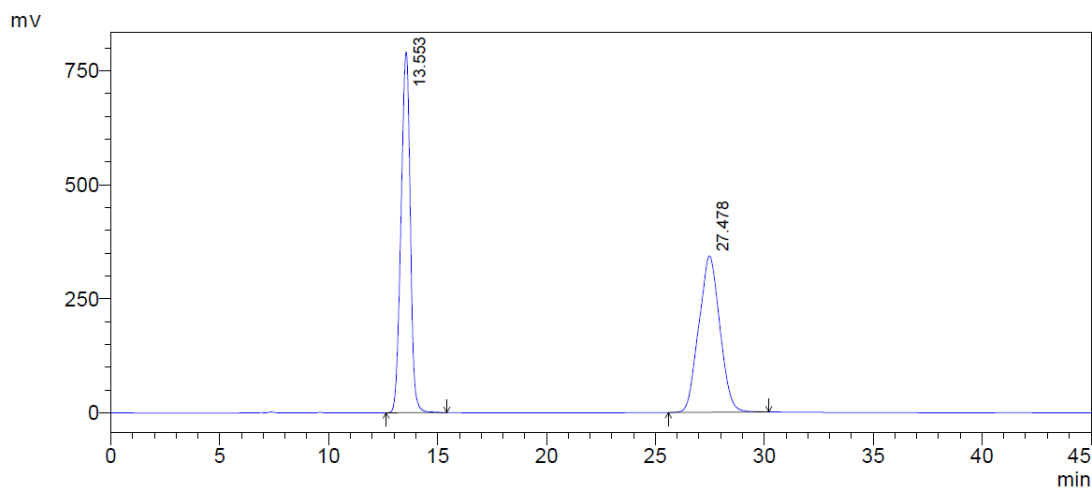
mV



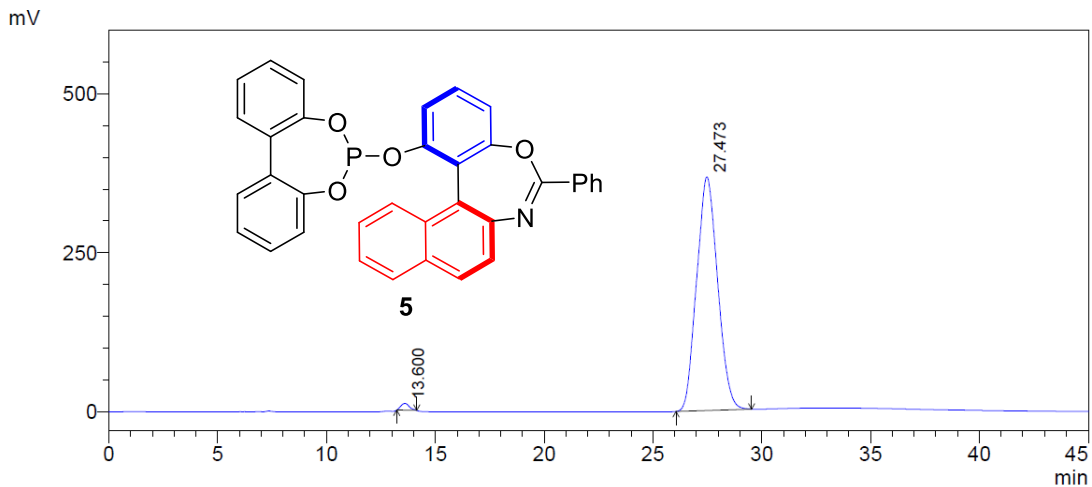
mV





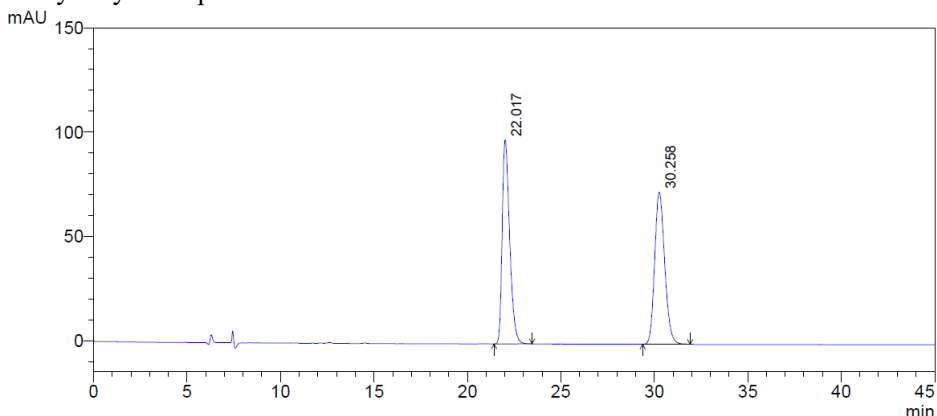


Peak#	Ret. Time	Area	Height	Area %	Height %
1	13.553	23364834	789969	50.403	69.750
2	27.478	22991588	342596	49.597	30.250
Total		46356422	1132566	100.000	100.000



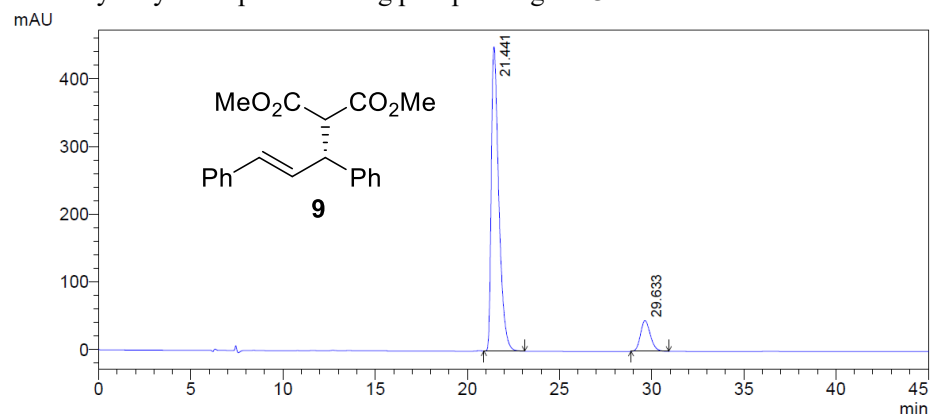
Peak#	Ret. Time	Area	Height	Area %	Height %
1	13.600	291765	10815	1.172	2.863
2	27.473	24612532	367006	98.828	97.137
Total		24904296	377822	100.000	100.000

Racemic alkyl allylation product



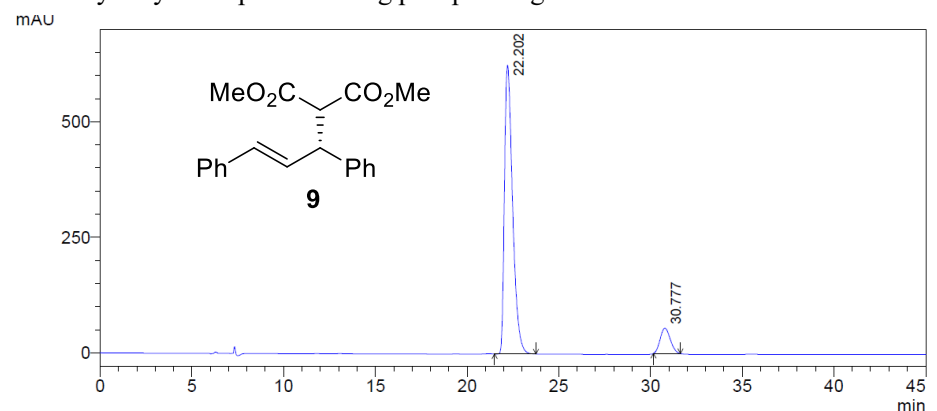
Peak#	Ret. Time	Area	Height	Area %	Height %
1	22.017	2718418	97876	49.971	57.288
2	30.258	2721547	72973	50.029	42.712
Total		5439965	170849	100.000	100.000

Asymmetric alkyl allylation product using phosphite ligand **5**



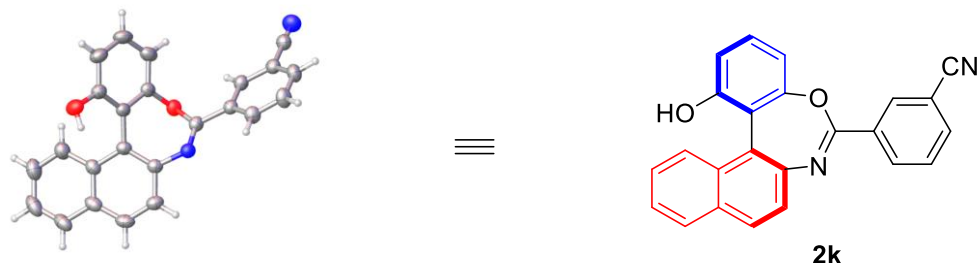
Peak#	Ret. Time	Area	Height	Area %	Height %
1	21.441	12775931	449403	88.322	90.829
2	29.633	1689227	45377	11.678	9.171
Total		14465158	494780	100.000	100.000

Asymmetric alkyl allylation product using phosphite ligand **6**



Peak#	Ret. Time	Area	Height	Area %	Height %
1	22.202	19269035	624663	90.149	91.923
2	30.777	2105691	54884	9.851	8.077
Total		21374726	679546	100.000	100.000

X-ray structure of **2k**



Deposition No. CCDC 2182790

References

- [1] a) Yang, G.; Guo, D.; Meng, D.; Wang, J. *Nat. Commun.* **2019**, *10*, 3062; b) Lu, S.; Poh, S. B.; Rong, Z.; Zhao, Y. *Org. Lett.* **2019**, *21*, 6169–6172.
- [2] Bai, S.-T.; Kluwer, A. M.; Reek, J. N. H. *Chem. Commun.* **2019**, *55*, 14151–14154.
- [3] Ahmed, A.; Bragg, R. A.; Clayden, J.; Lai, L. W.; McCarthy, C.; Pink, J. H.; Westlund, N.; Yasin, S. A. *Tetrahedron* **1998**, *54*, 13277–13294.

Full reference for Gaussian software:

Gaussian 16, Revision B.01, Frisch, M. J.; Trucks, G. W.; Schlegel, H. B.; Scuseria, G. E.; Robb, M. A.; Cheeseman, J. R.; Scalmani, G.; Barone, V.; Mennucci, B.; Petersson, G. A.; Nakatsuji, H.; Caricato, M.; Li, X.; Hratchian, H. P.; Izmaylov, A. F.; Bloino, J.; Zheng, G.; Sonnenberg, J. L.; Hada, M.; Ehara, M.; Toyota, K.; Fukuda, R.; Hasegawa, J.; Ishida, M.; Nakajima, T.; Honda, Y.; Kitao, O.; Nakai, H.; Vreven, T.; Montgomery Jr., J. A.; Peralta, J. E.; Ogliaro, F.; Bearpark, M.; Heyd, J. J.; Brothers, E.; Kudin, K. N.; Staroverov, V. N.; Kobayashi, R.; Normand, J.; Raghavachari, K.; Rendell, A.; Burant, J. C.; Iyengar, S. S.; Tomasi, J.; Cossi, M.; Rega, N.; Millam, J. M.; Klene, M.; Knox, J. E.; Cross, J. B.; Bakken, V.; Adamo, C.; Jaramillo, J.; Gomperts, R.; Stratmann, R. E.; Yazyev, O.; Austin, A. J.; Cammi, R.; Pomelli, C.; Ochterski, J. W.; Martin, R. L.; Morokuma, K.; Zakrzewski, V. G.; Voth, G. A.; Salvador, P.; Dannenberg, J. J.; Dapprich, S.; Daniels, A. D.; Farkas, Ö.; Foresman, J. B.; Ortiz, J. V.; Cioslowski, J.; Fox, D. J. Gaussian, Inc., Wallingford CT, **2016**.

- (1) Bannwarth, C.; Ehlert, S.; Grimme, S. GFN2-XTB - An Accurate and Broadly Parametrized Self-Consistent Tight-Binding Quantum Chemical Method with Multipole Electrostatics and Density-Dependent Dispersion Contributions. *J. S114*

- Chem. Theory Comput.* **2019**, *15* (3), 1652–1671.
- (2) Grimme, S.; Bannwarth, C.; Shushkov, P. A Robust and Accurate Tight-Binding Quantum Chemical Method for Structures, Vibrational Frequencies, and Noncovalent Interactions of Large Molecular Systems Parametrized for All Spd-Block Elements (Z = 1–86). *J. Chem. Theory Comput.* **2017**, *13* (5), 1989–2009.
- (3) Bannwarth, C.; Caldeweyher, E.; Ehlert, S.; Hansen, A.; Pracht, P.; Seibert, J.; Spicher, S.; Grimme, S. Extended Tight-Binding Quantum Chemistry Methods. *Wiley Interdiscip. Rev. Comput. Mol. Sci.* **2021**, *11* (2).
- (4) Grimme, S. Exploration of Chemical Compound, Conformer, and Reaction Space with Meta-Dynamics Simulations Based on Tight-Binding Quantum Chemical Calculations. *J. Chem. Theory Comput.* **2019**, *15* (5), 2847–2862.
- (5) Pracht, P.; Bohle, F.; Grimme, S. Automated Exploration of the Low-Energy Chemical Space with Fast Quantum Chemical Methods. *Phys. Chem. Chem. Phys.* **2020**, *22* (14), 7169–7192.
- (6) Weigend, F.; Ahlrichs, R. Balanced Basis Sets of Split Valence, Triple Zeta Valence and Quadruple Zeta Valence Quality for H to Rn: Design and Assessment of Accuracy. *Phys. Chem. Chem. Phys.* **2005**, *7* (18), 3297–3305.
- (7) Weigend, F. Accurate Coulomb-Fitting Basis Sets for H to Rn. *Phys. Chem. Chem. Phys.* **2006**, *8* (9), 1057–1065.
- (8) Li, Y. P.; Gomes, J.; Sharada, S. M.; Bell, A. T.; Head-Gordon, M. Improved Force-Field Parameters for QM/MM Simulations of the Energies of Adsorption for Molecules in Zeolites and a Free Rotor Correction to the Rigid Rotor Harmonic Oscillator Model for Adsorption Enthalpies. *J. Phys. Chem. C* **2015**, *119* (4), 1840–1850.
- (9) Luchini, G.; Alegre-Requena, J. V.; Funes-Ardoiz, I.; Paton, R. S.; Pollice, R. GoodVibes: Automated Thermochemistry for Heterogeneous Computational Chemistry Data. **2020**, *9*, 291.
- (10) Contreras-García, J.; Johnson, E. R.; Keinan, S.; Chaudret, R.; Piquemal, J. P.; Beratan, D. N.; Yang, W. NCIPILOT: A Program for Plotting Noncovalent Interaction Regions. *J. Chem. Theory Comput.* **2011**, *7* (3), 625–632.

- (11) Schrödinger, L. *The PyMOL Molecular Graphics Development Component, Version 1.8*; 2015.
- (12) Lv, Y.; Luo, G.; Liu, Q.; Jin, Z.; Zhang, X.; Chi, Y. R. Catalytic Atroposelective Synthesis of Axially Chiral Benzonitriles via Chirality Control during Bond Dissociation and CN Group Formation. *Nat. Commun.* 2022 **13** (1), 1–9.
- (13) Fukui, K. The Path of Chemical Reactions - The IRC Approach. *Acc. Chem. Res.* **1981**, *14* (12), 363–368.
- (14) Fukui, K. Formulation of the Reaction Coordinate. *J. Phys. Chem.* **2005**, *74* (23), 4161–4163.
- (15) Ess, D. H.; Houk, K. N. Distortion/Interaction Energy Control of 1,3-Dipolar Cycloaddition Reactivity. *J. Am. Chem. Soc.* **2007**, *129* (35), 10646–10647.
- (16) Bickelhaupt, F. M.; Houk, K. N. Analyzing Reaction Rates with the Distortion/Interaction-Activation Strain Model. *Angew. Chem. Int. Ed.* **2017**, *56* (34), 10070–10086.
- (17) Bickelhaupt, F. M. Understanding Reactivity with Kohn-Sham Molecular Orbital Theory: E2-SN2 Mechanistic Spectrum and Other Concepts. *J. Comput. Chem.* **1999**, *20* (1), 114–128.
- (18) Fernández, I.; Bickelhaupt, F. M. The Activation Strain Model and Molecular Orbital Theory: Understanding and Designing Chemical Reactions. *Chem. Soc. Rev.* **2014**, *43* (14), 4953–4967.
- (19) Wolters, L. P.; Bickelhaupt, F. M. The Activation Strain Model and Molecular Orbital Theory. *Wiley Interdiscip. Rev. Comput. Mol. Sci.* **2015**, *5* (4), 324–343.
- (20) Vermeeren, P.; van der Lubbe, S. C. C.; Fonseca Guerra, C.; Bickelhaupt, F. M.; Hamlin, T. A. Understanding Chemical Reactivity Using the Activation Strain Model. *Nat. Protoc.* **2020**, *15* (2), 649–667.